FUNCTIONAL CHARACTERIZATION OF SMALL MAF TRANSCRIPTION

FACTORS MAFG AND MAFK IN MAMMALIAN LENS HOMEOSTASIS

by

Smriti Akshay Agrawal

A thesis submitted to the Faculty of the University of Delaware in partial fulfillment of the requirements for the degree of Masters of Science in Biological Sciences

Summer 2014

UMI Number: 1567789

UMI

Dissertation Publishing

UMI 1567789

ProQuest®

FUNCTIONAL CHARACTERIZATION OF SMALL MAF TRANSCRIPTION FACTORS MAFG AND MAFK IN MAMMALIAN LENS HOMEOSTASIS

by

Smriti Akshay Agrawal

Approved: _____
Salil A. Lachke, Ph.D.
Professor in charge of thesis on behalf of the Advisory Committee

Approved: _____
Randall Duncan, Ph.D.
Chair of the Department of Biological Sciences

Approved: _____
George H. Watson, Ph.D.
Dean of the College of Arts and Sciences

Approved: _____
James G. Richards, Ph.D.
Vice Provost for Graduate and Professional Education

ACKNOWLEDGMENTS

TABLE OF CONTENTS

Chapter

LIST OF TABLES

ABSTRACT

Elucidating the regulatory events that underlie formation and maintenance of lens transparency is critical for understanding the etiology of its associated disease termed cataract. Thus far, mutations or functional compromise in only 26 genes are described to cause non-syndromic or isolated pediatric cataract. The majority of these genes exhibit highly enriched-expression in lens fiber cells suggesting that regulation of their expression in these cells is essential to maintenance of lens transparency. However, so far only five transcription factors (Pax6, c-Maf, Prox1, Sox1, and Hsf4) have been primarily associated with fiber cell gene expression. In my thesis, I have identified and characterized a new function of the small Maf transcription factors MafG and MafK in regulating gene expression in mouse lens fiber cells, disruption of which causes lens defects including cataract.

I used the bioinformatics tool *iSyTE* (integrated Systems Tool for Eye gene discovery, http://bioinformatics.udel.edu/Research/iSyTE) to first identify *MafG* as a candidate gene with highly enriched expression in the lens. Moreover, my analysis using *iSyTE* also indicated that mRNAs encoding several transcriptional regulatory protein partners of MafG were enriched in the lens. Based on these analyses, I hypothesized that MafG and its associated regulatory partner proteins function to control gene expression in lens fiber cells. Previous studies on small Maf proteins MafG, MafK, and MafF in non-eye related cells/tissues suggest a functional redundancy among these regulatory proteins. To identify which other small Maf members are

expressed in the lens and how their expression compares to that of MafG, I analyzed *iSyTE* for expression of *MafG*, *MafK*, and *MafF* and performed real time quantitative RT-PCR to test expression of these genes in postnatal lens tissue. While MafG exhibits highly enriched expression in embryonic and postnatal lens, *MafK* is expressed in these stages, albeit at low levels and *MafF* expression is undetected in the lens, indicating that *MafG* and *MafK* may function in lens development or homeostasis. *In situ* expression analysis of wild type embryonic mouse lens confirmed the highly enriched expression of *MafG* transcripts in lens fiber cells.

Thus, to investigate the function of *MafG* and *MafK* in the lens, I bred previously generated germline knock-out mouse mutants to derive various combinations of *MafG* and *MafK* compound mutant mice. *MafG-/-:MafK+/-* compound mouse mutants exhibit fully penetrant lens defects, including smaller lens (evident postnatal day 60 (P60) and later), a subset of which develop severe cataract (evident P120 and later). Examination of the lens fiber cell ultrastructure by scanning electron microscopy (SEM) analysis demonstrated that *MafG-/-:MafK+/-* compound mutant lens exhibit disruption of membrane protrusions in cortical fiber cells compared to *MafG+/-:MafK+/-* control lens. Interestingly, *MafG+/-:MafK-/-* compound mutant or *MafG-/-:MafK+/+* and *MafG+/+:MafK-/-* single gene mutant lenses do not exhibit any lens defects that are detectable by either light microscopy or SEM analysis. Moreover, *MafG-/-:MafK-/-* mouse mutants, that exhibit perinatal lethality and therefore cannot be analyzed at postnatal stages, but do not exhibit lens defects at embryonic stage E16.5. To gain insight into the molecular changes underlying these lens defects in *MafG-/-:MafK+/-*

mice, I performed microarray-based transcript profiling analysis on *MafG-/-:MafK+/-* mutant and control lens at 2 month age, prior to development of cataract phenotype, and identified altered expression of several genes functional in distinct cell response pathways such as DNA damage response, cell cycle regulation, and apoptosis. At 1.5-fold levels, 949 genes were found to be up- or down-regulated in *MafG-/-:MafK+/-* mutant lens. Among other pathways, stress response genes such as *Hsp27*, *Hmox1* and *Ddit3* were mis-regulated in *MafG-/-:MafK+/-* mutant lens.

In silico analyses of genomic regions surrounding a subset of these target genes identified conserved ARE (Antioxidant Response Element) *cis*-regulatory binding sites recognized by MafG/K and Cap n' Collar (CNC)/Bach heterodimers. Furthermore, I performed an integrated analysis based on *iSyTE* data on lens-enrichment or lens expression, as well as previously published ChIP (Chromatin Immuno-Precipitation) data on Nrf2, a small Maf binding partner, to identify genes with anti-oxidant response elements (ARE) to prioritize candidates from the extensive list of differentially regulated genes in *MafG-/-:MafK+/-* mutant lens. This analysis led to the identification of 24 genes that are promising direct targets of MafG/MafK and their co-regulatory protein partners in the lens.

In sum, my thesis research has led to the identification and functional characterization of the transcription factors MafG and MafK in regulation of gene expression that control diverse pathways functional in stress response, apoptosis, and cell cycle regulation in lens fiber cells. Moreover, my research demonstrates that deficiency of these genes in a compound mouse mutant model causes severe lens fiber

cell defects, including cataract. These findings imply *MafG* and *MafK* as important new candidate genes for further examination in human cataract patients.

Chapter 1

INTRODUCTION

1.1 The Structure and Function of the Ocular Lens

The human eye is a complex organ with multiple tissue components that coordinately function to enable high-resolution vision. Located in the anterior compartment of the eye is the lens - an avascular, transparent, and a highly structured tissue that, along with the cornea, refracts and focuses light on the retina (Figure 1.1). The photoreceptor cells of the retina detect the focused light and convert it into signaling information that is relayed to the brain via the optic nerve. Thus, the function of the lens, and hence the visual acuity of the animal, is dependent on the maintenance of its transparency, which should ideally persist throughout the life. Lens development begins in the latter part of the first trimester in human, and the morphological changes

Figure 1.1. Anatomy of the human eye. The lens is located in the anterior portion of the eye, where along with the cornea, it functions to refract and focus light on the retina. (adopted from http://webvision.med.utah.edu)

1

associated with this process have been generally well understood in mammals, including human and mouse, as well as in frog, chicken and zebrafish.

The onset of mammalian lens development is first observed in late gastrulation, when coordinate interactions between the optic vesicle and the overlying surface ectoderm result in the thickening of the surface ectoderm into the lens placode (Figure 1.2). In mouse embryogenesis, this process initiates early around the 20-25 somite stage or on embryonic day 9.5 (E9.5) (Huang et al., 2011; McAvoy et al., 1999).

As these tissues develop further, the lens placode invaginates along with the optic vesicle to form the lens pit and early optic cup (E10.0), respectively. Subsequently, the lens pit pinches off from the ectodermal surface and proceeds to close in and form a spherical structure termed the lens vesicle.

As the lens vesicle develops further, two types of cells can be distinguished based on their morphology and gene expression profiles. Cells located in the anterior region of the lens vesicle form the anterior epithelium of the lens (AEL), while those located posteriorly elongate into differentiating primary fiber cells, which lose their organelles and nuclei and contribute to the central core of the lens (Grainger et al., 1992; Graw, 1999; Lovicu & Robinson, 2004). The AEL comprises of a single layer of cells that are metabolically active and in a specific region mitotically active as well. In post-natal lens, the AEL serves as a resource of cells that proliferate in the mitotically active zone, and at the transition zone exit the cell cycle to differentiate into secondary fiber cells at the equatorial region of the lens (Bassnett, 2002; Bassnett & Shi, 2010; Martinez & de Iongh, 2010). Similar to primary fiber cells, the terminal differentiation of

secondary fiber cells is accompanied by degradation of organelles and nuclei, which is

necessary to form a transparent tissue for effective refraction and transmission of light

(Bassnett, 2002, 2009; Slingsby et al., 2013; Wride, 2011; Zandy et al., 2005).
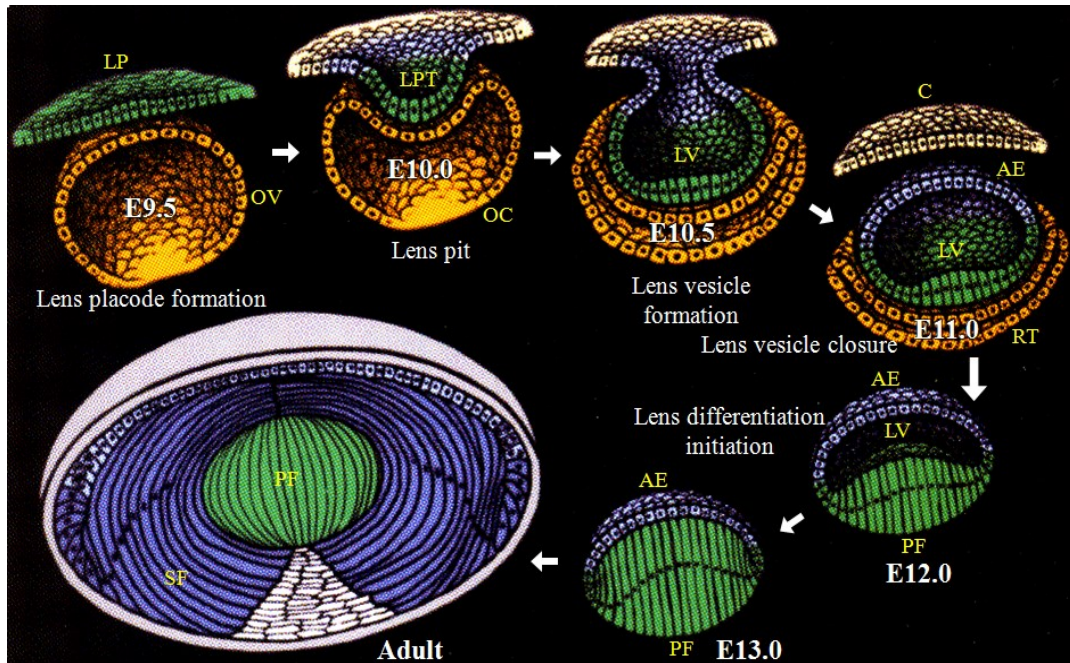
Figure 1.2. Schematic of mammalian lens development. Several morphological events can be distinguished during embryonic development of the lens in mammals. At mouse embryonic day (E) 9.5, the lens placode (green) is induced, which in subsequent stages (E10.0 through E10.5) invaginates along with the optic cup (orange) to form the lens pit that in turn forms the lens vesicle. Primary fiber cells form as a result of elongation of the posteriorly localized cells in the lens vesicle at E11.0, which continue to fill the lens vesicle (green) and eventually lose their organelles. The anterior epithelium (blue) of the lens is a single layer made of metabolically active cells that serve as a reservoir for differentiating into secondary fiber cells. The process of secondary fiber cell differentiation occurs throughout the life of the animal. (Modified from Kuszak and Brown, 1994)

The process of lens secondary fiber cell differentiation continues throughout the life of the animal, whereby new fiber cells continue to form in the outermost layer and compile on top of the previously differentiated secondary fiber cells. During this stage, water-soluble proteins called crystallins are expressed in high concentrations and account for over 90% of the soluble protein profile in the lens (Ueda et al., 2002). There are many distinct regulatory processes, including transcriptional control, post-transcriptional modifications by RNA binding proteins, and micro-RNA mediated silencing that have been shown to control expression of crystallins in the lens (Conte et al., 2010; Cvekl & Duncan, 2007; Lachke & Maas, 2011; Shaham et al., 2013).

For instance, transcription factors such as Prox1, Sox1 and c-Maf regulate the expression of critical lens fiber cell specific genes encoding crystallins (*e.g.* αA-crystallin and αB-crystallin) (Nishiguchi et al., 1998; Ring et al., 2000; Robinson & Overbeek, 1996; Wigle et al., 1999), transport channels proteins (*e.g.* MIP, Aquaporin 0) (Chepelinsky, 2003; Varadaraj et al., 2010; Varadaraj et al., 2008), and gap junction proteins (*e.g.* Connexin 43, Connexin 46, and Connexin 50) (Gong et al., 2007; Mathias et al., 2010). Indeed, mutations or functional compromise of genes encoding these proteins cause congenital or pediatric cataracts (Santana & Waiswo, 2011; Shiels et al., 2010; Shiels & Hejtmancik, 2013). Thus, regulation of lens development and homeostasis is critical for the lens to remain transparent throughout life.

1.2   Cataract: Opacification of the Lens

Loss of lens transparency, clinically termed "cataract", is the leading cause of blindness worldwide (Javitt et al., 1996; Petrash, 2013; Shichi, 2004). To allow clear high-resolution vision, the lens functions to refract and focus light on the retina. Therefore, opacity of the lens obstructs transmission of light and its focus on to the retina, thus altering the refractive index of the lens (Benedek, 1971; Delaye & Tardieu, 1983) (Delaye and Tardieu, 1983, Benedek, 1971, (Hejtmancik & Kantorow, 2004) (Figure 1.3). Lens opacity can result from structural changes in fiber cells (*e.g.* vacuole formation) or qualitative or quantitative alterations in proteins such as crystallins (*e.g.* protein aggregation) (Benedek, 1971; Cheng et al., 2010).

Cataract is a multifactorial disease that can result from environmental factors, genetics, gender, or diseases such as diabetes (Gilbert & Foster, 2001; Shiels & Hejtmancik, 2013; Yi et al., 2011). Based on the 2012 World Health Organization report, it is estimated that blindness is prevalant in 39 million people, and cataract is responsible for about 50% of the blindess worldwide (Petrash, 2013; Rao & Perry, 2011). Depending on its onset, cataract can be classified as congenital/pediatric or age-related (Hejtmancik, 2008; Shiels & Hejtmancik, 2013). Congenital cataract occurs at birth, while pediatric cataract develops during childhood and causes visual impairment or blindness in infancy (Santana & Waiswo, 2011). About twenty-five to fifty percent of all congenital cataract cases have been predicted to have a genetic cause, and are a result of genetic perturbations (*e.g.* mutations in genes encoding crystallins) (Francis & Moore, 1999; Santana & Waiswo, 2011).

Congenital cataract can also result from infections (*e.g.* Rubella) that the mother could have contracted during pregnancy, or due to certain inherited syndromes such as Alport's syndrome, Fabry disease, among others (Dewan & Gupta, 2012; Orssaud et al., 2003; Trumler, 2011). Other factors causing loss of visual acuity include exposure to ultraviolet light or radiation, secondary effects of diseases such as diabetes, other metabolic diseases, hypertension, or trauma, as well as other environmental risk factors such as cigarette smoking, alcohol consumption, obesity, and corticosteroid exposure or other medications, common in patients with age-related or secondary cataracts (Hejtmancik & Kantorow, 2004; McCarty & Taylor, 2001).
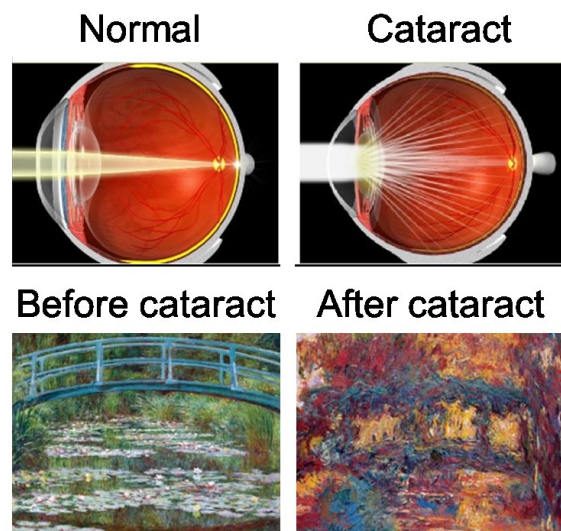
Figure 1.3.   **Cataract results from loss of lens transparency.** In people with normal vision, the lens along with the cornea refracts and focuses light onto the retina. In patients with cataract, the passage of light through the lens is obstructed, causing its scattering. This prevents light from being focused onto the retina and results in loss of clear vision. Paintings by Claude Monet before he developed cataract and after he developed cataract are dramatically different. (NEI and http://www.biologyjunction.com/EXCR_SCIAM-DyingToSee.pdf)

As we age, lens proteins undergo modifications and structural changes that contribute to the lens becoming thicker and less flexible (Petrash, 2013). These processes are often accelerated in the presence of oxidative or osmotic stress or other insults to fiber cells. As these conditions prevail during aging, they cause the lens tissue to break down and crystallin proteins to aggregate, resulting in clouding of small areas of the lens. With time, cataract progresses as the clouding becomes denser and spans a greater portion of the lens, resulting in blindness (Petrash, 2013; Sharma & Santhoshkumar, 2009)

Although cataract surgery is a common procedure performed routinely, it can result in complications such as endophthalmitis, posterior capsular opacification, and retinal detachment (Chan et al., 2010; Durand, 2013; Sinha et al., 2013). Approximately 1.35 million cataract operations are performed annually in the US alone, accounting for 2% of the total Medicare budget according to the National Eye Institute (Babizhayev et al., 2004). With the general aging of human population worldwide, combined with increased life expectancy, the number of cataract cases is expected to climb. Over the past two decades, the genetic causes of cataracts have become more approachable as our understanding of congenital and age-related cataracts has improved (Hejtmancik, 2008; Shiels & Hejtmancik, 2013; Yi et al., 2011). To accomplish the goal of developing approaches to prevent or delay the onset of cataracts, it is critical to first understand the genetic and physiological basis of lens transparency by characterizing the mechanism of lens development in general, and fiber cell differentiation, in particular. These efforts will help determine the critical regulatory processes involved

in normal lens homeostasis, and provide insights into factors that underlie cataract development.

Of the 26 human cases of human congenital or pediatric isolated (non-syndromic) cataract to which a genetic mutation is presently assigned, greater than 80% of the candidate genes exhibit high expression in fiber cells (Santana & Waiswo, 2011; Shiels et al., 2010; Shiels & Hejtmancik, 2013). In consideration of the above data, our understanding of regulation of gene expression in fiber cells is remarkably inadequate. Indeed only five transcription factors (TFs) (Pax6, c-Maf, Prox1, Sox1, and Hsf4) have been studied to some detail in this context. Thus, characterization of new TFs that function in lens fiber cell biology and identification of their downstream targets will lead to identification of potential new candidate genes that are associated with human cataract.

1.3 Transcriptional Regulation in the Lens

In the past two decades, molecular analysis of vertebrate lens development has led to identification of several transcription factors (TFs) that function in the initial stages of lens induction (Cvekl & Duncan, 2007; Lachke & Maas, 2010). Based on knowledge gained from these studies, a gene regulatory network for lens induction encompassing the TFs Six3, Pax6 and Sox2, which function in the formation of the lens placode, can be defined (Donner et al., 2006; Lachke & Maas, 2010).

Pax6 (paired box six) is one of the most critical transcriptional regulators of vertebrate lens development and is essential for lens placode formation (Ashery-Padan

et al., 2000; Cvekl & Duncan, 2007; Graw, 2010; Shaham et al., 2009). While heterozygous mutations in *Pax6* cause ocular abnormalities such as aniridia, cataracts and glaucoma in humans, and small eye in mice and rat (Hill et al., 1991; Hogan et al., 1986; Matsuo et al., 1993), homozygous null mutations cause an arrest in optic vesicle development and lens placode formation, and therefore the lens, fails to initiate (Ashery-Padan et al., 2000). Pax6 is regulated by members of the TALE family of TFs, *e.g.* Meis1 and Pknox1 (Rowan et al., 2010; Zhang et al., 2002) and by Six3, Sox2/Oct1 or by directly binding to its own enhancer in a feedback loop (Donner et al., 2007; Liu et al., 2006). Pax6 in turn regulates the TFs Sox11 and AP-2a that are involved in lens placode invagination and lens vesicle separation, respectively (Pontoriero et al., 2009; Wurm et al., 2008). Another downstream TF, Pitx3, is required for maintenance of the anterior epithelium of the lens (AEL) (Ho et al., 2009). Pax6 also activates the TF Mab21l1 (male abnormal 21 like 1), which in turn regulates Foxe3, a highly lens-enriched forkhead family TF involved in lens vesicle closure. Foxe3 functions to negatively regulate expression of yet another TF, Prox1, in lens AEL (Blixt et al., 2000; Yamada et al., 2003). In later stages, expression of Foxe3 and Prox1 in AEL and differentiating fiber cells function to fine-tune the control of cell cycle exit and initiation of fiber cell differentiation (Landgren et al., 2008)

In contrast to the detailed understanding of the TF circuitry that functions in lens placode induction and maintenance and proliferation of the AEL, our understanding of TFs that function in lens fiber cells is limited (Lachke & Maas, 2010). Studies on animal ocular mutants and human inherited cataract patients have led to the identification of

five TFs – Pax6, Prox1, Sox1, Hsf4 and the large Maf family member, c-Maf – that function to regulate critical downstream genes (*e.g.* genes encoding alpha, beta and gamma crystallins, among others) in differentiating fiber cells (Kawauchi et al., 1999; Kim et al., 1999; Nishiguchi et al., 1998; Ring et al., 2000; Wigle et al., 1999; Xie & Cvekl, 2011)

Numerous studies on Pax6 provide evidence that this gene plays cell-autonomous roles in the lens (Huang et al., 2011; Shaham et al., 2009). When Pax6 was conditionally knocked-out from the lens after the lens vesicle stage, the mice appeared to have smaller eyes resulting from a decrease in lens tissue. Pax6-deficient mice lens also exhibited failure of lens epithelial fiber cell differentiation and failed to exit the cell cycle at the lens equator, showing that Pax6 is essential for initiation of the lens fiber differentiation program and cell cycle exit in the lens (Huang et al., 2011; Shaham et al., 2009). Its lens tissue-related function is a result of its interactions with other lens-tissue enriched TFs such as c-Maf, AP-2α, and Sox2, as well as via interactions with other TFs pRb and TFIID that are not necessarily lens-enriched or restricted (Cvekl et al., 2004). In essence, Pax6 regulates a multitude of genes important during ocular development, including αA, αB, and δ1 crystallins in the lens of mice and chicken (Cvekl & Piatigorsky, 1996), as well as a broad range of genes including other transcriptional regulators such as Six3, c-Maf, and Prox1 (Ashery-Padan et al., 2000; Goudreau et al., 2002; Sakai et al., 2001), and various cell adhesion molecules like α5β1 integrins (Duncan et al., 2000).

Prox1 is another critical transcription factor that functions in lens fiber cell differentiation (Duncan et al., 2002). Prox1 is expressed in the mouse lens placode at E9.5, as well as in the lens vesicle at E10.5 and the fiber cell nuclei at E12.5. It regulates the transcription of several crystallin genes such as βB1-crystallin and γF-crystallins, as well as cell-cycle inhibitors p27KIP1 and p57KIP2, and is required for normal lens development (Duncan et al., 2002). Mouse *Prox1* homozygous deletion mutation results in failure of fiber cell elongation to fill up the lens vesicle, resulting in a hollow lens (Wigle et al., 1999). *Sox1* belongs to the Sox-family of transcription factors that have a HMG domain, and targeted deletion of this transcription factor in mice results in failure of fiber cell elongation, causing ocular abnormalities such as microphthalmia and cataract (Graw, 2009). Sox1 promotes transcription of γ-crystallin encoding genes, and *Sox1* mutant embryos exhibit down-regulation of γA, γB, and γF at E12.5, and all γ-crystallins, including γC and γE, by 15.5 dpc (Nishiguchi et al., 1998). Mutations in human heat shock transcription factor gene *HSF4* causes congenital cataract (Yi et al., 2011). Hsf4 encodes a DNA-binding protein that specifically binds heat shock promoter elements (HSE) (Cui et al., 2012; Yi et al., 2011). Studies on *Hsf4* deletion mouse mutants have elucidated its critical role in fiber cell differentiation during lens development, and HSF4 mutations in humans lead to both congenital and age-related cataract (Fujimoto et al., 2004; Min et al., 2004). Hsf4 is a critical transcription factor required in regulating the expression of all γ-crystallins in the lens. Hsf4 also promotes the expression and DNase activity of Dlad (Dnase2β), which is essential for degradation of nuclear DNA required for lens fiber differentiation (Cui et al., 2013). When *Hsf4* was

deleted in mice, phenotypic abnormalities such as abnormal lens fiber cells containing inclusion-like structures were observed (Fujimoto et al., 2004).

Studies in various species, including human, mouse, rat, chicken, quail, frog and fish have established that basic region/leucine zipper (bZIP) transcription factors critically function in eye development (Graw, 2009; Reza & Yasuda, 2004). The Maf (*m*usculo*a*poneurotic *fi*brosarcoma) oncogene family encodes basic region-leucine zipper transcription factors that contain a bZIP domain that is responsible for protein-protein and protein-DNA interactions (Blank & Andrews, 1997). While the basic region binds to DNA, the leucine zipper region facilitates dimerization of DNA binding regions. The large Maf family gene, *c-Maf* (*MAF* in human), is initially expressed in the lens placode and vesicle, but becomes progressively restricted to lens fiber cells (Kawauchi et al., 1999; Ring et al., 2000; Sakai et al., 2001). Homozygous null *c-Maf* mouse mutants exhibit ocular developmental abnormalities such as incomplete fiber cell elongation, lack of secondary fiber cell differentiation, and reduced αB, βB, and γ-crystallin expression (Figure 1.4) (Kim et al., 1999; Ring et al., 2000; K. Yoshida et al., 2001). c-Maf has been shown to regulate αA-crystallin directly, similar to Pax6 and CREB (Y. Yang et al., 2006). Ocular abnormalities, including congenital cataract, have been identified due to *c-MAF* mutations in human patients (Figure 1.4, Figure 1.5) (Jamieson et al., 2002; Lyon et al., 2003). These studies provide substantial evidence that Maf TFs, particularly c-Maf, function in lens development and homeostasis and regulate genes involved in maintaining lens transparency.
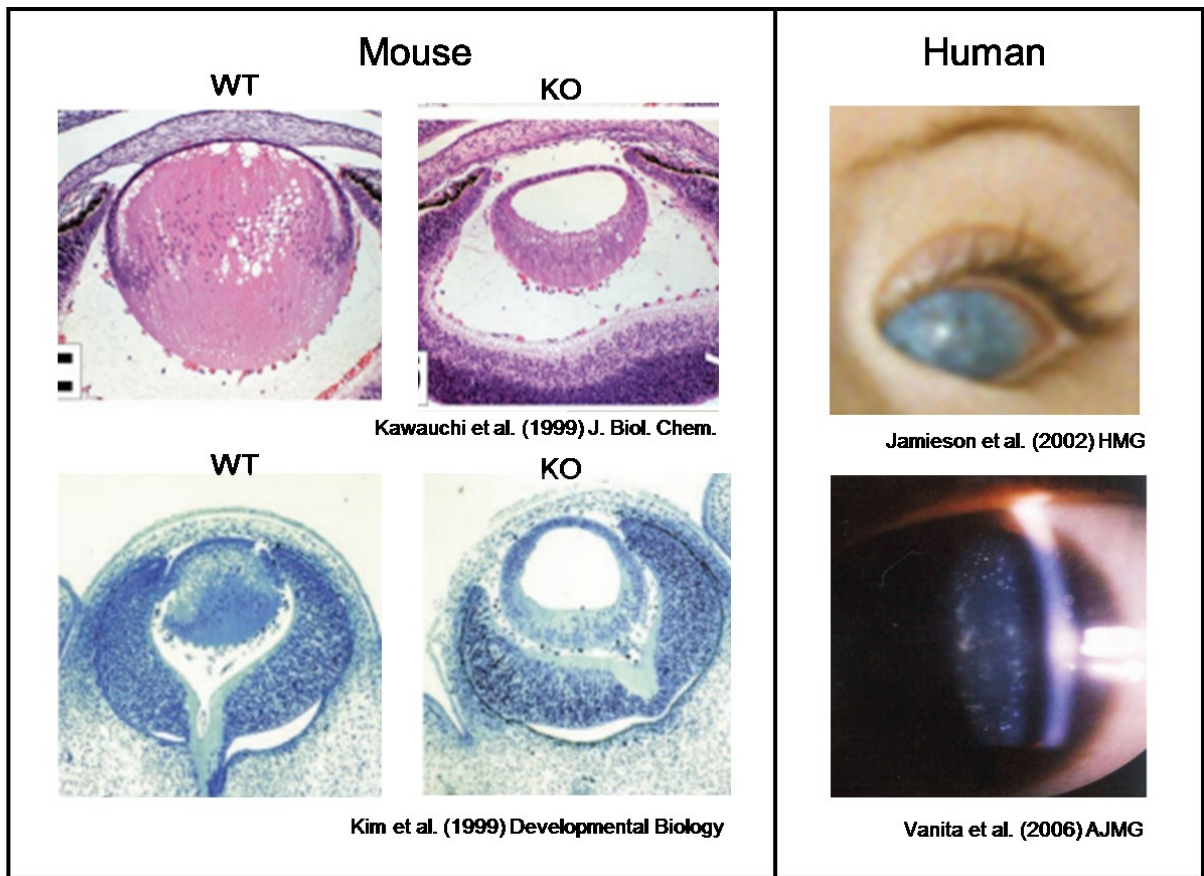
Figure 1.4. c-Maf deficiency causes fiber cell differentiation defects and cataract. Histological analysis of embryonic *c-Maf-/-* mutant and normal eyes (KO and WT respectively) demonstrates defective elongation of posterior lens fiber cells in *c-Maf-/-* mutants. Human mutations in *c-Maf* cause congenital cataracts. Adapted and modified from Kawauchi et al., 1999, Kim et al., 1999, Jamieson et al., 2002, Vanita et al., 2006.
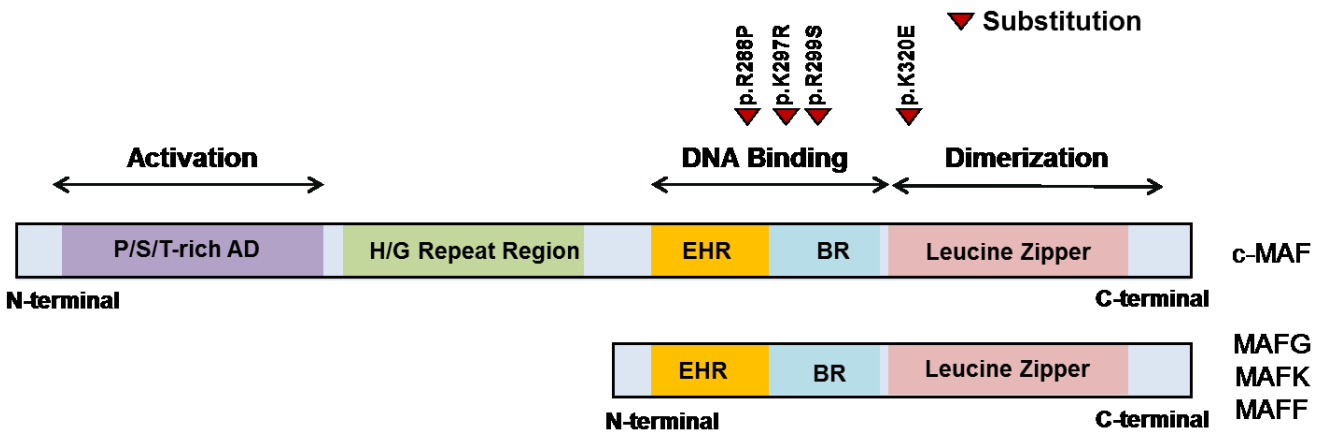
Figure 1.5. Comparison of large and small MAF proteins. Structure of large MAF family protein c-MAF (A). c-MAF protein structure consists of a proline/serine/threonine- rich acidic domain (P/S/T-rich AD) and a histadine/glycine (H/G) repeat region. It also consists of three regions that are shared with the small MAFs- an extended homology region (HER), a basic region (BR), and a leucine zipper domain. Note: mutations in *c-MAF* from inherited cataract patients that affect DNA binding and dimerization domains are indicated by red inverted triangle. c-Maf shares the DNA binding region with small Mafs (B), which lack the N terminal regions including the P/S/T-rich activation domain.

Thus, although we have some insights into the function of transcription factors that are involved in lens fiber cell differentiation, it is critical to identify new regulatory molecules that are involved in this process, which will allow the identification of new candidate genes associated with cataract. My research focuses on the small *Maf* family of TF proteins (*MafG, MafK,* and *MafF*) whose function in the lens remains uncharacterized.

1.4   1.4 *iSyTE* predicts Small Maf Trancription Factor MafG Function in the Lens

iSyTE   (integrated   Systems   Tool   for   Eye   gene   discovery,

http://bioinformatics.udel.edu/Research/iSyTE)   is   a   web-based   bioinformatics

approach for identification of genes with potential function in the lens that are also likely

to be associated with cataract (Lachke, Ho, et al., 2012). *iSyTE* has been highly effective

in identifying known as well as novel genes associated with cataract. This approach is

based on a novel processing of embryonic lens microarray datasets to identify genes that

exhibit highly lens-enriched expression.   This is achieved by comparing the lens

expression datasets with E10.5, E11.5 and E12.5 whole embryonic body tissue (WB)

expression dataset to allow *t*-statistic-based computation of "lens enrichment" *p*-values

for each probe on the microarray. Based on lens-enrichment *p*-values, a ranked list of

lens-enriched genes is generated which is viewed as embryonic stage-specific *iSyTE*

lens tracks in the UCSC Genome browser that in turn can be used to identify candidate

genes with potential lens function within specific genomic regions. In a heat map key,

genes with high lens-enrichment are represented by bright red color while non lens-

enriched genes are represented by dark blue color.

When *iSyTE* was tested on previously mapped intervals of 24 genes associated

with isolated or non-syndromic congenital cataract in human, it identified the known

cataract associated gene in 88% of the cases by ranking it within the top 2 genes among

all genes present in the locus (Lachke, Ho, et al., 2012). More recently, it has facilitated

the characterization of several genes that function in lens biology and are associated

with mammalian cataract (Lachke et al., 2011; Lachke, Higgins, et al., 2012; Lachke,

Ho, et al., 2012; Manthey et al., 2014; Wolf et al., 2013). By analyzing *iSyTE* tracks on

a large genomic interval (2.0 Mb) on chromosome 17 in human (or chromosome 11 in

mouse), *MAFG* was identified among the genes that received an extremely high lens

enrichment score – within the top 1% of lens-expressed genes – strongly indicating it as

a putative candidate gene associated with lens biology and cataract (Figure 1.6). *MAFG*

encodes a small Maf transcription factor protein with DNA binding properties (Blank,

2008; Motohashi et al., 1997).
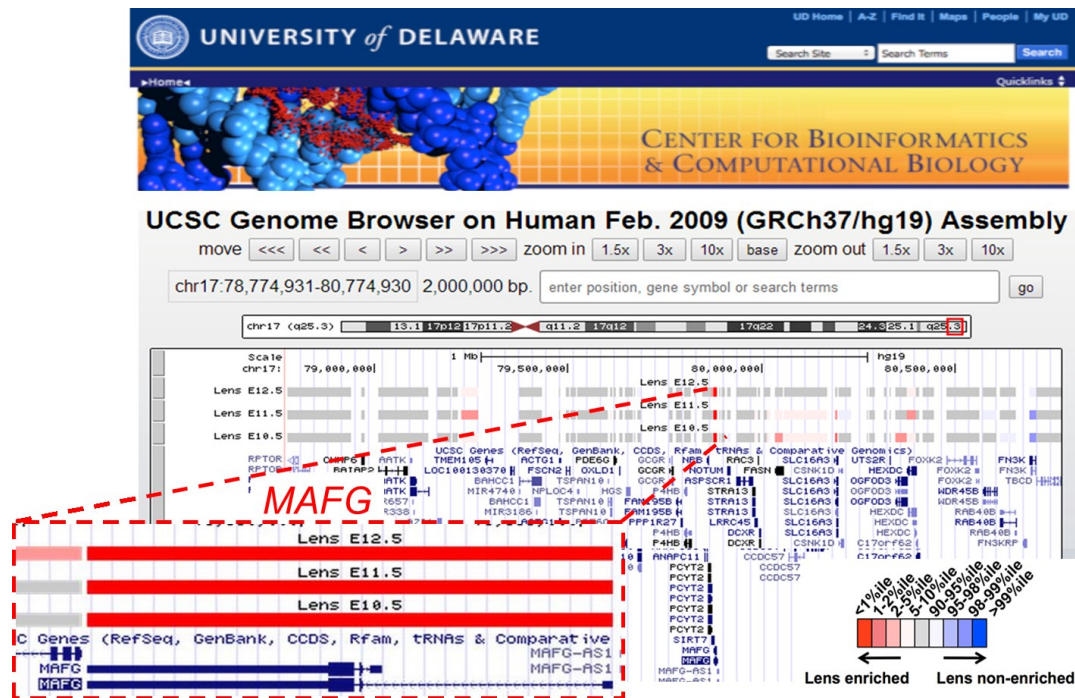
Figure 1.6. ***iSyTE* predicts *MAFG* as a new lens-enriched transcription factor.** *iSyTE* (integrated Systems Tool for Eye gene discovery, http://bioinformatics.udel.edu/Research/iSyTE) is a bioinformatics tool used to predict genes that are important in lens development and disease. *MAFG* (musculoaponeurotic fibrosarcoma oncogene homolog G) was highly lens-enriched during critical embryonic time-points E10.5, E11.5, and E12.5). The heat map key represents genes with high lens-enrichment by bright red color while non lens-enriched genes are represented by dark blue color.

The small MAF transcription factor subgroup includes the proteins MafF, MafG, and MafK, all of which are similar in size (18kDa) and share high homology. Numerous studies have demonstrated that small MAFs are critical regulators of various cellular processes ranging from stress signaling to hematopoiesis (Blank, 2008). *MafG* knockout mice develop thrombocytopenia and motor ataxia, while *MafG* and *MafK* double knockout mice develop severe thrombocytopenia and central nervous system neuronal degradation (Kobayashi et al., 2011; Onodera et al., 1999; Onodera et al., 2000). Small Maf deletion mutations in all three genes *MafG*, *MafK*, and *MafF* result in embryonic lethality and fetal liver apoptosis (Yamazaki et al., 2012). Small Mafs have a dynamic expression pattern during embryogenesis (Murphy & Kolstø, 2000; Onodera et al., 2000), and adult mice express small Mafs in a variety of tissues including the brain, heart, skeletal muscle, placenta, as well as all hematopoietic cell linages (Shimokawa et al., 2000; Toki et al., 1997). These proteins exhibit a modular structure containing a basic domain that mediates DNA binding, and a leucine zipper region that facilitates dimerization of the DNA binding regions. In this aspect, small Maf proteins are similar to large MAF proteins (Figure 1.5). Both the small and large MAFs also share an extended homology region (EHR), which is critical for DNA binding (Blank, 2008; Motohashi et al., 1997).

One of the primary differences between these two sub-families is that small Maf proteins lack the Histidine/Glycine Repeat region and a P/S/T-rich distinctive acidic domain present in large MAF proteins (Figure 1.5), which is the domain with known trans-activation function (Kannan et al., 2012). Thus, small Maf proteins when bound

17

to DNA alone are not expected to have trans-activation function. There is evidence supporting the function of both homodimers and heterodimers of the small MAF proteins in transcriptional regulation of gene expression in development, differentiation, and oncogenesis (Cvekl et al., 2004; Eychène et al., 2008; Kataoka, 2007). The first identified protein partner of small MAF TFs was p45, which was initially isolated as the large subunit of transcription factor NF-E2 (Andrews et al., 1993). Together, the small MAF and p45 heterodimers bind Maf Recognition elements (MARE) and activate transcription (Figure 1.7). This study also provided evidence that homodimers of the small MAF proteins act as negative regulators, while heterodimers composed of MafG and p45 activate transcription *in vivo*. Since this finding, several other transcription factors belonging to the Cap 'N' collar (CNC) domain family such as Nrf1 (/LCRF1/TCF11), Nrf2 (/ECH), Bach1, and Bach2 family proteins (Shavit et al., 1998) that interact with small MAF proteins have been identified (Table 1).
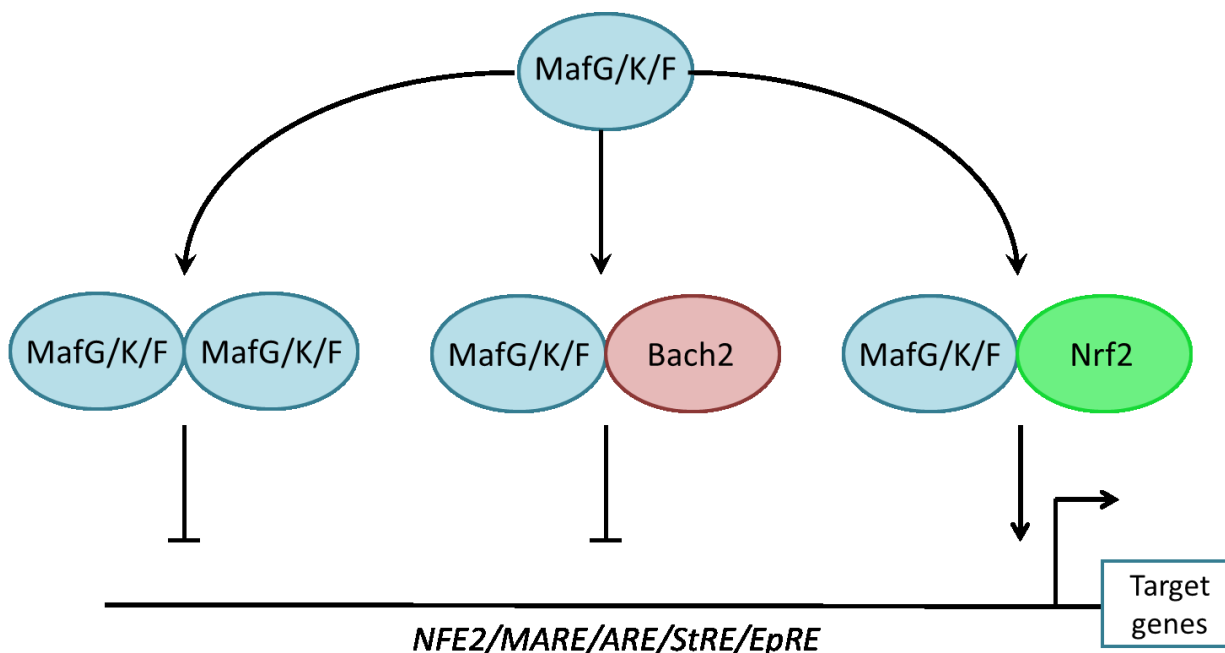
Figure 1.7. Transcriptional regulation of small Mafs proteins. Small Mafs TFs can homo- or hetero-dimerize and bind to specific *cis*-regulatory sites near their target genes and depending upon binding-partner context, function as either transcriptional activators or repressors. Some of the target genes are involved in stress response, hematopoiesis, CNS function, and inflammation.

Proteins in the CNC family of TFs lack the capacity to bind DNA on their own and therefore require small MAF proteins as obligatory dimerization partners to function as transcriptional regulators. Binding partners of small Maf TFs highlighted in Table 1 have provided insights into the cellular function of these transcriptional regulatory proteins (Kannan et al., 2012). Further, identification of HIF1A (hypoxia inducible factor 1, alpha subunit), a member of the bHLH-PAS family of proteins, as a binding partner of small Maf TFs has indicated their involvement in regulating hypoxic response (Kannan et al., 2012). In a separate example, in addition to

Table 1.1.　　Small MAF proteins interact with various transcription factors. Adapted and modified from M.B. Kannan et al., 2012.

Protein	References
Leucine zipper proteins	
MAFF	Kataoka et al., 1995
MAFG	Kataoka et al., 1995
MAFK	Kataoka et al., 1995
BACH1	Oyake et al., 1996
BACH2	Oyake et al., 1996
NFE2 (P45)	Toki et al., 1997, Kataoka et al., 1995 and Marini et al., 2002
NFE2L1	Toki et al., 1997, Marini et al., 2002, Johnsen et al., 1996 and Marini et al., 1997
NFE2L2	Toki et al., 1997, Kataoka et al., 1995, Marini et al., 2002, Marini et al., 1997, Itoh et al., 1995 and Massrieh et al., 2006
NFE2L3	Kobayashi et al., 1999 and Chenais et al., 2005
FOS	Kataoka et al., 1995
FOSB	Shimokawa et al., 2005
MIP	Ye et al., 2006
Other proteins	
PAX6	Kataoka et al., 2001
MHOX/PRX1/PHOX1/PMX1	Kataoka et al., 2001
HOX12	Kataoka et al., 2001

regulating its transcriptional activity, MafG is important in regulating the intracellular localization of the transcriptional regulator protein Nfe2l2 (W. Li et al., 2008) .

　　　　Considering the important functions that small MAF TFs have in various cellular processes, its structural similarity to c-Maf TF – which has previously been associated with congenital cataract, and *iSyTE's* prediction that MafG is a highly lens-enriched

transcription factor, I hypothesized that small Maf proteins MafG (and potentially other members) have an important role in transcriptional control of gene expression in the lens. The specific aims of my Master's thesis were to test this hypothesis by using previously generated *MafG:MafK* compound mutant mice to perform a detailed phenotypic and molecular characterization of their lens.

Chapter 2

MATERIALS AND METHODS

2.1 Animals

All animals in this study were bred and housed at the University of Delaware Animal Facility (Newark, DE) in accordance with the Association of Research in Vision and Ophthalmology (ARVO) statement for the use of animals in ophthalmic and vision research. The University of Delaware Institutional Animal Care and Use Committee (IACUC) approves all animal protocols (approval number: 1226, Appendix). Small Maf germline compound mutants *MafG+/-:MafK+/-* generated by intercrossing *MafG+/-* and *MafK-/-* mutant mice (129/CD1 mixed hybrid background) (Shavit et al., 1998).

These germline knockout mice were generated by deleting the entire coding sequence and replacing them with selectable markers. For *MafG*, the targeting vector consisted for loxP sites surrounding the MC1neo/MC1HSVtk cassette, and for MafK, the loxP sites surrounding the phosphoglycerate kinase (PGK)-neo cassette. The lacZ gene was inserted immediately 5' to these markers and it replaced the endogenous translation initiation sites that were present in exon two of both *MafG* and *MafK*. For the *MafG* cassette, Diphtheria toxin was used as the negative selection marker, while thymidine kinase were used for negative selection in the *MafK* targeting cassette. The LoxP-flanked PGK-neo/TK or PGK-neo cassettes in all targeted alleles were removed by mating with *Ayu1-Cre* mice. *MafG:MafK* compound mutants were generated by Dr.

Onodera and colleagues by intercrossing *MafG+/-* with *MafK-/-* mutant mice (129/CD1 mixed hybrid background) to generate *MafG+/-:MafK+/-* compound mutant mice (Onodera et al., 2000).

For my research, these *MafG+/-:MafK+/-* mice were obtained from Dr. Hozumi Motohashi (Tohoku University, Japan) and housed in the animal facility at the University of Delaware. Mice were housed in a 14 h light to 10 h dark cycle. For timed pregnancies, crosses were set up in the evening and the females were tested for the presence of a vaginal plug in the morning of the following day. Vaginal plug discovery was designated embryonic day E0.5. The compound heterozygote mice (*MafG+/-:MafK+/-*) were cross-bred to generate various combinations of compound mutant progeny. In addition to wild type (*MafG+/+:MafK+/+*) controls, all combinations of *MafG:MafK* compound mouse mutants were examined, including the following genotypes: *MafG+/+:MafK+/-*, *MafG+/-:MafK+/+*, *MafG+/-:MafK+/-*, *MafG+/+:MafK-/-*, *MafG-/-:MafK+/+*, *MafG+/-:MafK-/-*, *MafG-/-:MafK+/-*, and *MafG-/-:MafK-/-*. Compound mutants *MafG-/-:MafK+/-*, which appeared to be smaller in size and developed hind-limb paralysis evident at the time of weaning, were placed in separate cages and provided with supplemental food gels.

Mice between the ages of 2-7 months were physically evaluated for the presence of lens defects and cataracts, euthanized, and processed as required. Mice older than 4 weeks were sacrificed by carbon-dioxide inhalation and cervical dislocation using a standard protocol. Younger mice collected at embryonic (E10.5-E17.5) or early post-natal (P0-P2) stages were sacrificed by decapitation.

2.2 DNA Isolation for Genotyping

Genomic DNA was extracted from mouse tails of adult *MafG:MafK* compound mutants using the Puregene® Genomic DNA Purification Kit (Gentra Systems, catalog no. 158622, Minneapolis, MN) as per manufacturer's instructions. Mice were genotyped for both *MafG* and *MafK* (T100 Thermal Cycler, Bio-rad, 186-1096EDU, Hercules, CA) and DNA concentrations were quantified using the NanoDrop ND-1000 UV-Vis Spectrophotometer (Nanodrop Technologies; Software V3.8.1). Samples were stored at room temperature until use.

PCR reactions for *MafG* were set up using the following recipe per reaction: 19.87 µl nuclease free water (Corning Cell Gro, Fisher Scientific), 2.5 µl 10X CoralLoad PCR buffer, 0.5 µl dNTPs (10 µM), 0.5 µl forward primer (25 µM), 0.5 µl reverse primer (25 µM), 0.125 µl Taq polymerase (5 units/µl) (Qiagen), and 1 µl of isolated DNA (approximately 100 ng) to a 0.2 mL microcentrifuge tube. Multiplex PCR for *MafK* genotyping was performed using the following recipe per reaction: 15.75 µl nuclease free water (IDT, Coralville, IA), 5 µl 10X CoralLoad PCR buffer, 1 µl dNTPs (10 µM), 1 µl forward primer (25 µM), 0.5 µl reverse primer (25 µM), 0.5 µl mutant primer (25 µM), 0.125 µl Taq polymerase (5 units/µl), and 1 µl of isolated DNA (approximately 100 ng) to a 0.2 mL microcentrifuge tube. The sequences of primers used for this analysis are provided in Table 2.1. *MafG* and *MafK* PCR reactions were performed with 40 cycles of 94ºC for 30 seconds, 60ºC for 20 seconds, 72ºC for 75 seconds, with a final extension at 72ºC for 5 minutes. Gel electrophoresis was performed on 1.2% agarose gel using 1x TBE buffer with ethidium bromide (Thermo Fisher Scientific, Waltham,

Massachusetts). A 100 bp ladder was used to determine the molecular weight of PCR

products (ThermoScientific Fermentas GeneRuler, Fisher Scientific). The amplicon

sizes of the expected wild-type (WT) and mutant alleles for *MafG* and *MafK* are as

follows: *MafG* WT: 417 bp, *MafG* Mut: 870 bp, *MafK* WT: 252 bp, *MafK* Mut: 579 bp.

MafG:MafK compound mutants were genotyped for a lens-specific member of the

intermediate beaded-filament structural protein 2 (*Bfsp2*/*CP49*) since *CP49* mutations

in 129 strain mice have been previously reported to cause loss of optical properties

(Sandilands et al., 2004). The primer sequences used for PCR analysis are listed in table

2.1.

Table 2.1.   Primers for PCR analysis of *MafG:MafK* compound mutant mice. *MafG*
and *MafK* primer sequences were obtained from Onodera et al., 2000. CP49 primer
sequences were obtained from Sandilands et al., 2003.

Allele	Sequence
MafG	MafG36: 5'-GCATGACTCGCCAGGAACAG-3' MafG433: 5'-CCCAAGCCCAGCCTCTCTAC-3'
MafK	MafKEx2.1: 5'-CCTACCGTTTCTGTCTTTCCAG-3' MafKln346: 5'-AATTCCTGAGGACAAAGCTGAC-3'
LacZ	LacZ4: 5'-CCTGTAGCCAGCTTTCATCAAC-3'
CP49	f: 5′-AGT GCT TAC AGA GGC CAG AAG AAG G-3′ d′: 5′-CCT CTG ACA AAG TCT TGA GCT CTC-3′ c: 5′-TGG GGT TGG GCT AGA AAT CTC AGA-3′ e′: 5′-AGC CCC TAC GAC CTG ATTTTT GAG-3′

2.3 RNA Isolation and cDNA Preparation

Total RNA from *MafG+/-:MafK+/-* control and *MafG-/-:MafK+/-* compound mutant adult (age 2 month) lenses was extracted using the RNeasy Mini Kit (Qiagen, catalog no. 74106). Dissected lens tissue was flash frozen in a 1.5 ml eppendorf and stored at -80ºC until beginning of RNA isolation. For RNA isolation, 600 µl of RLT lysis buffer provided by manufacturer was added to the sample. The lens tissue was disrupted by repeated pipetting in lysis buffer and 600 µl of the lysate was pipetted to a Qiagen QIAshredder homogenizer, and centrifuged for 3 minutes at full speed (14,000 rpm) to fully homogenize the sample. The column was discarded, and 600 µl of 70% molecular grade ethanol was added to the lysate in the 2 ml collection tube. The lysate and ethanol were mixed by gently pipetting. A white precipitate was observed consisting of nucleic acids and proteins. 600 µl of the sample along with the precipitate was pipetted to a Qiagen RNeasy Mini spin column and centrifuged for 30 seconds at 14,000 rpm, and the flow through was discarded, and this was repeated twice. 350 µl of buffer RWI (Qiagen) was used to wash the membrane-bound RNA by adding to the RNeasy spin column and centrifuged at 14,000 rpm for 30 seconds, and the flow through was discarded.

The RNase-free DNase Set (Qiagen, catalog no. 79254) was used to prepare a mastermix (buffer RDD, DNase I stock solution) in a 1.5 ml eppendorf, and 80 µl of DNase I incubation mix was added directly to the RNeasy spin column membrane and incubated at RT for 15 minutes. 350µl of buffer RW1 was added to the spin column and centrifuged at 14,000 rpm for 30 seconds, and 500 µl buffer RPE was added to the

RNeasy spin column, spun for 30 seconds, and the flow through was discarded both times. This step was repeated again. The RNeasy spin column was placed in a new 1.5 ml eppendorf and 30 μl of RNase-free water was added to the column membrane. The samples were centrifuged at 14,000 rpm for 1 minute to elute the RNA, which was collected and stored at -80ºC after determining the RNA concentration by using Nanodrop (Nanodrop Technologies; Software V3.8.1)

The total RNA isolated was used to make cDNA using an iScript cDNA synthesis kit (Bio-Rad). RNA was diluted to 0.5 μg/ul, and used to prepare cDNA by adding RNase/DNase free water, iScript Pre-mix (5x), and iScript Enzyme (reverse transcriptase) in a PCR tube. The thermo cycler settings are as follows: 5 minutes at 25ºC, 30 minutes at 42ºC, 5 minutes at 85ºC, and stored at 4ºC until needed. Regular PCR was performed by preparing each reaction as follows: 20.375 μl water, 2.5 μl coral red buffer (10x), 0.5 μl dNTP (10 μM), 0.5 μl forward primer (25 μM), 0.5 μl reverse primer (25 μM), 0.5 μl template cDNA, and 0.125 μl taq polymerase (5 units/μl) (Qiagen). The thermal cycler was set to the following conditions: 2 minutes at 94ºC, repeated 40 times- 15 seconds at 94ºC, 30 seconds at 57ºC, and 30 seconds at 72ºC. This was followed by holding at 72ºC for 7 minutes and hold at 4ºC. The resulting PCR products were run on 1.2% agarose gel and imaged.

2.4 Immunostaining

Embryonic head tissues were collected, fixed in 4% paraformaldehyde (PFA) on ice for 30 min, then treated with 30% sucrose overnight, and were embedded in optimum sectioning temperature media (OCT, Tissue Tek, Torrence CA). Frozen sections of

16µm thickness were obtained (Leica CM3050 cryostat, Leica Microsystems, Buffalo Grove, IL, USA) and blocking was performed with 1% BSA diluted in 1x phosphate buffered saline (PBS) (Abcam). Slides were washed three times in PBS, and incubated with commercially available MafG MaxPab rabbit polyclonal antibody (Santa Cruz, SC-133770, 1:100) overnight at 4ºC. After 3x washes with 1x PBS (R.T., 5 min each wash), slides were incubated for 2.5 hr at room temperature in dark with a 1:200 dilution of chicken anti-rabbit secondary antibody conjugated to Alexa 594 fluorophore (Invitrogen). Slides were washed again 3X in 1x PBS (R.T., 5 min each wash).

Slides were mounted with VECTASHIELD mounting medium with DAPI (Vector Laboratories, Inc., Burlingame, CA, USA) and covered with cover slips. Confocal microscopy (Zeiss 780 LSM or Zeiss 510 LSM) was performed to obtain all images. Optimal adjustment of brightness/contract was performed in Adobe Photoshop and applied consistently for all images. All expression patterns among the slides were compared in data generated from the same staining experiment on the same day and imaged on the same day under consistent conditions and imaging settings.

2.5   RNA *in situ* hybridization

Mouse embryonic head tissues at E12.5 were dissected and fixed overnight in 4% PFA, dehydrated, and embedded in Optimum Cutting Temperature Media (OCT, Tissue Tek, Torrence, California). Coronal sections of 16µm thickness were obtained using standard procedures on the Leica CM3050 cryostat (Leica Microsystems, Buffalo Grove, IL, USA), and stored at -80°C until needed. To generate *MafG* RNA probes,

28

forward and reverse primers against *MafG* cDNA were designed and SP6 and T7 sequences were added to the 5' of forward and reverse primers as described previously (Lachke et al. 2012a). *MafG* cDNA was amplified by PCR, and the products were run on 1% agarose gel. Purification of PCR was performed (QIAquick Spin Kit), and DNA quality was analyzed by gel electrophoresis and visualized using a transilluminator. The DNA fragment was excised with a razor blade under the transilluminator carefully and placed in nuclease-free water in 1.5 mL eppendorf. The gel fragment was weighed and 3 volumes of buffer QG (Qiagen QIAqick Spin Kit reagent) was added per 1 volume of gel. The sample was incubated at 50°C for 10 minutes and vortexed for 2 minutes until dissolved. One gel volume of isopropanol was added to the sample and mixed, and it was transferred to the spin column and centrifuged for 1 minute at 13,000 rpm. The flow through was discarded and 750 µl of buffer PE was added to the spin column and centrifuged for 1 minute at 13,000 rpm. The column was placed in a 1.5 mL Eppendorf and centrifuged again for 1 minute to remove any residual buffer PE. The column was placed in a new eppendorf and DNA was eluted with deinonized RNase-free water by centrifugation for 1 minute at 13,000 rpm. DNA quality was tested by gel electrophoresis.

The PCR purified DNA was used to synthesize RNA probes by *in vitro* transcription. The sense probe was generated using the MAXIscript SP6 kit (Invitrogen, catalog no. AM1308), and the anti-sense probe was generated using MAXIscript T7 kit (Invitrogen, catalog no. AM1312). The transcription reaction was validated using gel electrophoresis.

Slides with frozen sections were air dried for 15 to 20 minutes at room temperature (RT), and were placed in Tissue-tek slide holder. The holder was placed in a staining dish containing 4% PFA/PBS on shaker for 10 minutes at RT. The slides were rinsed with PBT buffer (1x PBS, 0.1% Tween-20) quickly, and washed twice with fresh PBT for 5 minutes each at RT. The slides were washed in 1µg/ml solution of Proteinase K in 1x PBS, incubated and rotated for 10 minute at RT to inactivate RNases and DNases and digest the tissue. The slides were placed in PBT again for 5 minutes (two rounds) on the rotator at RT. The slides were placed in 4% PFA/PBS and rotated for 5 minutes at RT. PBT washes were repeated again four times, followed by acetylation of the sections in 0.1M triethanolamine/0.25% acetic anhydride for 15 minutes at RT. The slides were washed twice for 5 minutes with PBT at RT by shaking gently, and rinsed with nuclease free water.

One microliter of RNA probe was added per 100 µl of pre-warmed hybridization solution (10mM Tris pH7.5, 600mM NaCl, 1mM EDTA, 0.35% SDS, 10% Dextran Sulfate (American Bioanalytical 50% solution), 1X Denhardt's, 200 (American Bioanalytical 50% solution), 1X Denhardt's, 200µg/ml yeast tRNA (Gibco), 50% formamide) and kept at 57ºC for 10 minutes to decrease viscosity. 100 µl of RNA probe was added to each slide and hybri-slips (Sigma, #H0784) were applied. Slides were stored in a container with paper towels soaked with 5X saline sodium citrate buffer (SSC) (American Bioanalytical, #AB13156) /50% formamide, and incubated in hybridization oven at 57ºC overnight. Slides were rinsed in 5x SSC solution and placed in staining dish containing pre-warmed 1x SSC/50% formamide in 65ºC for 30 minutes.

Slides were washed with TNE (10mM Tris pH7.5, 500 mM NaCl, 1 mM EDTA) for 10 minutes in a 37 ºC water bath, and washed with TNE solution containing RNase A (20µg/ml, Roche) for 30 minutes at 37ºC. Slides were washed again with TNE for 10 minutes at 37ºC, followed by washing with 2x SSC and 0.2x SSC for 20 minutes each at 65ºC twice. Slides were washed with MABT (100 mM Maleic acid, 150 mM NaCl, 0.1% Tween-20, pH 7.5) for 5 minutes at RT twice. Slides were placed on a flat surface and 20% heat inactivated sheep serum (HISS) diluted in MABT was added to each slide for 1 hour at RT. One ml of anti-DIG antibody (Roche, catalog no. 50-720-3750) at 1:2500 dilution in 5% HISS/MABT was added to each slide and incubated overnight at 4ºC.

The following day, slides were rinsed in staining dish with fresh MABT repeated four times, followed by washing with NTM (100 mM NaCl, 100mM Tris pH 9.5, 50mM $MgCl_2$) for 10 minutes on shaker. Antibody substrate (BCIP/NBT tablet, Gibco) was reconstituted, and 1 ml was added to each slide. Samples were incubated in the dark for 3 hours at RT, and rinsed with NTM. The slides were washed with 1x PBS on shaker for 5 minutes twice, and fixed in 4% PFA/PBS for 30 minutes while shaking. The slides were washed again in 1x PBS for 5 minutes and rinsed with nuclease-free water. Slides were mounted in gelvatol mounting medium and allowed to dry. Imaging was performed on the Zeiss Axiophot light microscope (Car Zeiss Microscopy, Thornwood, NY).

2.6   Western blotting

Lenses were harvested from heterozygous *MafG+/-:MafK+/-* mutant mice at 2 months of age and tissue was homogenized in cold lysis buffer (50 mM Tris HCl pH 8.8, 150 mM NaCl, 0.1% SDS, 1% NP-40 (Tergitol), 0.8% Na-deoxycholate, 1x protease inhibitor and phosphatase inhibitor (Roche cat no. 04693124001). The tissue lysate was centrifuged at 14,000 rpm for 30 minutes at 4°C, and the supernatant was saved. Protein concentration in the lysate was quantified using the NanoDrop ND-1000 UV-Vis Spectrophotometer (Nanodrop Technologies; Software V3.8.1).

The purified lysate with the known protein concentration was diluted to 100 ug with water, and then was denatured by adding 1x Lamelli buffer and boiling for five minutes at 95°C. A 7% resolving gel (1.5 M Tris pH 8.8, 10% APS, 10% SDS, 40% Acrylamide/Bis, TEMED) with a 4% stacking gel (0.5 M Tris pH 6.8, 10% APS, 10% SDS, 40% Acrylamide/Bis, TEMED) was prepared. The western blot gel tank was assembled with the gel and 1x tris-glycine electrophoresis running buffer (25mM Tris, 250 nm glycine pH 8.3, 0.1% SDS), and 25 μl of protein sample (100μg) and 10 μl of marker were loaded in the wells, and the gel was run at 90V for 90 minutes at 4°C. The PVDF membrane (Fisher Scientific, catalog #PI88518) was soaked in 100% methanol for five minutes and equilibrated. Transfer cassette was set up, and transfer was done onto PVDF membrane overnight (120 amps at 4°C) in transfer buffer (25 mM Tris, 250 mM glycine pH 8.3, and 0.1% SDS). The membrane was equilibrated with TBST for 5 minutes, and blocked for three hours in blocking solution (1x TBS, 0.1% Tween 20, 5% non-fat dry milk) at room temperature. Anti-rabbit MafG polyclonal primary antibody

(1:100 dilution in blocking buffer) (SC-133770) was added in blocking solution, and the blot was incubated in solution overnight at 4°C.

Three 15 minutes washes with TBST buffer (0.05 mM at Tris pH 7.5, 0.18 M NaCl, 0.05% Tween-20) were performed, and the blot was incubated for 1 hour at room temperature with secondary antibody (1:1000 dilution in blocking buffer) (anti-rabbit IG catalog no. 7074, Cell Signaling Technology, Danvers, Massachusetts). The blot was washed again three times in TBST, followed by addition of chemilumicescent substrate (Cell signaling, 1x LumiGLO and 1x Peroxide solution) for two minutes. Imaging was performed using a FluorChemTM Q Imaging System (Protein Simple, Santa Clara, California). For loading control, the blot was stripped with stripping buffer (ThermoScientific, Waltham, Massachusetts), and blocked for two hours at room temperature. For housekeeping protein loading control, rabbit polyclonal beta-actin primary antibody (Abcam, Catalog no. 8227) was used for hybridization overnight at 4°C, washed three times with TBST for 15 minutes, and the blot was incubated for 1 hour at room temperature with secondary antibody. Imaging was performed as described above following addition of chemilumicescent substrates.

2.7   Morphological Analysis by Light Microscopy and Histology

Eyes were dissected from mutant and control mice and carefully cleaned in 1x PBS solution under a dissecting microscope. Eyes were photographed under light field and dark field optics. Lens was extracted, cleaned, placed in pre-warmed media 199, 1x (with Earle's salts and L-glutamine) (Cellgro, Mediatech, Inc., Manassas, VA) and

imaged on a 200-mesh electron microscopy grid to observe the refractive property of the tissue. For histological analysis using Hematoxylin and Eosin (H&E) staining, whole eyes (postnatal mice) or heads (embryos) were collected from WT and mutant mice at appropriate stages. Samples were fixed in 4% paraformaldehyde overnight, rinsed in 1x PBS, and transferred to 2 ml of 70% ethanol. Paraffin-embedding was performed at the Comparative Pathology lab at the College of Agriculture and Natural Resources, University of Delaware. Serial paraffin sections (6 μm thickness) were stained with hematoxylin and eosin (H&E) visualized with a Zeiss Axiophot light microscope (Carl Zeiss Microscopy, Thornwood, NY).

2.8 Scanning Electron Microscopy of Lens

Scanning electron microscopy was performed on 2-7 month old *MafG+/+:MafK+/+* and *MafG+/-:MafK+/-* mouse lenses (used as controls) and *MafG-/-:MafK+/-*, *MafG+/-:MafK-/-* compound mutant lenses. Briefly, eyes were enucleated from mice, lenses were dissected, briefly cleaned and transferred to a fixative (0.08M sodium cacodylate, 1.25% glutaraldehyde, 1% paraformaldehyde) (Electron Microscopy Sciences (EMS), Hatfield, PA) and incubated at room temperature for 48 hours. After fixation, lenses were washed in 1x PBS and dehydrated through an alcohol dilution series (25%, 50%, 70%) as described previously (Duncan et al., 2000). After overnight incubation in 100% ethanol, lenses were washed in two additional 2.5 h rounds of washes in ethanol. Lenses were dried in 1:2 hexamethyldisilazane (EMS, Hatfield, PA) (HMDS)/ethanol for 1 h followed by 2:1 ratio of HMDS to ethanol for 1

h, and 100% HMDS for 30 min twice. Lenses were transferred on to filter paper placed in a 6-well plate container and placed in a vacuum desiccator overnight. Lenses were mounted on aluminum stubs covered with carbon adhesive tabs (EMS, Hatfield, PA) and painted with silver conductive paint (EMS, Hatfield, PA). Lenses were dried and prepared for sputter coating with gold/palladium and imaged using the Hitachi S-4700 Field-Emission Scanning Electron Microscope (FE-SEM)). At least three biological replicates were used for SEM analysis for control and compound mutant lenses.

2.9 cDNA Preparation and Real Time Quantitative Reverse Transcriptase-Polymerase Chain Reaction

RNA from *MafG+/-:MafK+/-* control and *MafG-/-:MafK+/-* compound mutants extracted using the RNeasy Mini Kit (Qiagen Ltd., Crawley, UK) was used to synthesize cDNA using an iScript cDNA synthesis kit (Bio-Rad) followed by conventional PCR at varying cycles for semi-quantitative RT-PCR. Quantitative Reverse-Transcription PCR (qRT-PCR) was performed using RealMasterMix Fast Probe Kit (5 PRIME, Gaithersburg, MD) on the ABI 7500 Fast Real-Time PCR System and Software v2.0.3 (Applied Biosystems: Carlsbad, CA).

All samples were prepared in a 96-well reaction plate with three biological replicates (independent samples from those used for microarray analysis) and technical triplicates. The master-mix was prepared as follows: 8.5 µl molecular grade water, 10 µl 5PRIME RealMasterMix Fast SYBR Low ROX, 0.5 µl of forward and reverse primers each, and 0.5 µl of cDNA (25 µM) per sample. The following cycling

conditions were used for all experiments: 40 cycles of 30 seconds at 95ºC, 15 seconds at 58ºC and 15 seconds at 68ºC. A select list of differentially regulated genes, identified by microarray analysis, was used for validation and is provided in supplemental Table 1. Mean fold change (F.C.) was calculated using log (base 10) transformed data in a nested ANOVA by determining the mean and standard deviations. These values were then back transformed to obtain the final F.C. values.

2.10 Microarray Analysis

Total RNA was extracted from *MafG+/-:MafK+/-* and *MafG-/-:MafK+/-* compound mouse mutant lenses at 2 months of age for gene expression profiling by microarrays. For microarray analysis of wild type mouse embryonic lens for expression of *MafG*, *MafK*, and *MafF*, micro-dissected mouse embryonic/post-natal lenses and whole embryonic tissue minus the eye portion at various stages (from stages E10.5, E11.5 and E12.5) were used as described (data analysis used for *iSyTE*, described in detail in Lachke et al., 2012a, Kakrana et al. manuscript in preparation). RNeasy Mini Kit (Qiagen Ltd., Crawley, UK) was used to extract RNA from embryonic and post-natal lens samples as described in section 2.4, and shipped on dry ice to the Molecular Genetics Core Facility at the Children's Hospital in Boston. RNA quantity and quality were assessed by nanodrop ND-1000 UV-Vis Spectrophotometer (Nanodrop Technologies; Software V3.8.1, Wilmington, DE) and bioanalyzer. Standard Affymetric procedures were used to make cDNA and biotin labeled cRNA using *in vitro* transcription, and qualitative and quantitative quality control were performed on the

36

labeled cDNA. For microarray analysis of the lenses, Expression BeadChip (MouseWG-6 v2.0, Illumina, San Diego, CA) array platform was used for hybridization at the Molecular Genetics Core Facility at Children's Hospital in Boston. cRNA was hybridized to a mouse WG-6 v2.0 Beadchip and scanned by the Illumina BeadArray reader.

Analysis of Microarray datasets was performed under 'R' statistical environment (http://www.r-project.org/) through Bioconductor suite (www.bioconductor.org). The raw files were imported using lumi package and background correction was performed followed by Rank Invariant based normalization. Present-absent calls were generated using lumi inbuilt function and probe-sets present in more than two samples were retained for analysis. The probe-level analysis was converted to gene-level by selecting the probe-set (out of probe-sets for a single gene) that has highest expression across samples to represent a gene. Package limma (ref: http://link.springer.com/chapter/10.1007%2F0-387-29362-20 0_23) was used to identify differentially expressed genes from the normalized expression estimates. Linear model was fitted to log-expression values using lmfit function of limma and a moderated t-test was performed. To reduce false positives, *p*-values were further corrected using Benjamini Hochberg FDR (Benjamini et al. 2001) correction algorithm. To determine differentially regulated genes in *MafG* in *MafG-/-:MafK+/-* mutant lens, a FC cutoff of 1.5 for both up-regulation and down-regulation was chosen in order to avoid missing potentially important biological signals. The differentially regulated

genes (DRGs) identified in *MafG* in *MafG-/-:MafK+/-* mutant lens using microarray analyses are described in Chapter 3.

To examine the functions of the differentially expressed genes (p-value < 0.05, 1.5 F.C. cut-off), the functional annotation tool provided by the Database for Annotation, Visualization, and Integrated Discovery (DAVID), version 6.7 (Huang et al., 2009), was utilized. The two lists of predicted DRGs (up-regulated and down-regulated genes) were separately submitted to DAVID. The DRG targets were annotated by the Kyoto Encyclopedia of Genes and Genomes (KEGG) pathway analysis (http://david.abcc.ncifcrf.gov/). This analysis was performed using the high classification stringency criteria with the similarity threshold of 0.50 and the enrichment threshold of 1. Each functional category considered significant included at least three genes per annotation term, and redundant pathways were manually excluded.

Since the DAVID functional annotation analysis revealed a broad range of categories that the DRGs were classified under (Figure 3.16 and Figure 3.18), I used an integrated approach to further elucidate the role of MafG and MafK in the lens, and to gain insight into small Maf-mediated gene regulation. *iSyTE* was used to analyze the expression of DRGs to identify genes that exhibited lens-expression. Both up-regulated and down-regulated candidate genes were subjected to this analysis.

Previously, human small Mafs have been identified to form heterodimers with CNC (cap and collar) family transcription factors and recognize the NRF2 (nuclear factor erythroid-derived 2-like; NFE2L2) motif (Kataoka, 2007; W. Li et al., 2008; Toki et al., 1997). I utilized *iSyTE* to observe enrichment of *NRF2* in the lens during

developmental time-points. A previous study performed ChIP-seq (chromatin immunoprecipitation) experiments with human lymphoblastoid cells (Chorley et al., 2012) to identify the direct targets of Nrf2. All the genes that consisted of an antioxidant response element (ARE) motif that Nrf2 directly binds to were compared with the list of DRGs from microarray analysis of *MafG-/-:MafK+/-* mutant lenses (present data). *iSyTE* was used to evaluate the expression of the filtered genes that consisted of ARE motifs in the lens. Genes that were lens enriched or lens expressed, as well as genes that had biological relevance based on literature were further analyzed to gain insights into their role in lens biology.

Chapter 3

FUNCTION OF SMALL MAF PROTEINS MAFG AND MAFK IN

MAINTENCE OF LENS TRANSPARENCY

3.1   MafG and MafK are Expressed in the Mouse Lens

As described in the Introduction section, *iSyTE* predicted MafG to be enriched in

the lens (Figure 1.4). In order to study the expression of MafG and MafK in the mouse

embryonic lens as it transitions from the placode invagination stage through the adult

stage, I first performed an analysis of previously published or generated lens microarray

gene expression profiles. The expression analysis indicates that while expression of

MafK and *MafF* is low or absent in lens tissue, respectively, *MafG* is highly expressed

and enriched in the lens in these stages, especially in embryonic stages (Figure 3.1).

Interestingly, although *MafG* expression remains lens-enriched in postnatal lens

development, it exhibits progressive reduction in overall expression in the lens. *MafK*

expression in embryonic as well as post-natal stages remains at largely unchanged low

levels (Figure 3.1). In contrast, *MafF* expression is not significantly expressed in the

lens at any embryonic or post-natal stages tested. This suggests that in MafG may be

the major small Maf protein in the embryonic lens contributing primarily to the total

small Maf protein activity in the lens during these stages. However, in the post-natal

lens, contribution of *MafG* to total small Maf protein activity is comparatively lowered

and therefore in post-natal stages, both MafG and MafK proteins may be equally

important. qPCR of *MafG*, *MafK* and *MafF* on wild type lens at post-natal stages supported this trend in small Maf expression in lens (Figure 3.2).
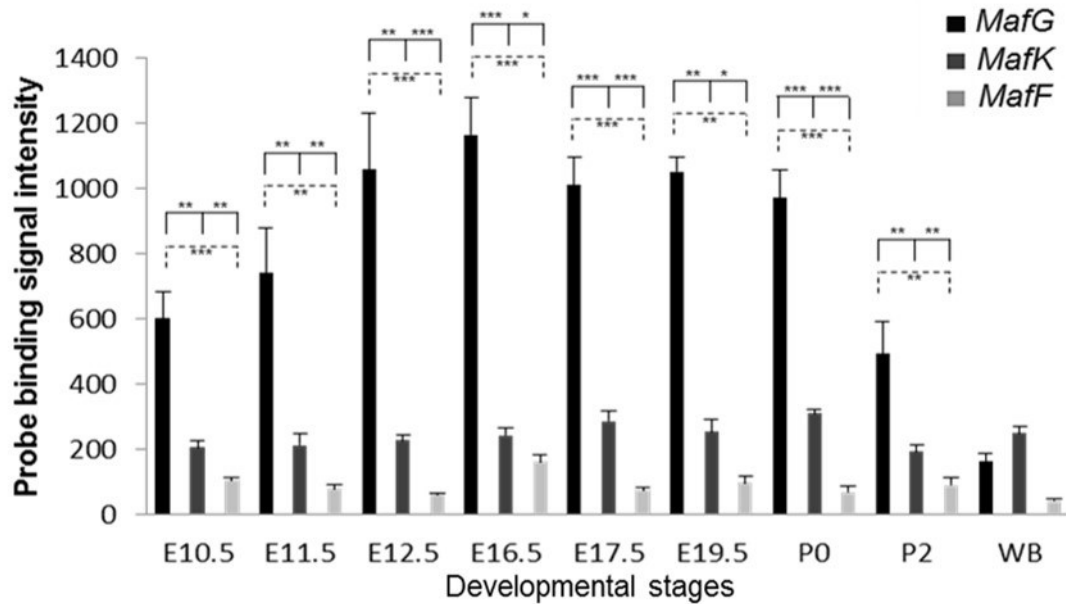
Figure 3.1. *MafG* is highly expressed and enriched in embryonic stages and *MafK* is expressed at similar levels in embryonic and post-natal stages in the lens. *MafG* expression is highly enriched in mouse lens development during embryonic stages E10.5-E19.5. *MafK* expression is lower compared to *MafG* but similar in both embryonic and post-natal stages. *MafF* exhibits low expression or is absent in the lens at all stages tested. * denotes $p<0.05$, ** denotes $p<0.005$, *** denotes $p<0.001$
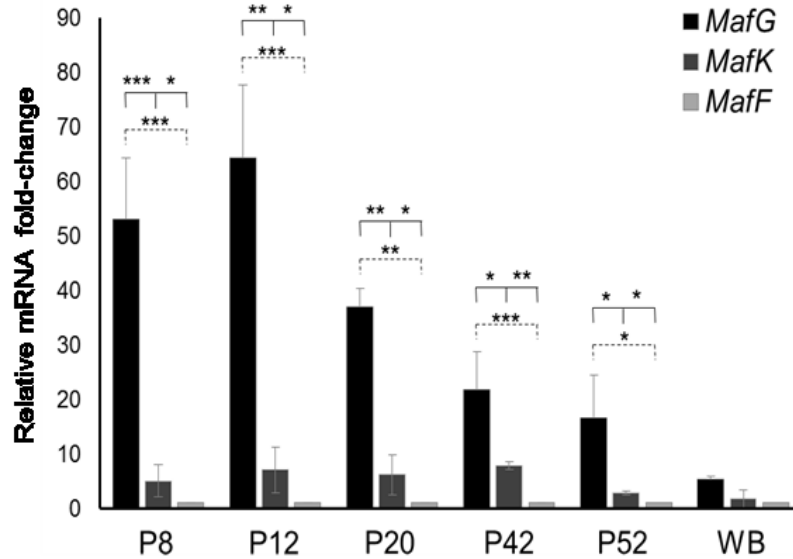
Figure 3.2. **While *MafF* is absent, *MafG* and *MafK* are both expressed at postnatal stages in the lens.** Quantitative real-time PCR was performed to confirm that both *MafG* and *MafK*, and not *MafF* are expressed in the lens at various post-natal stages (P8, P12, P20, P42, P52). * denotes $p<0.05$, ** denotes $p<0.01$, *** denotes $p<0.005$. Fold-change of *MafG* and *MafK* was normalized using *Actnb* and compared to *MafF* expression value set as 1. Expression analysis was also performed by normalizing fold-change using *Gapdh* and *Hprt* and was consistent with this result (data not shown). Each bar represents ±SD for experiments performed using biological replicates and technical triplicates. Statistical analysis was performed using nested-ANOVA test.

Next, the lens microarray datasets were analyzed to examine the expression of genes that encode small Maf-binding transcriptional regulators. *Nfe2l1*, *Nfe2l2,* and *Bach2* were specifically enriched in the embryonic lens, while *Nfe2l3*, *Nfe2* and *Bach1* exhibit low expression or are absent in the lens (Figure 3.7). Together with the above data, this suggested that initial efforts to functionally characterize small Mafs in the lens

should focus on *MafG* and *MafK* and the three small Maf binding proteins Nfe2l1, Nfe2l2, and Bach2. Importantly, expression analysis of mouse AEL or fiber cells at E12.5 indicated that all the above lens-enriched genes are also enriched in fiber cells [*MafG* (5.5-fold)*, Nfe2l1* (2.2-fold)*, Nfe2l2* (4.0-fold)*, Bach2* (1.3-fold), David Beebe, personal communication] - thus identifying a new set of TFs that potentially regulates fiber cell gene expression.
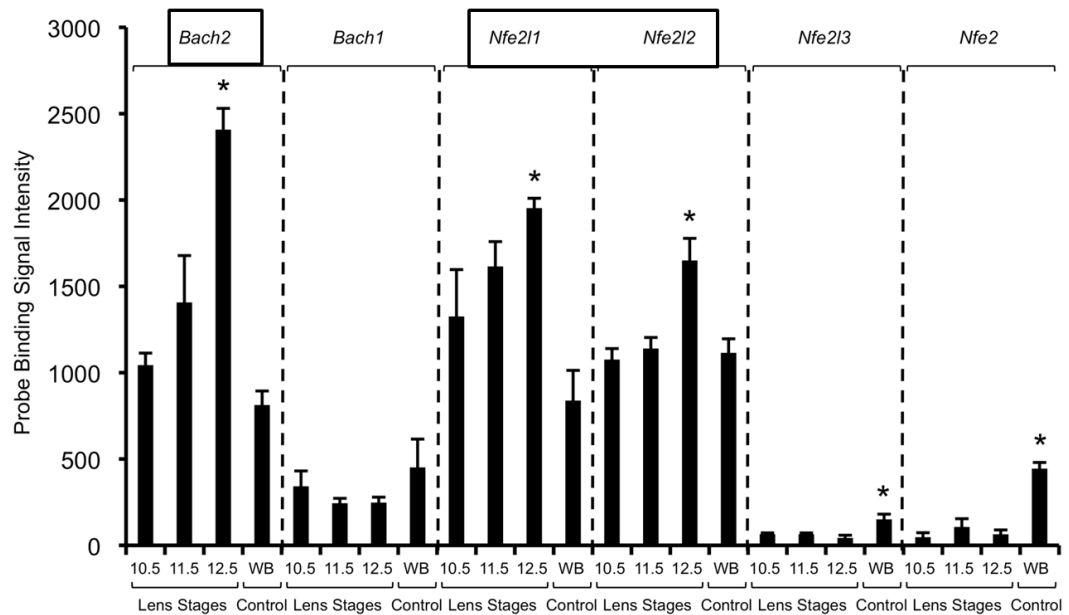
Figure 3.3. Expression of genes encoding small Maf binding proteins in the lens. Expression of small Maf binding partners was analyzed from microarray data at mouse embryonic developmental stages E10.5, 11.5, and E12.5, and compared to the expression in the whole body control (WB). Probe binding signal intensity ranged from 1000-2400 (arbitrary units). *Bach2, Nfe2l1,* and *Nfe2l2* are significantly enriched during mouse lens development compared to WB. Expression of *Bach1*, *Nfe2l3*, and *Nfe2* is either low or absent in the lens. In microarray analysis, genes with values below 200 are considered to have no expression or down-regulation. Asterisk denotes *p<0.002*.

Furthermore, RNA *in situ* hybridization confirmed that *MafG* mRNA is expressed in the lens at E12.5 and is enriched in lens fiber cells. Examinatoin of MafG protein expression in the lens was not feasible due to a lack of a MafG specific anitbody. Alternatively, immunostaining was performed with a small Maf antibody with a human MafG etitope, which confirmed expression of small Maf proteins in lens fiber cells (Figure 3.4). Western blotting showed that small Maf proteins (18kDa) are present in the lens tissue collected at 2 months of age.
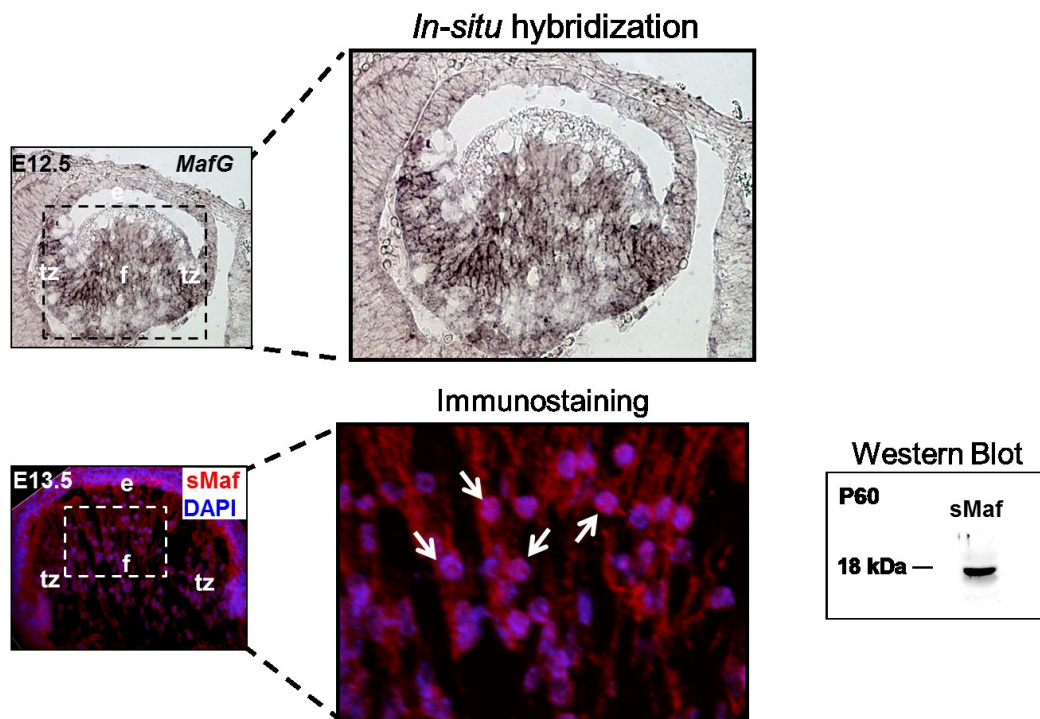
Figure 3.4. *MafG* **mRNA and small Maf proteins are expressed in the developing lens.** Expression of *MafG* mRNA was confirmed using RNA *in situ* hybridization. At E12.5, *MafG* mRNA is localized in the lens fiber cells. Immunostaining confirmed that small Maf proteins are expressed at the protein level in the lens. Western blotting shows the presence of 18kDa small Maf protein band in *MafG+/-:MafK+/-* lens tissue extracted from 2 month old animal.

3.2 Generation of *MafG* and *MafK* Mouse Mutants

In order to characterize the function of MafG and MafK in the lens, small Maf germline compound mutants *MafG+/-:MafK+/-* previously generated by intercrossing *MafG+/-* and *MafK-/-* mutant mice (129/CD1 mixed hybrid background) (Shavit et al., 1998, Onodera et al., 2000) were obtained from Dr. Hozumi Motohashi. Previous studies that initially generated germline knockout mouse models of *MafG* and *MafK* have shown that targeted disruption of *MafK* (*MafK-/-*) independently does not result in a particularly discernible phenotype (Kotkow & Orkin, 1996; Shavit et al., 1998), while *MafG* homozygous null mice exhibit mild thrombocytopenia (Shavit et al., 1998). Furthermore, *MafF* homozygous null mice appear to be normal. *MafG-/-:MafK+/-* compound mutant mice exhibit chronic posterior ataxia and also develop thrombocytopenia (Onodera et al., 2000). Also, deficiency of *MafG*, *MafK*, and *MafF* alone does not affect viability and fertility of mice. (Blank, 2008)

Since *MafG* and *MafK*, but not *MafF*, are expressed in the lens, I sought to generate *MafG* and *MafK* single and compound mutants. Generation of the original *MafG+/-* and *MafK-/-* germline mutants (Shavit et al., 1998) required to generate *MafG+/-:MafK+/-* compound heterozygous mutants (Onodera et al., 2000) is described in the methods section. *MafG+/-:MafK+/-* compound mutants were obtained from Dr. Hozumi Motohashi and used for this study. Genotypes of progeny of crosses between compound heterozygous *MafG+/-:MafK+/-* and compound *MafG+/-:MafK-/-* mouse mutants were determined by PCR (Figure 3.5). Various combinations of compound

MafG and *MafK* mouse mutants were generated as illustrated in the schematic (Figure 3.6).

(A)

Wild-type *MafG* locus:

chr11:120,629,771-120,629,837   chr11:120,630,190-120,630,209

417 bp

5'   3'

Exon 2   Exon 3

ATG

Wild-type *MafK* locus:

chr5:139,799,117-139,799,138   chr5:139,799,343-139,799,364

252 bp

5'   3'

Exon 2   Exon 3

ATG

Mutant *MafG* locus:

870 bp in *MafG*   3'

5'

LacZ   Exon 3

ATG

Mutant *MafK* locus:

579 bp in *MafK*   3'

5'

LacZ   Exon 3

ATG
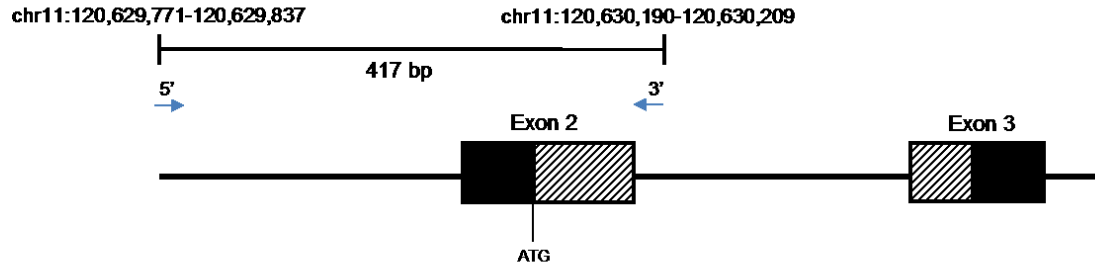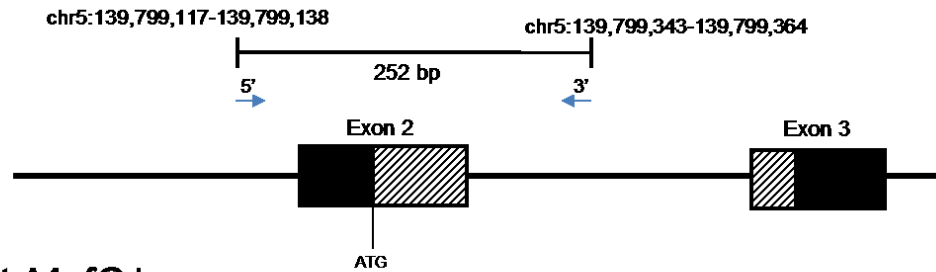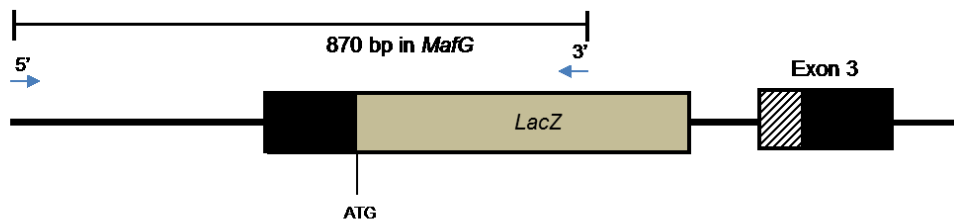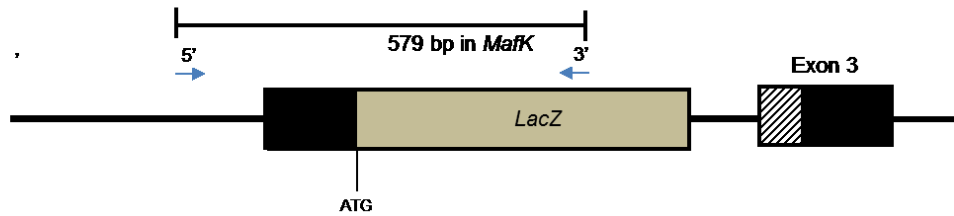
(B)
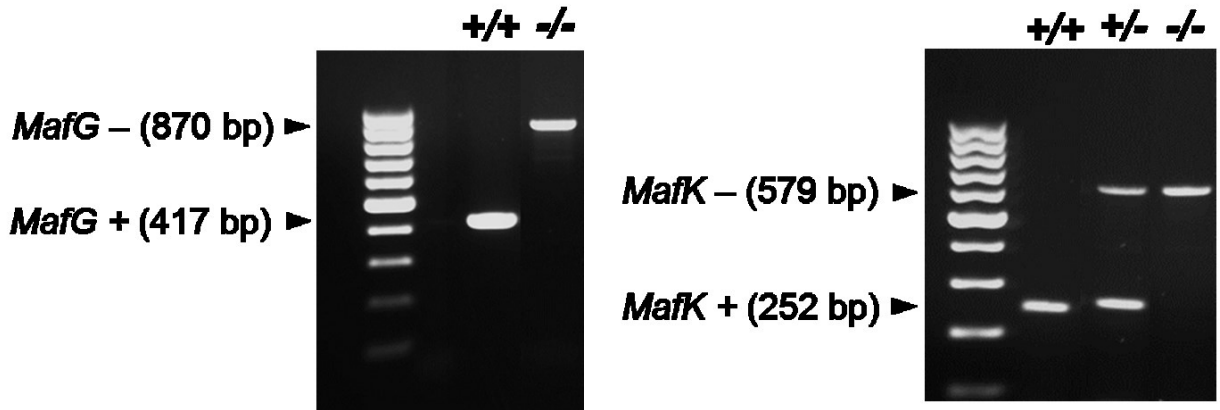
Figure 3.5. Structure and genotyping of *MafG* and *MafK* mutant alleles. (A) Wild-type *MafG* locus used to design primers spanned a 417 bp (base-pair) region and included coding Exon 2. The structure of *MafK* is similar to *MafG*. Primers designed for the wild-type *MafK* gene resulted in a 252 bp product. In order to knock-out *MafG* and *MafK*, the entire coding region of Exon 2 was deleted and replaced with *LacZ* for *MafG* and *MafK* respectively. The products size for *MafG* mutant region was 870 bp and 579 bp for *MafK*. (B) *MafG* and *MafK* mutant allele detection strategy was modified from that described in Onodera et al., 2000. Primers used in genotyping are provided in Table 1.1. *MafG* and *MafK* wild-type and mutants products were visualized on 1.2% agarose gels. Detailed description of the strategy is provided in materials and methods.
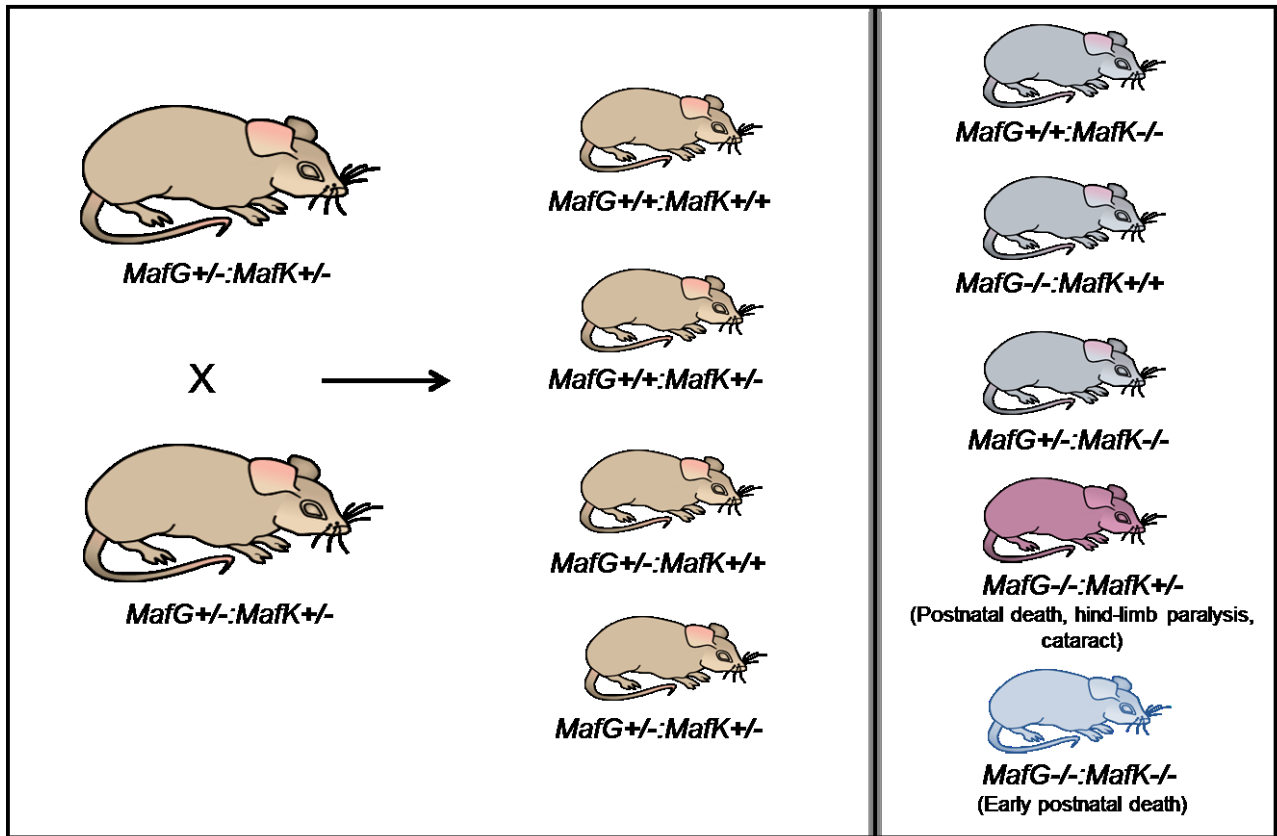
Figure 3.6. Breeding scheme for characterization of various combinations of MafG:MafK compound mouse mutants. Previously generated *MafG+/-:MafK+/-* compound heterozygous mutant mice were obtained and bred to derive various combinations of compound mutants as shown. Genotypes for mice depicted in brown were used as the control set, and genotypes depicted for mice in grey, red, and blue were characterized for potential lens defects and abnormalities.

Although *MafG+/+:MafK+/+*, *MafG+/-:MafK+/-*, *MafG+/+:MafK-/-*, *MafG-/-:MafK+/+*, and *MafG+/-:MafK-/-* were found to be present at the expected Mendelian ratio, *MafG-/-:MafK+/-* and *MafG-/-:MafK-/-* mutant mice were always obtained at less than expected Mendelian ratios. *MafG-/-:MafK+/-* compund mutant animals were viable and survived until adulthood, but developed hind-limb paralysis and ataxia within the first month after birth (Figure 3.7 A), which put them at a reproductive disadvantage. *MafG-/-:MafK-/-* double homozygous-null mutants were perinatal lethal (Figure 3.7 B). Physically they were significantly small in size compared to *MafG+/-:MafK+/-* compound control mice, and therefore appreared to have growth defects.

A

MafG+/-:MafK+/-   **MafG-/-:MafK+/-**

B
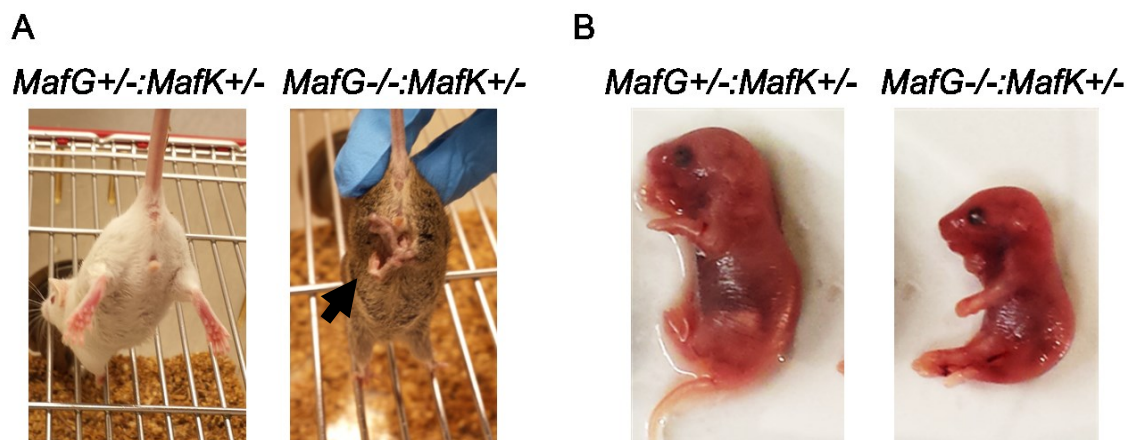
MafG+/-:MafK+/-   **MafG-/-:MafK+/-**

Figure 3.7. *MafG-/-:MafK+/-* **and** *MafG-/-:MafK-/-* **compound mouse mutants exhibit hind-limb paralysis and perinatal lethality, respectively.** (A) *MafG-/-:MafK+/-* compound mouse mutants exhibit hind limb paralysis/ataxia detected visually as early as 1 month of age compared to the *MafG+/-:MafK+/-* compound mouse mutants, which appear to be normal. (B) *MafG-/-:MafK-/-* compound mouse mutants appear to have growth retardation compared to *MafG+/-:MafK+/-* compound mouse mutants and die perinatally. Both compound mutant mice are obtained at significantly lower numbers than expected from Mendelian ratios.

Furthermore, mouse strain 129 has been previously reported to harbor a natural mutation in a lens specific beaded filament structural protein (*Bfsp2/CP49*) (Sandilands et al., 2004). This mutation carries a 6-kb deletion in *CP49*, and causes alterations in the lens optical quality and results in disruption of the lens cytoskeleton. Since the compound mutant mice are 129/CD-1 strains, PCR analysis was performed to confirm that lens defects observed in MafG-/-:MafK+/- mice was independent of mutations in *Bfsp2*. None of the mice tested (*MafG-/-:MafK+/-, MafG+/-:MafK+/-, MafG+/-:MafK-/-*) were homozygous null for *Bfsp2*. Mice that were heterozygoues *(Bfsp2+/-)* are not used for breeding, and the selection of breeding pairs used for generating compound mutant mice has been modified to only include mice that homozygous for wild-type *CP49* and lack the mutant allele (Figure 3.8 A).   *CP49* mRNA expression was analyzed in *MafG+/-:MafK+/-*   and *MafG-/-:MafK+/-* mice at 2 months of age from the microarray data, and there was no significant difference observed (Figure 3.8 B).
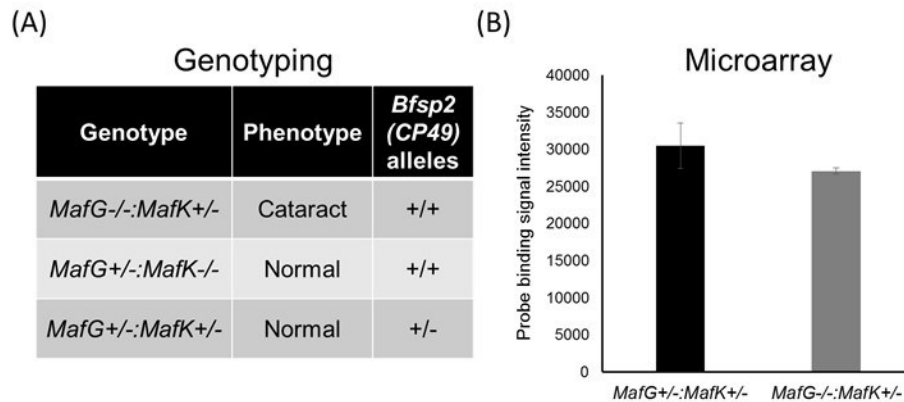
Figure 3.8. *CP49* **expression is unchanged in** *MafG:MafK* **compound mutant mice.** (A) Genotyping for *Bfsp2 (CP49)* was performed on *MafG-/-:MafK+/-* compound mutant mice and *MafG+/-:MafK-/-* and *MafG+/-:MafK+/-* control mice. None of these compound mutants were homozygous null for *Bfsp2*. (B) Expression of *Bfsp2 (CP49)*, a gene encoding lens specific beaded filament protein was compared between *MafG+/-:MafK+/-* and *MafG-/-:MafK+/-* compound mutant mice. Probe binding signal intensity of CP49 was unchanged in both compound mutants.

3.3 *MafG-/-:MafK+/-* Compound Mutants Exhibit Cataract.

To characterize the role of *MafG* and *MafK* in the lens, eyes from compound mouse mutants carrying different null mutant allele combinations of these genes were examined. A preliminary examination of eyes from 4 month old *MafG+/+:MafK+/+*, *MafG+/-:MafK+/-*, *MafG+/-:MafK-/-* and *MafG-/-:MafK+/+* mutant animals showed no obvious eye or lens defects (Figure 3.9). However, *MafG-/-:MafK+/-* compound mutants exhibited obvious haziness in the lens. Dark field imaging of *MafG+/+:MafK+/+*, *MafG+/-:MafK+/-*, *MafG+/-:MafK-/-*, *MafG-/-:MafK+/-*, and *MafG-/-:MafK+/-* confirmed that only *MafG-/-:MafK+/-* eyes have a visually overt

opacity (Figure 3.9). Analysis based on bright field view of lenses dissected from the above stated mutants provided further validation of the intense opacification of the lens specifically in *MafG-/-:MafK+/-* compound mutant animals (Figure 3.9).
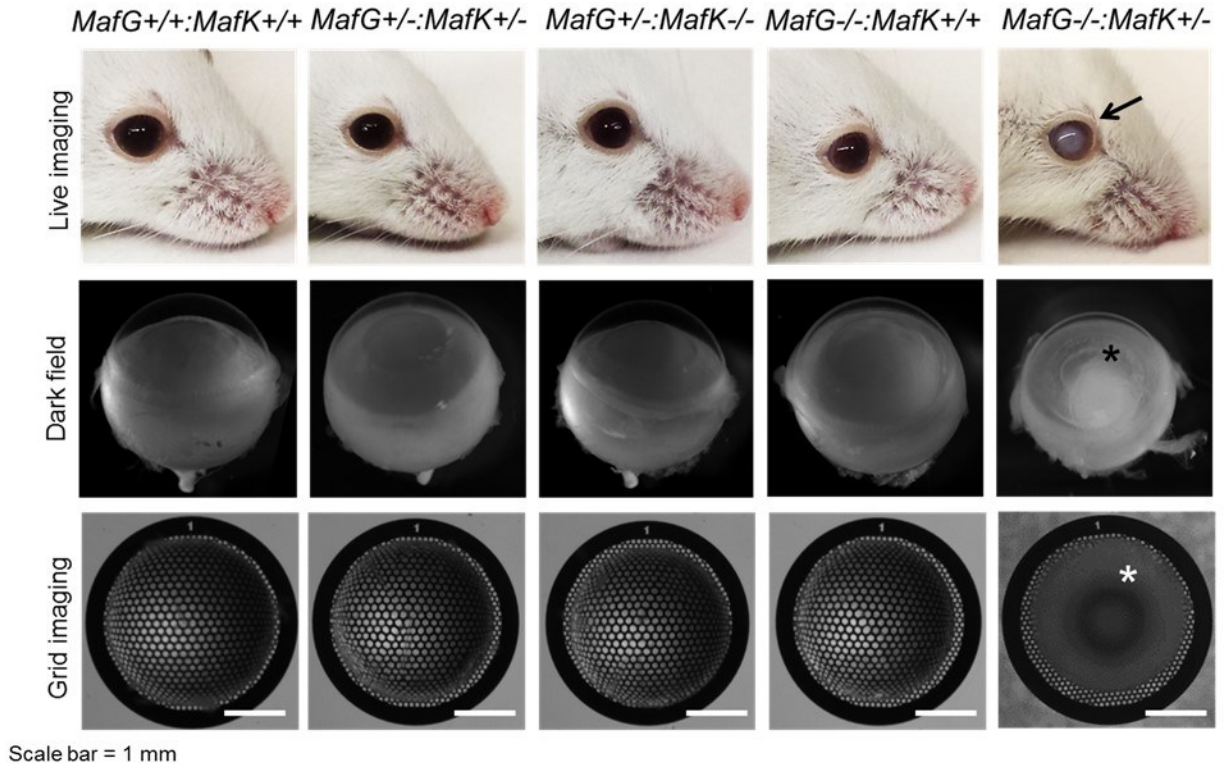
Figure 3.9. *MafG-/-:MafK+/- compound mutants exhibit cataract at 4 months age.* Physical examination of *MafG-/-:MafK+/-* compound mutant mice revealed an overt cataract phenotype starting at 4 months of age. Dark field view of cataractous *MafG-/-:MafK+/-* eye was observed in 4 month old animals. Bright field view of 4 month old lenses photographed on top of a hexagonal EM microscopy grid showed lack of patterns in *MafG-/-:MafK+/-* lens. Comparative analysis was performed with compound mutant animals including: *MafG+/+:MafK+/+*, *MafG+/-:MafK+/-*, *MafG+/-:MafK-/-*, *MafG-/-:MafK+/+* (represented above), *MafG+/-:MafK+/+*, *MafG+/+:MafK+/-* and *MafG+/+:MafK-/-* compound mutants. All of these compound animals lacked lens defects. At least 3 biological replicates were used in this experiment, with representative images illustrated above.

3.4 *MafG*:*MafK* Compound Mutants Exhibit Severe Lens Fiber Cell Defects

To gain insights into the etiology of fiber cell defects in *MafG-/-:MafK+/-* mutants at 4 months of age, histological analysis by hematoxylin and eosin staining of paraffin sections was performed on eye tissue and compared to *MafG+/-:MafK+/-* compound heterozygous and *MafG+/+:MafK+/+* wild-type control eyes (Figure 3.10). In both control samples, secondary fiber cell structure was normal and no defects were evident in the anterior epithelial region, transition zone, or the posterior region. However, in *MafG-/-:MafK+/-* mutants, the fiber cell compartment had large cortical vacuoles and profound fiber cell organization defects were evident. Additionally, a posterior capsular rupture of the fiber cells was evident in *MafG--/-:MafK+/-* mutants and was 75% penetrant (Figure 3.10).
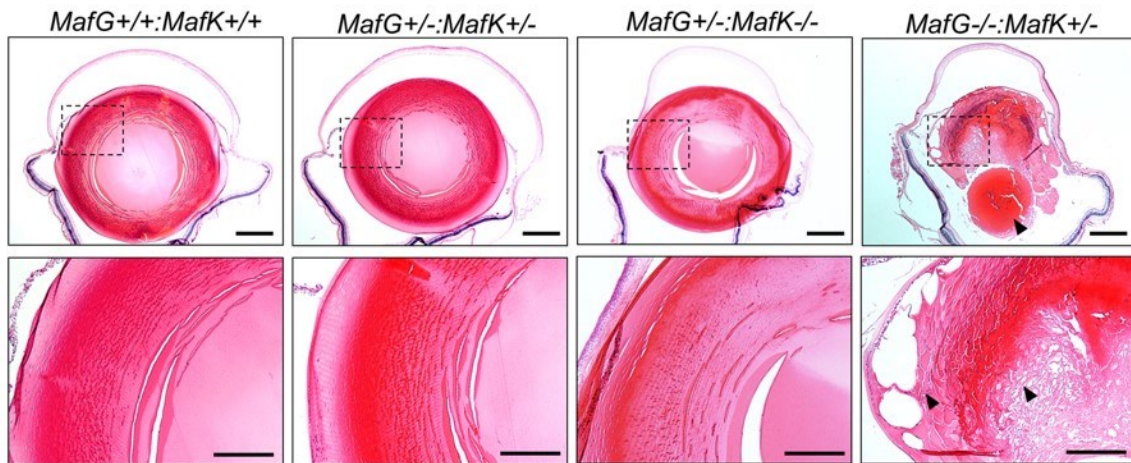
Top scale bars = 100 μm; bottom scale bars = 50μm

Figure 3.10. *MafG-/-:MafK+/-* **compound mutants exhibit fiber cell rupture defects at 4 months age**. Histological analysis of hematoxylin (purple) and eosin (pink) stained sections (6 μm thickness) showing large cortical vacuoles and profound fiber cell organization defects in lens obtained from *MafG-/-:MafK+/-* compound mutant mice. Morphology of the *MafG-/-:MafK+/-* compound mutant eyes were compared to eye sections obtained from *MafG+/+:MafK+/+*, *MafG+/-:MafK+/-*, and *MafG+/-:MafK-/-* sections which appeared to be normal. Top scale bars = 100 μm; bottom scale bars = 50μm

Interestingly, histological analysis of *MafG+/-:MafK-/-* eyes revealed no lens fiber cell defects and the tissue appeared to be normal, similar to the controls. This suggests that *MafG* function is more critical to lens homeostasis compared to *MafK*, which is in line with the observed difference in expression of these genes; *MafG* being more highly enriched than *MafK* in the lens. To characterize the morphology of the lens fiber cells from these mutants in further detail, scanning electron microscopy (SEM) was performed to examine the lens ultrastructure. The cortical fibers of lens were examined at 150-250 μm from the lens capsule of control and compound mutant *MafG+/-:MafK-/-* and *MafG-/-:MafK+/-* lens (Figure 3.11). SEM analysis revealed that lens obtained from 4 month old *MafG+/-:MafK+/-* and *MafG+/+:MafK+/+* control compound animals had organized cortical fiber cells in discrete aligned layers with interdigitating finger-like membrane protrusions. Cortical fiber cells in lens obtained from *MafG-/-:MafK+/-* compound mutant mouse at four months of age exhibited disorganized fiber cell packing, lack of membrane protrusions, and overall severe disruption of the cortical fibers. Interestingly, in sharp contrast, cortical fiber cells from *MafG+/-:MafK-/-* compound mutant mouse lens at 4 months age appeared to be normal in comparison to *MafG-/-:MafK+/-* compound mutant lens (Figure 3.11).
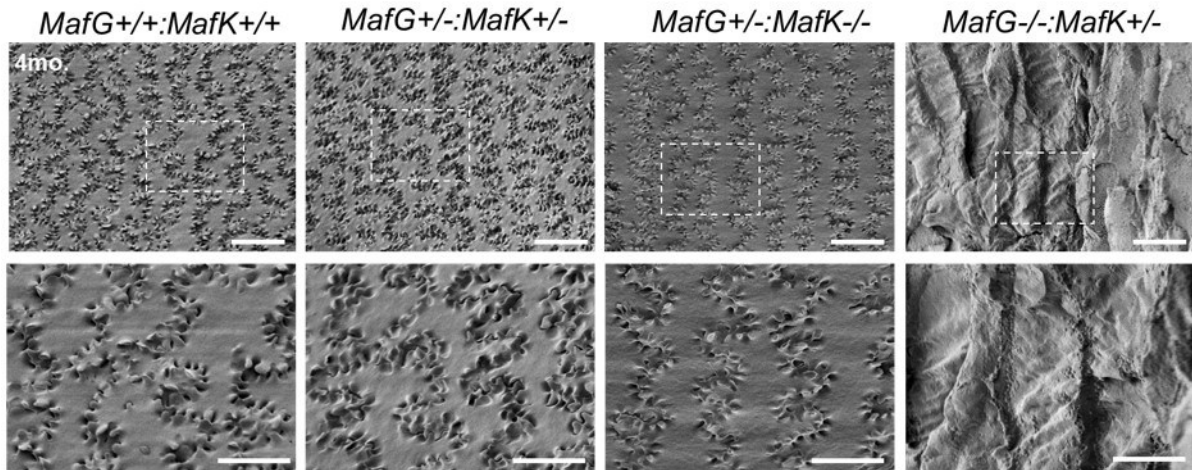
Figure 3.11. *MafG-/-:MafK+/-* **compound mutants exhibit cortical fiber cell defects at 4 months age**. High resolution scanning electron microscopy (SEM) of *MafG-/-:MafK+/-* compound mutant mice shows disorganization of fiber cell packing, lack of membrane protrusions, and overall severe disruption of the cortical fibers. In contrast, cortical fiber cells of *MafG+/-:MafK-/-* compound mutant mice lens at 4 months age appeared to be normal in comparison to *MafG-/-:MafK+/-* compound mutant lens. Comparative analysis was performed with compound mutant animals including: *MafG+/+:MafK+/+* and *MafG+/-:MafK+/-* compound mutant lens. All experiments were performed using at least 3 biological replicates. Scale bars for the top panel = 10µm; bottom panel = 5µm.

Although a subset of 4-month *MafG-/-:MafK+/-* compound mutants did not have overt cataract, in others, this lens opacity developed into severe cataract. The onset of cataract is variable, but the lens defect phenotype was fully penetrant in all tested *MafG-/-:MafK+/-* animals by 8 month age (Figure 3.12).
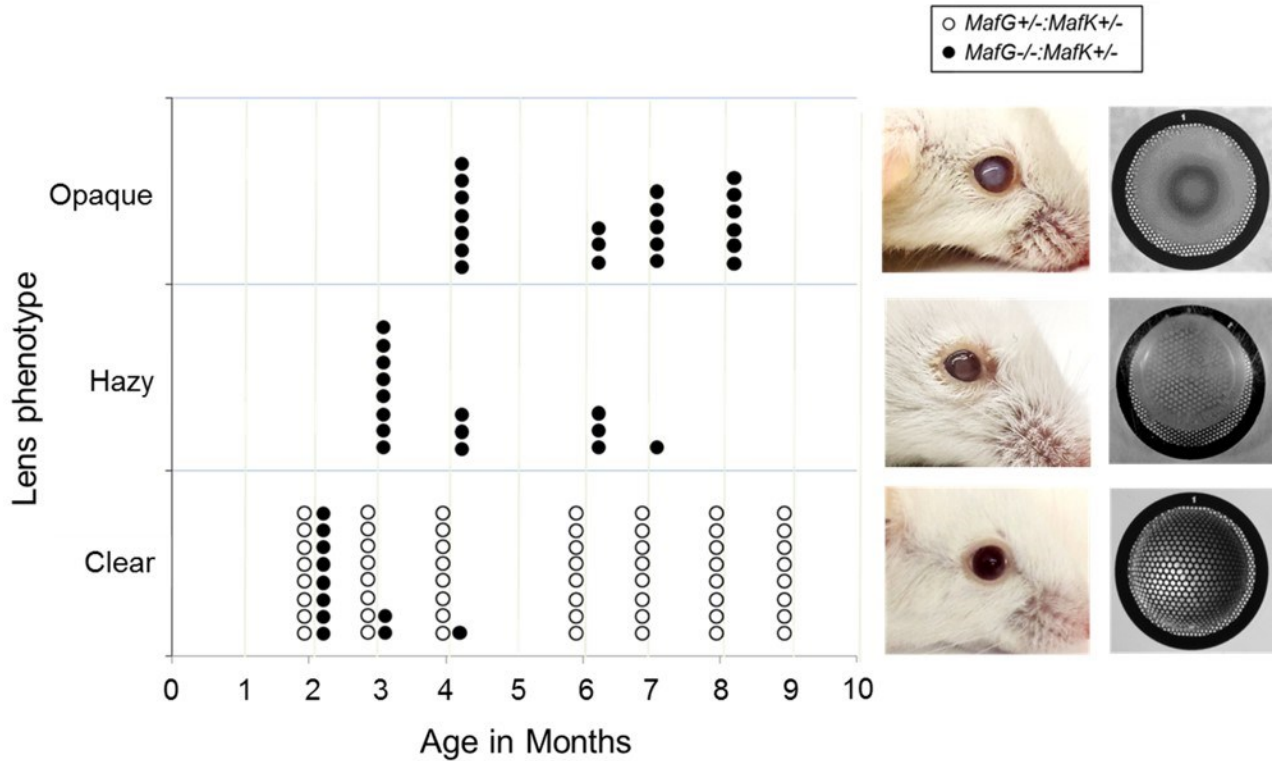
Figure 3.12. ***MafG-/-:MafK+/- compound mutants exhibit cataract at 4 months of age***. Progression of cataract was observed in mice ranging from ages 2 months to 9 months in *MafG-/-:MafK+/-* compound mutant mice and compared to eyes of *MafG+/-:MafK+/-* control mice. Cataract severity was scored as clear, hazy, or opaque. All *MafG+/-:MafK+/-* control compound mutants exhibited normal eye and lens at all stages. Starting at 3 months of age, hazy eyes were observed in *MafG-/-:MafK+/-* compound mutants. This analysis was performed in collaboration with Dr. Hozumi Motohashi (Kyoto, Japan).

Interestingly, I observed an isolated case of *MafG-/-:MafK+/-* compound mutant mouse that lacked overt cataract at 7 months of age. In order to characterize the phenotype, bright field view of a seven month old *MafG-/-:MafK+/-* revealed that the compound mutant had a mild cataractous lens (Figure 3.13). The hexagonal EM
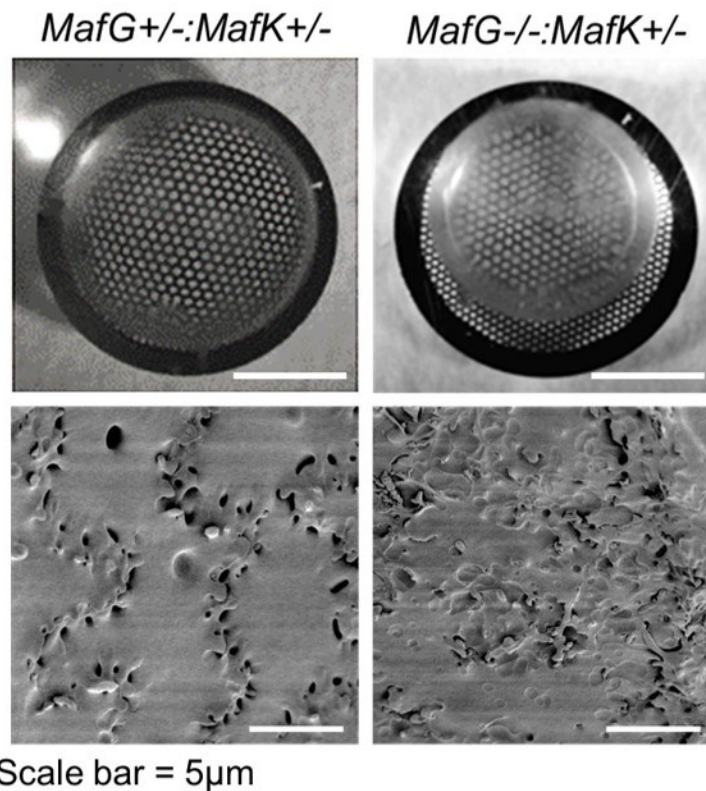
Figure 3.13. *MafG-/-:MafK+/-* **compound mutants exhibit fiber cell disruption in an apparently mild case of lens defect.** Bright field microscopy of *MafG+/- :MafK+/-* control lens on top of a hexagonal EM microscopy grid showing undistorted image typical of lens with normal refractive properties. In contrast, *MafG-/-:MafK+/-* mutant lens appears to have mild cataract and image is partially distorted. SEM based-analysis demonstrates normal cortical fibers with highly organized fiber cells and distinct membrane protrusions in *MafG+/- :MafK+/-* controls, while *MafG-/-:MafK+/-* lens cortical fiber cells show abnormal fiber cell organization. This indicates that although apparently a mild defect, the lens of a 7-month old *MafG-/-:MafK+/-* compound mouse mutant appears to have profound defects when analyzed at high resolution by SEM. Scale bar = 5µm.

microscopy grid is visible, but not as clearly as in the control *MafG+/-:MafK+/-* lens. However, when high resolution SEM was performed to examine the ultrastructure of the cortical fiber cells, it was evident that the *MafG-/-:MafK+/-* lens lacked organized fiber cell packing and membranes were structurally disrupted. This confirmed that even in a rare case of an apparently mild lens phenotype in *MafG-/-:MafK+/-* compound mutant at 7-month age, the lens on high resolution examination exhibited gross fiber cell defects.
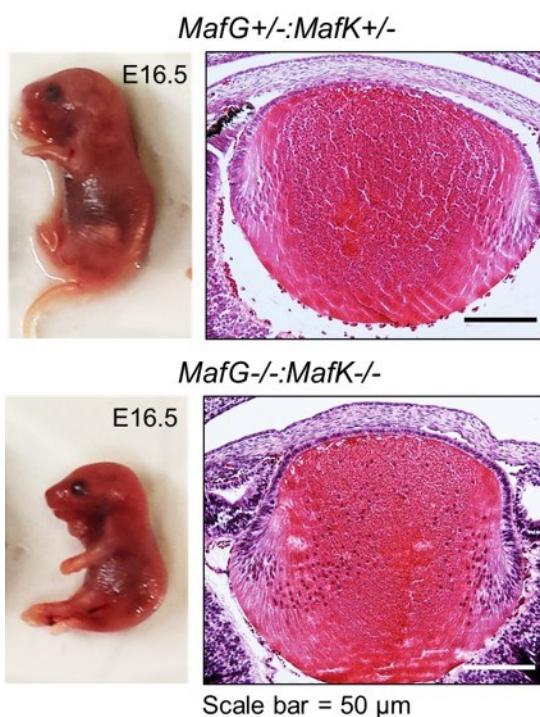
Since *MafG-/-:MafK-/-* compound homozygous null mutants are perinatal lethal and exhibit growth defects (Figure 3.14), characterization of lens was performed at late embryonic stage E16.5. Histological analysis by hematoxylin (purple) and eosin (pink) staining of sections obtained from E16.5 lens revealed no abnormalities in the lens in comparison to *MafG+/-:MafK+/-* control lens (Figure 3.14).

Figure 3.14. *MafG-/-:MafK-/-* **compound mouse mutants show no lens defects in embryonic development.** *MafG-/-:MafK-/-* compound mutants physically appear to be smaller and exhibit growth retardation defects compared to compound control animals at E16.5. Histological analysis of *MafG-/-:MafK-/-* compound mutant mice at E16.5 revealed lack of fiber cell defects in comparison to *MafG+/-:MafK+/-* compound mutant eyes. All experiments and imaging were performed under the same conditions. Scale bar = 50 μm.

3.5   Identification of Differentially Regulated Genes in *MafG-/-:MafK+/-* Mutant Lens.

I next sought to gain an understanding of the molecular changes underlying the phenotypic defects in *MafG-/-:MafK+/-* mutant lenses. To gain a global insight into gene expression changes in these mutants, I aimed to perform microarray-based gene expression analysis on lenses prior to their exhibiting an overt defect. Since *MafG-/-:MafK+/-* mutant lenses lacked overt opacities at 2 months age, and the only difference when compared to the controls is the smaller size of the lens (Figure 3.15), lenses from the *MafG-/-:MafK+/-* compound mutants and *MafG+/-:MafK+/-* controls were used to perform gene expression profiling by Illumina Mouse WG-6 microarrays.

To explore the expression changes of potential key genes and relevant biological processes in lens homeostasis and maintenance of transparency, microarray data from *MafG+/-:MafK+/-* control and *MafG-/-:MafK+/-* compound mutant lens samples were obtained and analyzed. Differentially regulated genes (DRGs) were identified using previously described method (Section 2.10), and cluster analysis of DRGs was performed following functional enrichment analysis with Database for Annotation, Visualization and Integrated Discovery (DAVID, Bioinformatics Resources 6.7) database. All genes with fold change of greater than ±1.5, which included 66 out of 90 genes in the up-regulated list and 949 out of 1200 genes were used in the DAVID analysis to perform Gene Ontology (GO) annotation and Kyoto Encyclopedia of Genes and Genomes (KEGG) pathway analysis for the DRGs.

MafG+/-:MafK+/-   **MafG-/-:MafK+/-**

Scale bar = 5μm
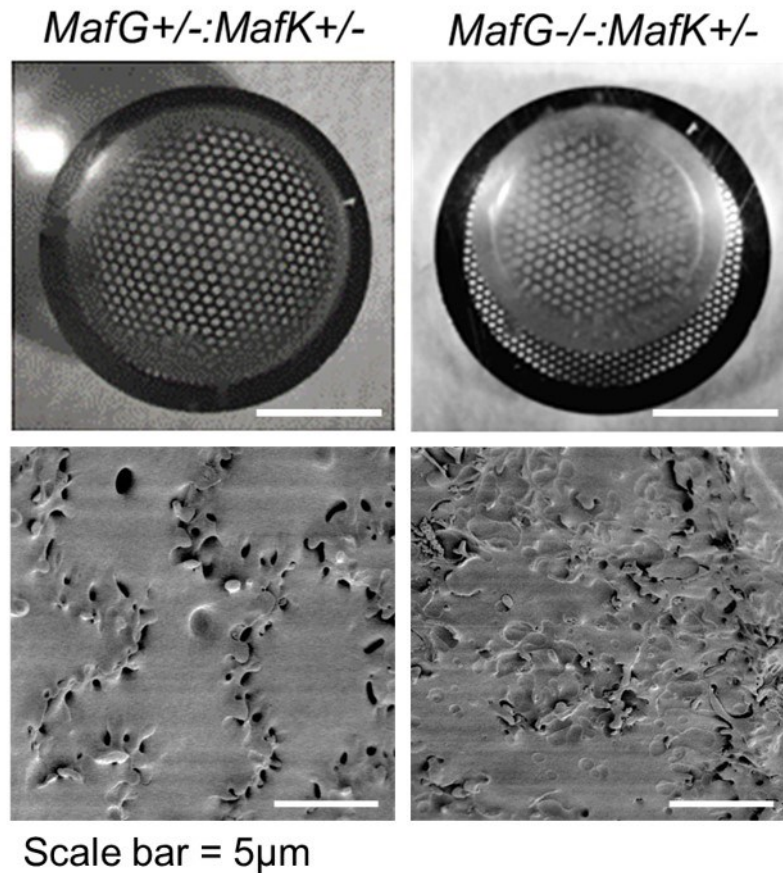
Figure 3.15. *MafG-/-:MafK-/-* **compound mutants lack overt lens defects including cataracts at 2 months age**. Dark field microscopy of *MafG+/-:MafK+/-* lens compared to *MafG-/-:MafK+/-* compound mutant mice demonstrates the presence of transparent lens in both animals, although the lens is smaller in size in *MafG-/-:MafK+/-* mutants. High resolution analysis using SEM also demonstrates normal fiber cell structure in *MafG+/-:MafK+/-* and *MafG-/-:MafK+/-* cortical fiber cells, indicating that by 2-month age, there are no gross defects in *MafG-/-:MafK+/-* compound mutant lens. Scale bar = 5μm.

After normalizing the expression data for up-regulated and down-regulated genes in *MafG-/-:MafK+/-* compound mutant lens, the curated list of genes were run through DAVID software to conduct functional annotation clustering. In total, 66 up-

regulated genes were used in the analysis, and 949 down-regulated genes were used to perform clustering using high classification stringency. Over 900 genes were down-regulated in the *MafG-/-:MafK+/-* compound mutant mice lens with a fold-change of -1.5 or below. DAVID analysis resulted in many of the genes clustered into categories including protein localization, apoptosis, extracellular matrix, cell division, response to DNA damage, defense response, etc. (Figure 3.16). Some other categories that had more than five genes clustered included cell adhesion junction, intracellular protein and lipid binding signaling, and regulation of cellular response to stress. One of the clusters was retinoic acid metabolic process, which included aldehyde dehydrogenase family
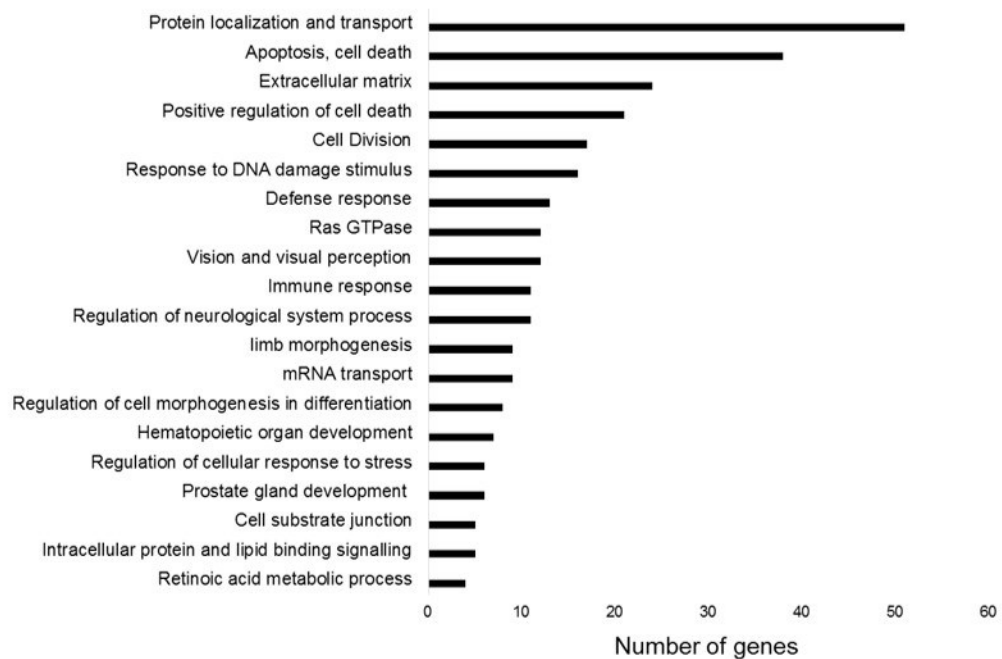
Figure 3.16. Down-regulated gene functional annotation clustering in *MafG-/-:MafK+/-* compound mutants. Cluster analysis of down-regulated genes was performed following functional enrichment analysis with Database for Annotation, Visualization and Integrated Discovery (DAVID, Bioinformatics Resources 6.7) database. All down-regulated genes with fold change of greater than 1.5 were used in the DAVID analysis.

proteins *ALDH3A1* (F.C. -3.64) and *ALDH1A7* (F.C. -1.51), as well as cellular retinoic acid binding protein II (*CRABP2*, F.C. -2.05). Genes identified in the vision cluster included ATP-binding cassette subfamily 1, member 4 (*ABCA4*, F.C. -1.91)), clarin 1 (*CLRN1*, F.C. -1.60), guanine nucleotide binding protein, alpha transducing 1 (*GNAT1*, F.C. -1.69), opsin 1 (OPN3, F.C. -1.54), phosphodiesterase 6B (*PDE6B*, F.C. -1.69), phosphodiesterase 6G (PDE6G, F.C. -2.20), protein phosphatase (*PTPN4*, F.C. -1.53), EF hand calcium-binding domain 2 (*EFCAB4B*, F.C. -1.52), rhodopsin (*RHO*, F.C. -1.63), spermatogenesis associated 7 (*SPATA7*, F.C. -1.56), and retinitis pigmentosa GTPase regulator (*RPGR*, F.C. -1.50).

Another important cluster was regulation of cell morphogenesis involved in differentiation, which included genes like transforming growth factor, beta 3 (*TGFB3*, -1.54 F.C.), tetratricopeptide repeat domain 3 (*TTC3*, -1.61 F.C.), reticulon 4 (*RTN4*, -1.51 F.C.) and ring finger protein (C3H2C3 type) 6 (*RNF6*, -1.64 F.C.). Another interesting gene that was down-regulated was *Hspb1* (-1.5 F.C.), a heat shock protein, that has been shown to play important roles in stress response and has also found to be down-regulated in *Tdrd7* null mutant lens (Lachke et al., 2011).

For the up-regulated genes (Figure 3.17), many of the functional categories included apoptosis, cell division, response to DNA damage stimulus, defense response, regulation of oxidative stress, vision and visual perception, etc. Of the genes that were up-regulated in *MafG-/-:MafK+/-* compound mutant lens, the top candidates based on fold-change (F.C.) were dynactin or P62 (*DCTN4,* 6.5 F.C.) which is a cytoskeleton protein, 3-Hydroxy-3-Methylglutaryl-CoA Synthase 1 (*Hmgcs1*, 4.1 F.C.) which is involved in sterol synthesis, DNA-damage-inducible transcript 3 (*DDIT3,* 3.2 F.C.)

which is involved in cell stress response and apoptosis, and heme oxygenase 1 (*HMOX1*, 2.4 F.C) which is involved in oxidative stress response.
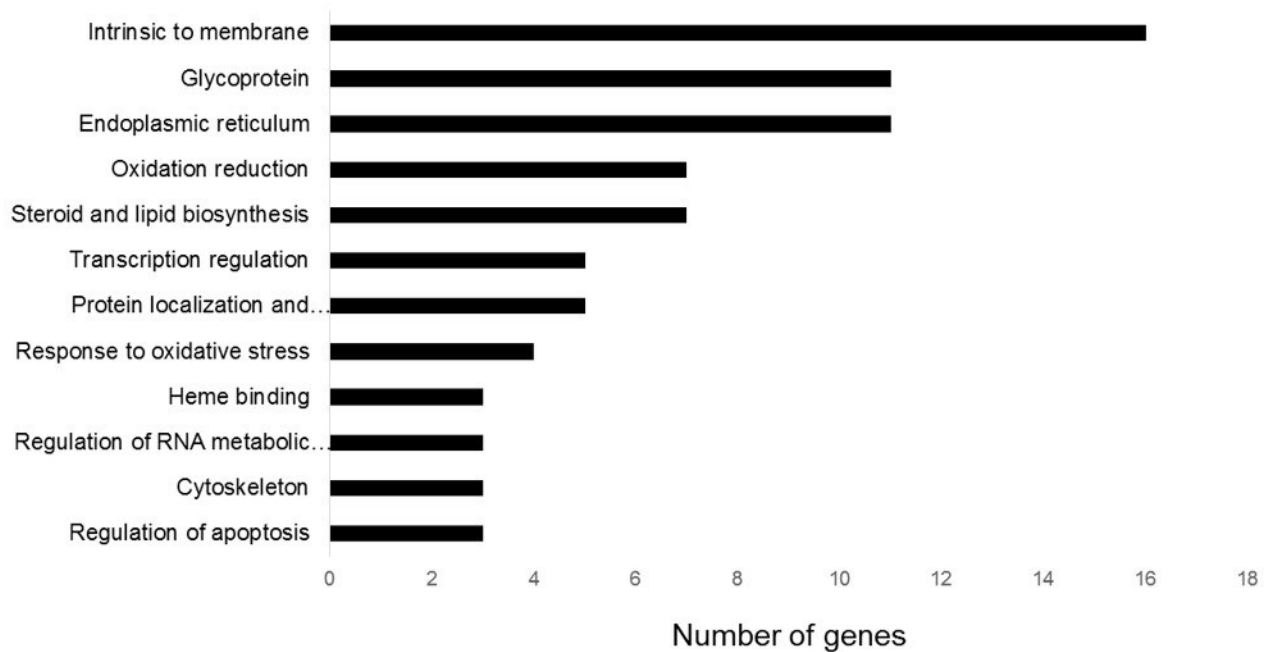
Figure 3.17. Up-regulated gene functional annotation clustering in *MafG-/-:MafK-/- compound mutants. Cluster analysis of up-regulated genes was performed following functional enrichment analysis with Database for Annotation, Visualization and Integrated Discovery (DAVID, Bioinformatics Resources 6.7) database. All genes with fold change of greater than 1.5 were used in the DAVID analysis.

Since majority of the genes were down-regulated at the 1.5 F.C. cut-off, the microarray data was analyzed at higher cut-off values to confirm that majority of the DRGs are down-regulate. At a 1.7 F.C cut-off, 491 genes were down-regulated while only 33 genes were up-regulated. At a 2.0 F.C. cut-off, 125 genes were down-regulated while only 20 genes were up-regulated. At a 2.5 F.C. cut-off, 31 genes were down-regulated while 10 genes were up-regulated. These results are interesting since small Mafs lack a transactivation domain and can only act as repressors if they dimerize with specific binding-partners such as Nrf2.

Down-regulation of both *Hspb1* and *Aldh3a1* were validated by qRT-PCR (figure 3.18), which confirmed that expression of these genes was reduced in *MafG-/-:MafK+/-* mutant lens. Up-regulation of both *Hmox1* and *Ddit3* were validated by qRT-PCR as well in the *MafG-/-:MafK+/-* compound mutant lens compared to the *MafG+/-:MafK+/-* compound control lens (Figure 3.19).
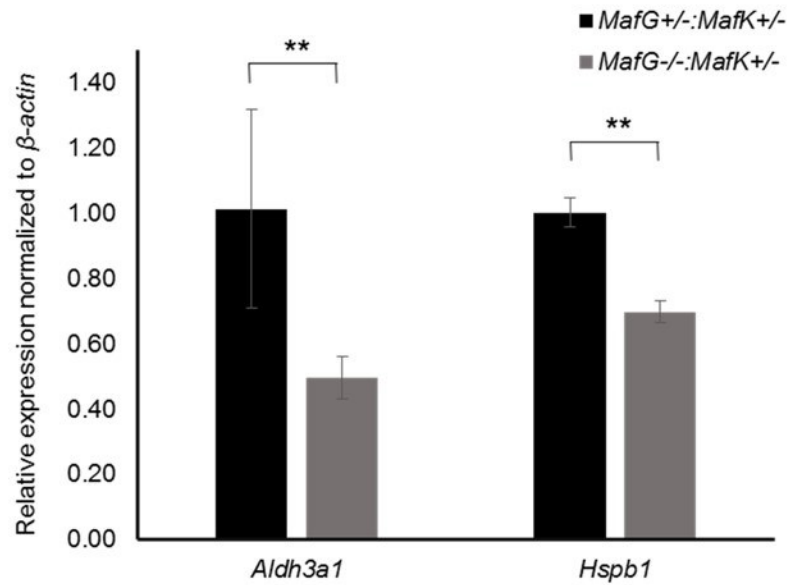
Figure 3.18. ***Aldh3a1*** **and** ***Hspb1*** **are down-regulated in** ***MafG-/-:MafK+/-***
compound mutants. Expression of up-regulated genes *Aldh3a1* and
Hspb1 was validated by qRT-PCR. Genes were normalized to *β-actin*
as housekeeping control. ** denotes p-value < 0.01.
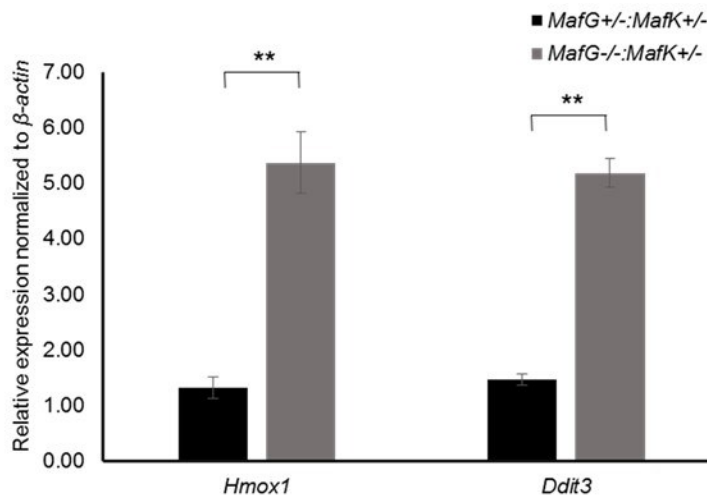
Figure 3.19. ***Hmox1*** **and** ***Ddit3*** **are upregulated in** ***MafG-/-:MafK+/-*** **compound**
mutants. Expression of up-regulated genes *Hmox1* and *Ddit3* was
validated by qRT-PCR. Genes were normalized to *β-actin* as housekeeping
control. ** denotes p-value < 0.01.

To further elucidate the role of MafG and MafK in the lens, and to gain insight into small Maf-mediated gene regulation, I developed an integrated approach to filter and select promising candidates from these lists of DRGs. *iSyTE* was used to analyze the expression of DRGs to identify genes that exhibited lens-expression or lens-enriched expression. Both, up-regulated and down-regulated candidate genes were subjected to this analysis. An alternative filter was applied which involved the overlay NRF2 direct target gene list to the list of DRGs in *MafG-/-:MafK+/-* lens. Previously, human small Mafs have been identified to form heterodimers with CNC (cap and collar) family transcription factors and recognize the NRF2 motif (Kataoka, 2007; W. Li et al., 2008; Toki et al., 1997). This list included genes that had an antioxidant response element (ARE) motif that Nrf2 (nuclear factor erythroid-derived 2-like; NFE2L2) binds to, and this data was obtained from ChIP (chromatin immunoprecipitation) experiments performed previously with human lymphoblastoid cells (Chorley et al., 2012).

After filtering the genes through this step, *iSyTE* was used to evaluate the genes that were in the top 5% lens enrichment percentile. For genes that were excluded from this analysis, gene expression in the lens was analyzed. For genes that were not expressed lens specifically, their relevance to biological function was assessed based on literature and if they were important in the eye, they were included as well. Based on this strategy, 25 genes were identified that had the ARE motifs to which small Mafs can bind to and regulate transcription of, and were either lens enriched, lens expressed, or had known biological role in the eye (Table 3.1). For each of these genes, ARE motifs were searched in 2.5 kb up and 2.5 kb down sequences. The analysis was also performed

66

based on *de novo* motif prediction to confirm if the motif is really present in the same set of sequences, which validated that the *NRF2* binding sites were present.

Table 3.1. Curated differentially regulated gene list with Anti-Oxidant Response (ARE) motifs.

Symbol	F.C. values	Lens enriched	Lens expressed	known biological role in eye
Aldh3a1	-3.6	yes	yes	yes
Hmox1	2.4	yes	yes	yes
B3gnt5	-1.9	yes	yes	no
Lpin1	-1.8	yes	yes	yes
Abcc5	-1.8	yes	yes	yes
Akap2	-1.5	yes	yes	yes
Insig1	1.9	no	yes	no
Wipi2	-1.5	no	yes	no
Dst	-1.9	no	yes	no
Mtf2	-1.8	no	yes	no
Gorasp2	-1.5	no	yes	no
Nln	-1.7	no	yes	no
Plk3	1.7	no	yes	no
Sspn	-1.8	no	yes	no
Ptges3	-1.9	no	yes	no
Brd2	-1.6	no	yes	no
Cep120	-1.7	no	yes	no
Adamts12	-1.6	no	no	yes
Rffl	-1.7	no	no	yes
Gcnt2	-1.5	no	no	yes
Mpdz	-1.5	no	no	yes
Ehmt1	-1.9	no	no	yes
Rgs3	-1.7	no	no	yes
Nqo2	-1.7	no	no	yes

Chapter 4

DISCUSSION

4.1   Characterization of Small Maf Transcription Factors in the Murine Lens

Small Maf basic leucine zipper (bZIP) proteins have been previously identified as crucial regulators of gene expression in specific mammalian cells and tissues. In particular, previous studies have shown that small Mafs dimerize with the Cap 'n' Collar (CNC) family of transcription factors and function in stress signaling, hematopoiesis, CNS function and oncogenesis. Moreover, small Maf genes are highly conserved in vertebrates, which suggests that they have important functional contribution in various processes. Homozygous null mouse mutant models for all three smalls Maf genes - *MafG*, *MafK*, and *MafF* (Yamazaki et al., 2012) have provided valuable insights into their role in several tissues.

Although there is redundancy between their functions, compound mutants carrying mutations in multiple candidates have proven to be informative to understand specific functions of these proteins. For example, *MafG-/-:MafK+/-* mutants exhibit chronic posterior ataxia – more severe than is observed in single *MafG-/-* mutants – and also develop thrombocytopenia (Onodera et al., 2000). In contrast, *MafF-/-:MafG-/-:MafK-/-* triple mutants die by embryonic day E13.5 and exhibit liver defects (Yamazaki et al., 2012). Clinically, small MAFs have been associated with various diseases such as thrombocytopenia, diabetes, carcinogenesis as well as neuronal disorders. Their large Maf related protein, c-MAF, has been shown to regulate lens development by

directly controlling expression of crystallin genes in lens fiber cell differentiation (Cvekl et al., 2004; Kawauchi et al., 1999; Kim et al., 1999; Ring et al., 2000; Xie & Cvekl, 2011), and mutations in its human ortholog (*MAF*) are known to cause congenital or juvenile cataracts (Jamieson et al., 2003; Vanita et al., 2006). However, the effect of small Maf mutations on ocular tissues remains uncharacterized. This work highlights a novel function of small Maf transcription factors, MafG and MafK in lens homeostasis and cataract development.

To elucidate the functional contributions of small Maf family factors to the lens, I set out to identify the small Maf factors that are specifically expressed in the mouse lens. While *MafG* and *MafK* are expressed in the lens, *MafF* expression is low or absent in the lens throughout development (Figure 3.1) as well as in post-natal stages through adulthood (Figure 3.2) Since the germline knockout mice have *LacZ* in place of the coding region, staining for β-galactosidase reporter indicated particularly intense expression in the epithelium of the intestine, skeletal muscle, lens, retina, brain, and cranial nerve and dorsal root ganglion cells (Shavit et al., 1998). Furthermore, using *iSyTE*, expression of *MafG* was found to be highly enriched in the lens compared to the whole embryonic body tissue reference dataset. These findings suggested that the lens represents a tissue where MafG may be functionally recruited. Since previous studies have shown that small Mafs bind with other transcriptional regulators and form heterodimers to exert their role on downstream genes, I examined the expression of various MafG-binding transcription factors in the lens. Specifically, *Nfe2l1*, *Nfe2l2*,

and *Bach2* were enriched in the lens, which suggested that both MafG as well as these binding partners may represent a new set of TFs that regulate fiber cell gene expression.

4.2   Generation of *MafG*:*MafK* Compound Germline Mutants.

Previously, it has been reported that targeted disruption of *MafK* independently does not result in a particularly discernible phenotype (Kotkow & Orkin, 1996; Shavit et al., 1998), while *MafG* germline knockout mice exhibit mild thrombocytopenia (Shavit et al., 1998). In order to characterize the ocular pathologies resulting from gene mutations in both *MafG* and *MafK*, I generated combinations of compound germline knockouts for these genes. *MafG+/-:MafK+/-* compound heterozygous mice were obtained from Dr. Hozumi Motohashi from Kyoto University in Japan. These mice were generated by intercrossing *MafG+/-* with *MafK-/-* mutant mice (129/CD1 mixed hybrid background) (Onodera et al., 2000; Shavit et al., 1998). All of the combinations of *MafG:MafK* were born in expected ratios with the exception of *MafG-/-:MafK+/-* (expected 12.5%, observed 6.0%, *n*=300) and *MafG-/-:MafK-/-* mutants (expected 6.2%, observed 1.4%, *n* = 300). This observation can be explained by the fact that a 100% of the *MafG-/-:MafK+/-* mutants exhibited a severe motor ataxia and hind limb paralysis neurological phenotype occurring within 3-4 weeks of age. This phenotype has been previously reported (Onodera et al., 2000), and my research confirms this results.

Further, compound homozygous null mutant animals have been previously characterized to be perinatal lethal and develop severe thrombocytopenia anemia, and

liver defects, which might explain the low observed to expected ratios. Interestingly, *MafG+/-:MafK-/-* animals did not exhibit any such defects and appeared to be normal in comparison to the wild-type *MafG+/+:MafK+/+* mice and compound heterozygous *MafG+/-:MafK+/-* mice. This suggested that while both *MafG* and *MafK* are important for overall viability, *MafG* is primarily indispensable for survival and at least one *MafG* allele is required for normal reproduction and survival.

4.3   Compound *MafG-/-:MafK+/-* Mutant Mice Exhibit Fiber Cell Defects and Cataract.

In order to characterize the lens pathology in *MafG:MafK* compound heterozygous mutant mice, various allelic combinations of *MafG* and *MafK* compound mutants were analyzed. Based on the results, it was evident that *MafG-/-:MafK+/-* compound mutants exhibit lens defects and cataract starting at 4 months of age. This observation is very interesting considering that *MafG-/-:MafK+/+* compound mutants and *MafG+/+:MafK-/-* compound mutants lack any overt lens phenotypes and do not develop cataract. Detailed characterization of lens from *MafG-/-:MafK+/-* compound mutants revealed that the fiber cells are severely disrupted and possess large cortical vacuoles in the fiber cell lens compartment with 100% penetrance. This phenotype is similar to a previously characterized lens phenotype in *Tdrd7*, a Tudor domain RNA binding protein that was predicted by *iSyTE* to be a lens-enriched gene.

Additionally, rupturing of the lens capsule that extrudes the fiber cell mass was evident in some *MafG-/-:MafK+/-* mutants but it was partially penetrant. Furthermore,

characterization of *MafG-/-:MafK+/-* based on high resolution scanning electron microscopy showed severe disruption of fiber cell arrangement marked by fiber cells lacking membrane protrusions and definitive cortical membranes. This analysis was performed at 4 months of age, and the phenotype was confirmed even in a rare mild-cataract case of *MafG-/-:MafK+/-* compound mutants at 7 months of age, where the fiber cells were severely disrupted. Interestingly, analysis of *MafG+/-:MafK-/-* mutants at 4 months of age revealed that the mice do not exhibit cataract and lack any overt fiber cell defects. These results demonstrate that while both MafG and MafK play an important role in the lens, MafG is essential for fiber cell homeostasis.

Furthermore, analysis of *MafG-/-:MafK-/-* showed that double null homozygosity for these genes leads to perinatal lethality, as previously reported (Onodera et al., 2000), and lens of these mice lack any lens or fiber cell defects at E16.5 discernable by histological analysis. In order to elucidate the lens phenotype resulting from deletion of both *MafG* and *MafK*, lens specific conditional knock-out models would be required to gain further insights.

4.4   Differentially Regulated Genes (DRGs) in *MafG+/-:MafK+/-* Compound Mutants Lens.

To understand the molecular phenotype of *MafG-/-:MafK+/-* mutant lens, I undertook a microarray-based expression analysis of isolated lenses from *MafG-/-:MafK+/-* compound mutants and *MafG+/-:MafK+/-* littermate controls focusing on 2 months stage or 8 weeks before the overt cataract appearance.   Comparison of

differentially regulated genes (DRGs) from these lens microarray data sets identified several biologically relevant genes. In particular, many of the up-regulated and down-regulated genes were grouped in categorizes such as apoptosis, cell division, response to DNA damage stimulus, defense response, regulation of oxidative stress, and vision and visual perception.

It is well understood that various stress stimuli, including oxidative stress insults, can activate the DNA binding of a heterodimer consisting of the basic-leucine zipper transcription factors Nrf2 and small Maf. Once bound to its recognition DNA sequence termed antioxidant-responsive element (ARE) or Maf-recognition element (MARE), Nrf2/small Maf heterodimers induce a set of genes important in oxidative stress response, inflammation, hematopoiesis, and CNS function. Of the interesting microarray targets, *Hmox1* that encodes heme oxygenase-1, a heat shock protein, was identified to be up-regulated in *MafG-/-:MafK+/-* compound mutants by microarrays and validated by qRT-PCR. Hmox1 has been previously shown to contribute to the scavenging of reactive oxygen species (ROS) (Kataoka, 2007; Zheng et al., 2010). *Hmox1* expression has previously been shown to be negatively regulated by Bach2, a small Maf dimerization partner belonging to the CNC family of transcription factors, in chronic myeloid leukemia (CML) (C. Yoshida et al., 2007). *Bach2* is highly expressed and enriched in the lens during embryonic development, and is known to induce apoptosis in response to oxidative stress. Based on these results, it can be hypothesized that MafG and Bach2 heterodimers are directly involved in repressing transcription of Hmox1. Furthermore, *iSyTE*-based analysis has indicated that *Hmox1* is a lens-enriched

73

gene, further suggesting that its regulation might be critical in the lens. Additionally, *Hmox1* has been shown to be regulated by Nrf2 (Chorley et al., 2012) in human lymphoblastoid cells by chromatin immunoprecipitation (ChIP) by binding to the ARE sites. Since Nrf2 requires small Maf proteins as obligatory dimerization partners to target the ARE, it would be interesting to investigate how the regulation of Nrf2-small Maf dimers compares with Bach2-small Maf mediated *Hmox1* repression, and if these heterodimers compete with each other to regulate *Hmox1*.

During fiber cell differentiation, it is known that transcription of crystallin genes are up-regulated as they are necessary in high protein levels and required for tight packing of the fiber cells that provides ocular transparency. One of the targets of MafG that is down-regulated in *MafG-/-:MafK+/-* compound mutants is a heat shock protein-*Hspb1* (*Hsp27*), which encodes a stress response chaperone protein. Hspb1 interacts with several lens crystallin proteins and stabilizes αA and B-crystallin proteins, which are very important in the lens (Fu & Liang, 2002, 2003). Further, Hspb1 has anti-oxidant properties that have been previously implicated in the regulation of apoptosis and reduction in the amount of reactive oxygen species (ROS) in cells exposed to oxidative stress (Arrigo et al., 2007). Thus, it can be hypothesized that *Hspb1* is a contributing factor to cataract in *MafG-/-:MafK+/-* compound mutants.

In addition to these candidate genes, 37 other genes involved in apoptosis were down-regulated in *MafG-/-:MafK+/-* compound mutant lenses (Table 4.1). Some of these genes encoded DnaJ (Hsp40) homolog (*DNAJA3*), a heat shock protein that stimulates the ATPase activity of Hsp70 chaperones, Caspase 4, an apoptosis-related

cysteine peptidase (*CASP4*), gap junction protein, beta 6 (GJB6), and reproductive homeobox 5 (*RHOX5*), all of which within the -1.5 fold cut-off for down-regulated expression.

Furthermore, other genes involved in regulation of apoptosis, namely 24-dehydrocholesterol reductase (*DHCR24*) and DNA-damage inducible transcript 3 (*DDIT3 or CHOP*) were up-regulated in *MafG-/-:MafK+/-* compound mutants. It has been previously established that cataractous lens has deficient defense systems against oxidative stress and UV (W. C. Li et al., 1995), and that cell stress can trigger lens epithelial cell apoptosis that can contribute to cataract development. Many cataractogenic stressors have been shown to induce UPR (unfolded protein response)-specific proteins (Shinohara et al., 2006, Ikesugi et al., 2006). Specifically, PERK is a kinase that phosphorylates translation initiation factor 2 α (eIF2α) which activates transcription factor ATF4 (Dey et al., 2010). Up-regulation of ATF4 activates *Ddit3*, which is evident in the microarray results of this study. Further, up-regulation of Ddit3 has been shown to down-regulate anti-apoptotic proteins in the cell death cascade (Dey et al., 2010; Ikesugi et al., 2006). Interestingly, two of these genes, B-cell lymphoma 2-like 1 (*BCL2l1*), and BCL2-like 2 (*BCL2L2*) are both down-regulated (-1.5 F.C. cut-off) in *MafG-/-:MafK+/-* compound mutant lens.

Table 4.1. Apoptosis associated down-regulated genes in *MafG-/-:MafK+/-* mutants.
All genes were down-regulated at the 1.5 F.C. value.

BCL2L1	BCL2-like 1
BCL2L2	BCL2-like 2
CD27	CD27 antigen
DNAJA3	DnaJ (Hsp40) homolog, subfamily A, member 3
FAIM	Fas apoptotic inhibitory molecule
FAIM2	Fas apoptotic inhibitory molecule 2
FAF1	Fas-associated factor 1
GRAMD4	GRAM domain containing 4; hypothetical protein LOC100045216
ASAH2	N-acylsphingosine amidohydrolase 2
PAWR	PRKC, apoptosis, WT1, regulator
RELT	RELT tumor necrosis factor receptor
2610301G19RIK	RIKEN cDNA 2610301G19 gene
SH3GLB1	SH3-domain GRB2-like B1 (endophilin)
STEAP3	STEAP family member 3
SHF	Src homology 2 domain containing F
TRAF6	TNF receptor-associated factor 6
WDR92	WD repeat domain 92
AIFM1	apoptosis-inducing factor, mitochondrion-associated 1
CASP4	caspase 4, apoptosis-related cysteine peptidase; hypothetical protein LOC100044206
C9	complement component 9
CUL1	cullin 1
DAP	death-associated protein
GJB6	gap junction protein, beta 6
GZMG	granzyme G
KIT	kit oncogene
MFSD10	major facilitator superfamily domain containing 10
MYCS	myc-like oncogene, s-myc protein
NR4A2	nuclear receptor subfamily 4, group A, member 2
PDCD4	programmed cell death 4
PSMG2	proteasome (prosome, macropain) assembly chaperone 2; similar to Clast3 protein
PPM1F	protein phosphatase 1F (PP2C domain containing)
PPP2R2B	protein phosphatase 2 (formerly 2A), regulatory subunit B (PR 52), beta isoform
P2RX1	purinergic receptor P2X, ligand-gated ion channel, 1
RHOX5	reproductive homeobox 5
RFFL	ring finger and FYVE like domain containing protein
SAP30BP	similar to transcriptional regulator protein; SAP30 binding protein
UNC5A	unc-5 homolog A (C. elegans)

In order to identify the candidate direct targets of MafG, DRGs identified by microarrays were overlapped with genes identified to have ARE in their promoter region. For this analysis, a dataset of all Nrf2- regulated genes identified previously by chromatin immunoprecipitation (ChIP)-sequencing experiments was obtained (Chorley et al., 2012).

Using this approach, 24 genes were identified to have ARE sites in the *MafG-/-:MafK+/-* lens DRGs list, and shown to be expressed based in the lens in embryonic (*iSyTE 1.0*) (Lachke, Ho, et al., 2012) and post-natal stages (*iSyTE 2.0*, unpublished Kakrana and Lachke, 2014). Genes that were lens-specifically enriched included *Aldh3a1, Hmox1, B3gnt5, Lpin1, Abcc5, Akap2*; genes that were lens-expressed included *Insig1, Wipi2, Dst, Mtf2, Gorasp2, Nln, Plk3, Sspn, Ptges3, Brd2* and *Cep120*. Of the 24 genes, seven of them did not have documented lens specific expression, but may be involved in the eye functionally. These genes are *Adamts12, Rffl, Gcnt2, Mpdz, Ehmt1, Rgs3,* and *Nqo2*.

Adamts12 belongs to the a disintegrin and metalloproteinase with thrombospondin type-1 motifs family that is involved in arthritis and inflammation (Wei et al., 2014). A recent study evaluated the promoter regions of Adamts12 by electrophoretic mobility shift assay and found that it contains a c-Maf recognition element (MARE) at position -61 (AGCTGAATCACTC), suggesting that c-Maf is directly involved in regulating *Adamts12* expression during chondryocyte differentiation (Hong et al., 2013). MARE sites are direct targets of small Mafs MafG and MafK. Therefore, it can be hypothesized that small Mafs might be regulating

Adamts12 mRNA expression directly in the lens. Ring domain-containing uqiquitin protein ligase (E3) (*Rffl*), also known as CARP2, has been previously shown to negatively regulate caspases-8 and -10 and is involved in inhibition of apoptosis (W. Yang et al., 2007). Also, based on RNA expression analysis and ChIP-chip studies, *Rffl* is expressed in the lens placode at E9.5 and is regulated directly by Pax6 (Xie et al., 2013). Based on the microarray analysis, *MafG* is lens enriched at early embryonic developmental stages. Since *Rffl* is 1.7-fold down-regulated in *MafG-/-:MafK+/-* mutant lens, and has the ARE sites and is expressed in the lens, it can be speculated that MafG might be directly regulating *Rffl* in the lens.

Furthermore, multiple PDZ domain protein (*Mpdz*) has been shown to be expressed in the lens at neonatal time points and related PDZ domain proteins (Scib and Dlg) have been shown to be required for cell cycle regulation and differentiation in the mouse lens (Nguyen et al., 2003). Although the biological relevance of Mpdz is unclear in the lens, it is possible that small Mafs might be regulating the *Mpdz* transcriptionally by binding the ARE sites that were identified in the promoter regions of this gene. A small Maf regulatory pathway was devised based on functional insights of these genes from literature, and it proposes direct involvement of small Maf along with their heterodimers in regulating down-stream target genes within distinct functional pathways (Figure 4.1).

Overall, my thesis research has led to the identification and functional characterization of the transcription factors, MafG and MafK, in regulation of lens fiber cell gene expression. Moreover, my research has demonstrated that deficiency of these

genes in a compound mouse mutant model causes severe lens fiber cell defects, including cataract. These findings imply *MafG* and *MafK* as important novel candidate genes for further examination in human cataract patients.
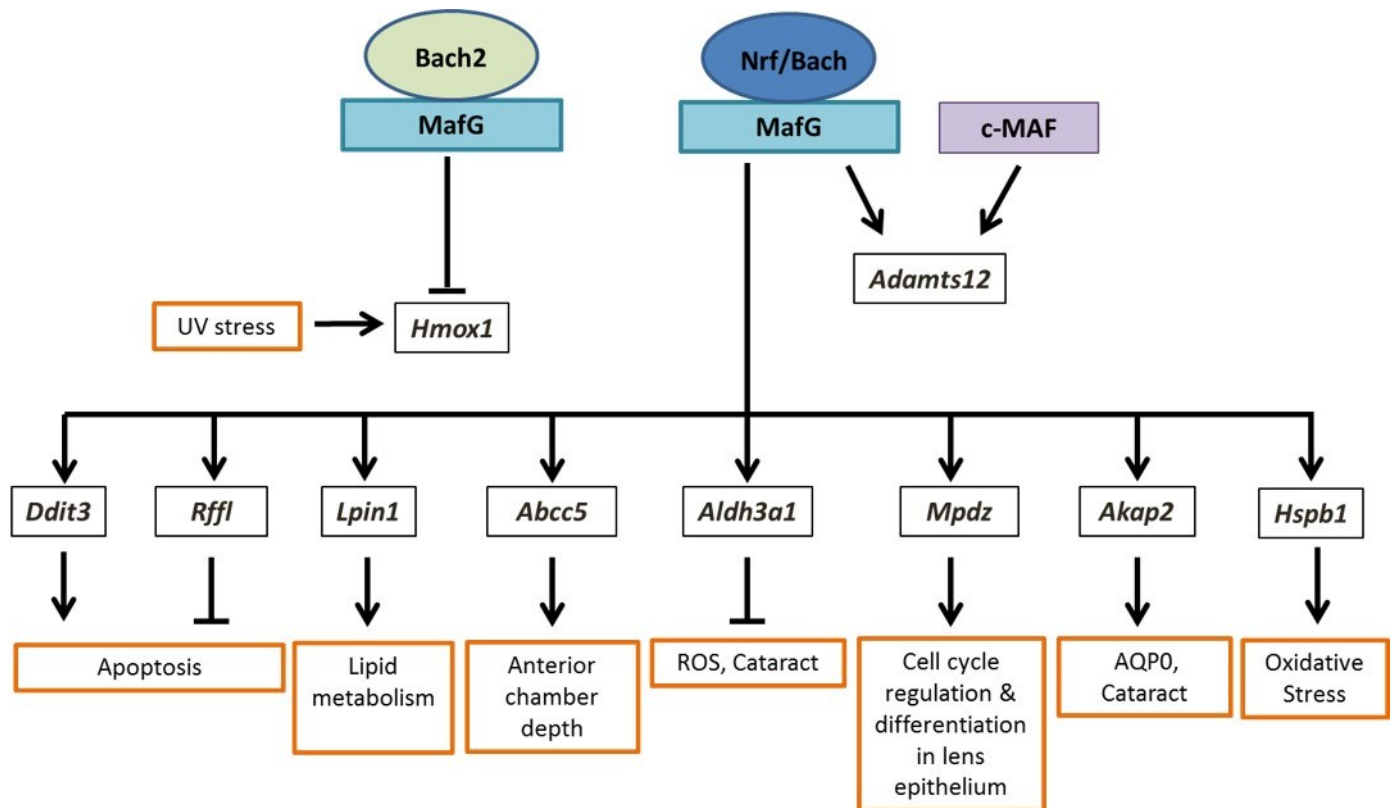
Figure 4.1. The small Maf regulatory pathway in the lens. Differentially regulated genes that had anti-oxidant response element (ARE) sites and exhibited lens-expression or lens-enriched expression, or had functional significance in lens biology, were utilized for the assembly of a preliminary gene regulatory pathway illustrating the contribution of small Maf TFs and their dimerization partners in the lens.

Chapter 5

FUTURE DIRECTIONS

Defining the role of small Maf proteins factors in the lens significantly advances our understanding of transcriptional regulatory mechanisms operational in fiber cells. Small Maf transcription factors MafG and MafK control gene regulation through complex mechanisms and can act as both transcriptional activators and repressors depending on their interactions with specific binding partners. This research establishes the function of MafG and MafK in lens homeostasis, and provides us with valuable insights into molecular alterations that are associated with lens pathology. Overall, this work contributes to the growing knowledge of regulatory factors alterations in which cause or are associated with the loss of lens transparency.

In order to characterize the morphological phenotype, I generated compound germline mutants for *MafG* and *MafK*, and demonstrated that complete loss of MafG, in combination with partial loss of MafK results in pre-senile cataracts in mice that can be observed at four months of age. *MafG-/-:MafK+/-* mice exhibit severe disruption of cortical fiber cells and membrane protrusions in the fiber cell compartment. *MafG-/-:MafK-/-* compound mutants are perinatal lethal and do not exhibit severe lens defects at embryonic day 16.5. Further examination of the fiber cell structure is required in lens from *MafG-/-:MafK-/-* compound mutants, but it has been speculated that there is a fiber cell migration defect and misplaced modiolus, and that the lens structure is not normal (Melinda Duncan, personal communication).

In order to gain insights into the regulation of MafG and MafK in the lens and understand the molecular mechanisms associated the etiology of cataract upon their compromise, I employed high throughput microarray-based gene expression profiling to identify genes that are differentially regulated in *MafG-/-:MafK+/-* compound mutant lens compared to *MafG+/-:MafK+/-* lens at two months of age. This analysis identified 1015 differentially regulated genes (DRGs) whose expression was altered in *MafG-/-:MafK+/-* compound mutants at 1.5-fold or above levels. These DRGs were subjected to integrated analysis of diverse selection filters based on lens expression, lens enriched expression, evidence of small Maf protein partner binding, biological function and literature-based evidence to identify promising candidates regulated by MafG and MafK in the lens.

Initial analysis based on these criteria led to the identification of 25 genes that have antioxidant response element (ARE) sites present in their near their genomic regions, and can represent as potential direct target candidates of small Mafs. Apart from ARE sites, small Mafs also recognize and bind to MARE (Maf recognition elements), TRE (12-O-tetradecanoyl phorbol 13-acetate (TPA)-responsive element), CRE (cAMP-responsive element) (Blank, 2007). In order to identify all the genes that have these sites, a comprehensive bioinformatics approach would have to be applied in future. Further, to validate these and other small Maf targets in the lens a chromatin immunoprecipitation (ChIP) experiment will need to be performed. ChIP can be followed by sequencing (ChIP-seq) or by qPCR of promising candidate regions predicted from the above bioinformatics study. ChIP may be challenging to perform

using whole lens tissue because the number of transcriptionally active cells may be a limiting factor for these experiments. However, recent research from the Lachke laboratory on the characterization of mouse and human lens epithelial cell cultures has determined these cells to express MafG and some of its binging partners and therefore can be used as reagents in ChIP assays. These experiments will lead to the identification of genes that are transcriptionally regulated by direct binding of MafG in lens cells.

These studies have opened up several new questions regarding the function of small Mafs in the lens that will be challenges for future work. Primarily, although my thesis research has led to the identification of several new target genes that are mis-expressed in *MafG-/-:MafK+/-* mutants, it remains to be determined how many of these are direct targets of these small Maf proteins. As small Maf transcription factors are known to dimerize with various binding partners in order to act as transcriptional activators or repressors, it will be interesting to investigate the nature of these interactions in the lens. Although I have shown that the expression of *Bach2*, *Nfe2l1*, and *Nfe2l2* are significantly enriched in mouse lens development, it is unknown whether binding of small Mafs to each or any of these factors affects transcriptional regulation of the downstream genes in a positive or negative manner. Binding to these specific proteins can be tested in co-immunoprecipitation assays. Thus, in order to address these concerns, further experimentation is required to gain a full understanding of the underlying molecular mechanisms regulated by small Mafs.

Finally, characterization of lens phenotypes in *MafG-/-:MafK-/-* compound mutant mice was challenging as these mice are perinatal lethal and therefore the

compound effect of these deleted genes could not be tested in post-natal stages. In order to comprehensively investigate the ocular pathology resulting when both copies of alleles are deleted for *MafG* and *MafK* in the lens, lens-specific conditional knock-out mice will need to be generated. This will provide further insights into the significance of MafG and MafK in the early postnatal lens. Furthermore, possible compensatory changes in MafK expression in the lens of mice homozygous null for MafG can provide us with additional insights into the transcriptional mechanisms by which MafG and MafK are regulated in the lens. This would also be helpful for analysis of the microarray data as it will be beneficial in identifying the specific targets. Thus, experiments discussed above will elucidate the molecular pathways regulated by small Maf proteins and their interactions with other regulatory factors in lens homeostasis.

REFERENCES

Andrews, N. C., Kotkow, K. J., Ney, P. A., Erdjument-Bromage, H., Tempst, P., & Orkin, S. H. (1993). The ubiquitous subunit of erythroid transcription factor NF-E2 is a small basic-leucine zipper protein related to the v-maf oncogene. *Proc Natl Acad Sci U S A, 90*(24), 11488-11492.

Arrigo, A. P., Simon, S., Gibert, B., Kretz-Remy, C., Nivon, M., Czekalla, A., . . . Vicart, P. (2007). Hsp27 (HspB1) and alphaB-crystallin (HspB5) as therapeutic targets. *FEBS Lett, 581*(19), 3665-3674. doi: 10.1016/j.febslet.2007.04.033

Ashery-Padan, R., Marquardt, T., Zhou, X., & Gruss, P. (2000). Pax6 activity in the lens primordium is required for lens formation and for correct placement of a single retina in the eye. *Genes Dev, 14*(21), 2701-2711.

Babizhayev, M. A., Deyev, A. I., Yermakova, V. N., Brikman, I. V., & Bours, J. (2004). Lipid peroxidation and cataracts: N-acetylcarnosine as a therapeutic tool to manage age-related cataracts in human and in canine eyes. *Drugs R D, 5*(3), 125-139.

Bassnett, S. (2002). Lens organelle degradation. *Exp Eye Res, 74*(1), 1-6. doi: 10.1006/exer.2001.1111

Bassnett, S. (2009). On the mechanism of organelle degradation in the vertebrate lens. *Exp Eye Res, 88*(2), 133-139. doi: 10.1016/j.exer.2008.08.017

Bassnett, S., & Shi, Y. (2010). A method for determining cell number in the undisturbed epithelium of the mouse lens. *Mol Vis, 16*, 2294-2300.

Benedek, G. B. (1971). Theory of transparency of the eye. *Appl Opt, 10*(3), 459-473.

Blank, V. (2008). Small Maf proteins in mammalian gene control: mere dimerization partners or dynamic transcriptional regulators? *J Mol Biol, 376*(4), 913-925. doi: 10.1016/j.jmb.2007.11.074

Blank, V., & Andrews, N. C. (1997). The Maf transcription factors: regulators of differentiation. *Trends Biochem Sci, 22*(11), 437-441.

Blixt, A., Mahlapuu, M., Aitola, M., Pelto-Huikko, M., Enerbäck, S., & Carlsson, P. (2000). A forkhead gene, FoxE3, is essential for lens epithelial proliferation and closure of the lens vesicle. *Genes Dev, 14*(2), 245-254.

Chan, E., Mahroo, O. A., & Spalton, D. J. (2010). Complications of cataract surgery. *Clin Exp Optom, 93*(6), 379-389. doi: 10.1111/j.1444-0938.2010.00516.x

Cheng, C., Xia, C. H., Huang, Q., Ding, L., Horwitz, J., & Gong, X. (2010). Altered chaperone-like activity of alpha-crystallins promotes cataractogenesis. *J Biol Chem, 285*(52), 41187-41193. doi: 10.1074/jbc.M110.154534

Chepelinsky, A. B. (2003). The ocular lens fiber membrane specific protein MIP/Aquaporin 0. *J Exp Zool A Comp Exp Biol, 300*(1), 41-46. doi: 10.1002/jez.a.10307

Chorley, B. N., Campbell, M. R., Wang, X., Karaca, M., Sambandan, D., Bangura, F., . . . Bell, D. A. (2012). Identification of novel NRF2-regulated genes by ChIP-Seq: influence on retinoid X receptor alpha. *Nucleic Acids Res, 40*(15), 7416-7429. doi: 10.1093/nar/gks409

Conte, I., Carrella, S., Avellino, R., Karali, M., Marco-Ferreres, R., Bovolenta, P., & Banfi, S. (2010). miR-204 is required for lens and retinal development via Meis2 targeting. *Proc Natl Acad Sci U S A, 107*(35), 15491-15496. doi: 10.1073/pnas.0914785107

Cui, X., Zhang, J., Du, R., Wang, L., Archacki, S., Zhang, Y., . . . Liu, M. (2012). HSF4 is involved in DNA damage repair through regulation of Rad51. *Biochim Biophys Acta, 1822*(8), 1308-1315. doi: 10.1016/j.bbadis.2012.05.005

Cvekl, A., & Duncan, M. K. (2007). Genetic and epigenetic mechanisms of gene regulation during lens development. *Prog Retin Eye Res, 26*(6), 555-597. doi: 10.1016/j.preteyeres.2007.07.002

Cvekl, A., & Piatigorsky, J. (1996). Lens development and crystallin gene expression: many roles for Pax-6. *Bioessays, 18*(8), 621-630. doi: 10.1002/bies.950180805

Cvekl, A., Yang, Y., Chauhan, B. K., & Cveklova, K. (2004). Regulation of gene expression by Pax6 in ocular cells: a case of tissue-preferred expression of crystallins in lens. *Int J Dev Biol, 48*(8-9), 829-844. doi: 10.1387/ijdb.041866ac

Delaye, M., & Tardieu, A. (1983). Short-range order of crystallin proteins accounts for eye lens transparency. *Nature, 302*(5907), 415-417.

Dewan, P., & Gupta, P. (2012). Burden of Congenital Rubella Syndrome (CRS) in India: a systematic review. *Indian Pediatr, 49*(5), 377-399.

Dey, S., Baird, T. D., Zhou, D., Palam, L. R., Spandau, D. F., & Wek, R. C. (2010). Both transcriptional regulation and translational control of ATF4 are central to the integrated stress response. *J Biol Chem, 285*(43), 33165-33174. doi: 10.1074/jbc.M110.167213

Donner, A. L., Episkopou, V., & Maas, R. L. (2007). Sox2 and Pou2f1 interact to control lens and olfactory placode development. *Dev Biol, 303*(2), 784-799. doi: 10.1016/j.ydbio.2006.10.047

Donner, A. L., Lachke, S. A., & Maas, R. L. (2006). Lens induction in vertebrates: variations on a conserved theme of signaling events. *Semin Cell Dev Biol, 17*(6), 676-685. doi: 10.1016/j.semcdb.2006.10.005

Duncan, M. K., Cui, W., Oh, D. J., & Tomarev, S. I. (2002). Prox1 is differentially localized during lens development. *Mech Dev, 112*(1-2), 195-198.

Duncan, M. K., Kozmik, Z., Cveklova, K., Piatigorsky, J., & Cvekl, A. (2000). Overexpression of PAX6(5a) in lens fiber cells results in cataract and upregulation of (alpha)5(beta)1 integrin expression. *J Cell Sci, 113 (Pt 18)*, 3173-3185.

Durand, M. L. (2013). Endophthalmitis. *Clin Microbiol Infect, 19*(3), 227-234. doi: 10.1111/1469-0691.12118

Eychène, A., Rocques, N., & Pouponnot, C. (2008). A new MAFia in cancer. *Nat Rev Cancer, 8*(9), 683-693. doi: 10.1038/nrc2460

Francis, P. J., & Moore, A. T. (1999). The lens. *Eye (Lond), 13 (Pt 3b)*, 393-394. doi: 10.1038/eye.1999.112

Fu, L., & Liang, J. J. (2002). Detection of protein-protein interactions among lens crystallins in a mammalian two-hybrid system assay. *J Biol Chem, 277*(6), 4255-4260. doi: 10.1074/jbc.M110027200

Fu, L., & Liang, J. J. (2003). Enhanced stability of alpha B-crystallin in the presence of small heat shock protein Hsp27. *Biochem Biophys Res Commun, 302*(4), 710-714.

Fujimoto, M., Izu, H., Seki, K., Fukuda, K., Nishida, T., Yamada, S., . . . Nakai, A. (2004). HSF4 is required for normal cell growth and differentiation during mouse lens development. *EMBO J, 23*(21), 4297-4306. doi: 10.1038/sj.emboj.7600435

Gilbert, C., & Foster, A. (2001). Blindness in children: control priorities and research opportunities. *Br J Ophthalmol, 85*(9), 1025-1027.

Gong, X., Cheng, C., & Xia, C. H. (2007). Connexins in lens development and cataractogenesis. *J Membr Biol, 218*(1-3), 9-12. doi: 10.1007/s00232-007-9033-0

Goudreau, G., Petrou, P., Reneker, L. W., Graw, J., Löster, J., & Gruss, P. (2002). Mutually regulated expression of Pax6 and Six3 and its implications for the Pax6 haploinsufficient lens phenotype. *Proc Natl Acad Sci U S A, 99*(13), 8719-8724. doi: 10.1073/pnas.132195699

Grainger, R. M., Henry, J. J., Saha, M. S., & Servetnick, M. (1992). Recent progress on the mechanisms of embryonic lens formation. *Eye (Lond), 6 (Pt 2)*, 117-122. doi: 10.1038/eye.1992.26

Graw, J. (1999). Cataract mutations and lens development. *Prog Retin Eye Res, 18*(2), 235-267.

Graw, J. (2009). Mouse models of cataract. *J Genet, 88*(4), 469-486.

Graw, J. (2010). Eye development. *Curr Top Dev Biol, 90*, 343-386. doi: 10.1016/s0070-2153(10)90010-0

Hejtmancik, J. F. (2008). Congenital cataracts and their molecular genetics. *Semin Cell Dev Biol, 19*(2), 134-149. doi: 10.1016/j.semcdb.2007.10.003

Hejtmancik, J. F., & Kantorow, M. (2004). Molecular genetics of age-related cataract. *Exp Eye Res, 79*(1), 3-9. doi: 10.1016/j.exer.2004.03.014

Hill, R. E., Favor, J., Hogan, B. L., Ton, C. C., Saunders, G. F., Hanson, I. M., . . . van Heyningen, V. (1991). Mouse small eye results from mutations in a paired-like homeobox-containing gene. *Nature, 354*(6354), 522-525. doi: 10.1038/354522a0

Ho, H. Y., Chang, K. H., Nichols, J., & Li, M. (2009). Homeodomain protein Pitx3 maintains the mitotic activity of lens epithelial cells. *Mech Dev, 126*(1-2), 18-29. doi: 10.1016/j.mod.2008.10.007

Hogan, B. L., Horsburgh, G., Cohen, J., Hetherington, C. M., Fisher, G., & Lyon, M. F. (1986). Small eyes (Sey): a homozygous lethal mutation on chromosome 2 which affects the differentiation of both lens and nasal placodes in the mouse. *J Embryol Exp Morphol, 97*, 95-110.

Hong, E., Yik, J., Amanatullah, D. F., Di Cesare, P. E., & Haudenschild, D. R. (2013). c-Maf Transcription Factor Regulates ADAMTS-12 Expression in Human Chondrogenic Cells. *Cartilage, 4*(2), 177-186.

Huang, J., Rajagopal, R., Liu, Y., Dattilo, L. K., Shaham, O., Ashery-Padan, R., & Beebe, D. C. (2011). The mechanism of lens placode formation: a case of matrix-mediated morphogenesis. *Dev Biol, 355*(1), 32-42. doi: 10.1016/j.ydbio.2011.04.008

Ikesugi, K., Yamamoto, R., Mulhern, M. L., & Shinohara, T. (2006). Role of the unfolded protein response (UPR) in cataract formation. *Exp Eye Res, 83*(3), 508-516. doi: 10.1016/j.exer.2006.01.033

Jamieson, R. V., Munier, F., Balmer, A., Farrar, N., Perveen, R., & Black, G. C. (2003). Pulverulent cataract with variably associated microcornea and iris coloboma in a MAF mutation family. *Br J Ophthalmol, 87*(4), 411-412.

Jamieson, R. V., Perveen, R., Kerr, B., Carette, M., Yardley, J., Heon, E., . . . Black, G. C. (2002). Domain disruption and mutation of the bZIP transcription factor, MAF, associated with cataract, ocular anterior segment dysgenesis and coloboma. *Hum Mol Genet, 11*(1), 33-42.

Javitt, J. C., Wang, F., & West, S. K. (1996). Blindness due to cataract: epidemiology and prevention. *Annu Rev Public Health, 17*, 159-177. doi: 10.1146/annurev.pu.17.050196.001111

Kannan, M. B., Solovieva, V., & Blank, V. (2012). The small MAF transcription factors MAFF, MAFG and MAFK: current knowledge and perspectives. *Biochim Biophys Acta, 1823*(10), 1841-1846. doi: 10.1016/j.bbamcr.2012.06.012

Kataoka, K. (2007). Multiple mechanisms and functions of maf transcription factors in the regulation of tissue-specific genes. *J Biochem, 141*(6), 775-781. doi: 10.1093/jb/mvm105

Kawauchi, S., Takahashi, S., Nakajima, O., Ogino, H., Morita, M., Nishizawa, M., . . . Yamamoto, M. (1999). Regulation of lens fiber cell differentiation by transcription factor c-Maf. *J Biol Chem, 274*(27), 19254-19260.

Kim, J. I., Li, T., Ho, I. C., Grusby, M. J., & Glimcher, L. H. (1999). Requirement for the c-Maf transcription factor in crystallin gene regulation and lens development. *Proc Natl Acad Sci U S A, 96*(7), 3781-3785.

Kobayashi, A., Tsukide, T., Miyasaka, T., Morita, T., Mizoroki, T., Saito, Y., . . . Yamamoto, M. (2011). Central nervous system-specific deletion of transcription factor Nrf1 causes progressive motor neuronal dysfunction. *Genes Cells, 16*(6), 692-703. doi: 10.1111/j.1365-2443.2011.01522.x

Kotkow, K. J., & Orkin, S. H. (1996). Complexity of the erythroid transcription factor NF-E2 as revealed by gene targeting of the mouse p18 NF-E2 locus. *Proc Natl Acad Sci U S A, 93*(8), 3514-3518.

Lachke, S. A., Alkuraya, F. S., Kneeland, S. C., Ohn, T., Aboukhalil, A., Howell, G. R., . . . Maas, R. L. (2011). Mutations in the RNA granule component TDRD7 cause cataract and glaucoma. *Science, 331*(6024), 1571-1576. doi: 10.1126/science.1195970

Lachke, S. A., Higgins, A. W., Inagaki, M., Saadi, I., Xi, Q., Long, M., . . . Maas, R. L. (2012). The cell adhesion gene PVRL3 is associated with congenital ocular defects. *Hum Genet, 131*(2), 235-250. doi: 10.1007/s00439-011-1064-z

Lachke, S. A., Ho, J. W., Kryukov, G. V., O'Connell, D. J., Aboukhalil, A., Bulyk, M. L., . . . Maas, R. L. (2012). iSyTE: integrated Systems Tool for Eye gene discovery. *Invest Ophthalmol Vis Sci, 53*(3), 1617-1627. doi: 10.1167/iovs.11-8839

Lachke, S. A., & Maas, R. L. (2010). Building the developmental oculome: systems biology in vertebrate eye development and disease. *Wiley Interdiscip Rev Syst Biol Med, 2*(3), 305-323. doi: 10.1002/wsbm.59

Lachke, S. A., & Maas, R. L. (2011). RNA Granules and Cataract. *Expert Rev Ophthalmol, 6*(5), 497-500. doi: 10.1586/eop.11.53

Landgren, H., Blixt, A., & Carlsson, P. (2008). Persistent FoxE3 expression blocks cytoskeletal remodeling and organelle degradation during lens fiber differentiation. *Invest Ophthalmol Vis Sci, 49*(10), 4269-4277. doi: 10.1167/iovs.08-2243

Li, W., Yu, S., Liu, T., Kim, J. H., Blank, V., Li, H., & Kong, A. N. (2008). Heterodimerization with small Maf proteins enhances nuclear retention of Nrf2 via masking the NESzip motif. *Biochim Biophys Acta, 1783*(10), 1847-1856. doi: 10.1016/j.bbamcr.2008.05.024

Li, W. C., Kuszak, J. R., Dunn, K., Wang, R. R., Ma, W., Wang, G. M., . . . Weiss, M. (1995). Lens epithelial cell apoptosis appears to be a common cellular basis for non-congenital cataract development in humans and animals. *J Cell Biol, 130*(1), 169-181.

Liu, W., Lagutin, O. V., Mende, M., Streit, A., & Oliver, G. (2006). Six3 activation of Pax6 expression is essential for mammalian lens induction and specification. *EMBO J, 25*(22), 5383-5395. doi: 10.1038/sj.emboj.7601398

Lovicu, F. J., & Robinson, M. L. (2004). *Development of the ocular lens*. Cambridge: Cambridge University Press.

Lyon, M. F., Jamieson, R. V., Perveen, R., Glenister, P. H., Griffiths, R., Boyd, Y., . . . Black, G. C. (2003). A dominant mutation within the DNA-binding domain of the bZIP transcription factor Maf causes murine cataract and results in selective alteration in DNA binding. *Hum Mol Genet, 12*(6), 585-594.

Manthey, A. L., Lachke, S. A., FitzGerald, P. G., Mason, R. W., Scheiblin, D. A., McDonald, J. H., & Duncan, M. K. (2014). Loss of Sip1 leads to migration

defects and retention of ectodermal markers during lens development. *Mech Dev, 131*, 86-110. doi: 10.1016/j.mod.2013.09.005

Martinez, G., & de Iongh, R. U. (2010). The lens epithelium in ocular health and disease. *Int J Biochem Cell Biol, 42*(12), 1945-1963. doi: 10.1016/j.biocel.2010.09.012

Mathias, R. T., White, T. W., & Gong, X. (2010). Lens gap junctions in growth, differentiation, and homeostasis. *Physiol Rev, 90*(1), 179-206. doi: 10.1152/physrev.00034.2009

Matsuo, T., Osumi-Yamashita, N., Noji, S., Ohuchi, H., Koyama, E., Myokai, F., . . . Iseki, S. (1993). A mutation in the Pax-6 gene in rat small eye is associated with impaired migration of midbrain crest cells. *Nat Genet, 3*(4), 299-304. doi: 10.1038/ng0493-299

McAvoy, J. W., Chamberlain, C. G., de Iongh, R. U., Hales, A. M., & Lovicu, F. J. (1999). Lens development. *Eye (Lond), 13 (Pt 3b)*, 425-437. doi: 10.1038/eye.1999.117

McCarty, C. A., & Taylor, H. R. (2001). The genetics of cataract. *Invest Ophthalmol Vis Sci, 42*(8), 1677-1678.

Min, J. N., Zhang, Y., Moskophidis, D., & Mivechi, N. F. (2004). Unique contribution of heat shock transcription factor 4 in ocular lens development and fiber cell differentiation. *Genesis, 40*(4), 205-217. doi: 10.1002/gene.20087

Motohashi, H., Shavit, J. A., Igarashi, K., Yamamoto, M., & Engel, J. D. (1997). The world according to Maf. *Nucleic Acids Res, 25*(15), 2953-2959.

Murphy, P., & Kolstø, A. (2000). Expression of the bZIP transcription factor TCF11 and its potential dimerization partners during development. *Mech Dev, 97*(1-2), 141-148.

Nguyen, M. M., Nguyen, M. L., Caruana, G., Bernstein, A., Lambert, P. F., & Griep, A. E. (2003). Requirement of PDZ-containing proteins for cell cycle regulation and differentiation in the mouse lens epithelium. *Mol Cell Biol, 23*(24), 8970-8981.

Nishiguchi, S., Wood, H., Kondoh, H., Lovell-Badge, R., & Episkopou, V. (1998). Sox1 directly regulates the gamma-crystallin genes and is essential for lens development in mice. *Genes Dev, 12*(6), 776-781.

Onodera, K., Shavit, J. A., Motohashi, H., Katsuoka, F., Akasaka, J. E., Engel, J. D., & Yamamoto, M. (1999). Characterization of the murine mafF gene. *J Biol Chem, 274*(30), 21162-21169.

Onodera, K., Shavit, J. A., Motohashi, H., Yamamoto, M., & Engel, J. D. (2000). Perinatal synthetic lethality and hematopoietic defects in compound mafG::mafK mutant mice. *EMBO J, 19*(6), 1335-1345. doi: 10.1093/emboj/19.6.1335

Orssaud, C., Dufier, J., & Germain, D. (2003). Ocular manifestations in Fabry disease: a survey of 32 hemizygous male patients. *Ophthalmic Genet, 24*(3), 129-139.

Petrash, J. M. (2013). Aging and age-related diseases of the ocular lens and vitreous body. *Invest Ophthalmol Vis Sci, 54*(14), ORSF54-59. doi: 10.1167/iovs.13-12940

Pontoriero, G. F., Smith, A. N., Miller, L. A., Radice, G. L., West-Mays, J. A., & Lang, R. A. (2009). Co-operative roles for E-cadherin and N-cadherin during lens vesicle separation and lens epithelial cell survival. *Dev Biol, 326*(2), 403-417. doi: 10.1016/j.ydbio.2008.10.011

Rao, R. C., & Perry, L. J. (2011). Decreased vision following eye trauma. *JAMA, 306*(23), 2606-2607. doi: 10.1001/jama.2011.1832

Reza, H. M., & Yasuda, K. (2004). Roles of Maf family proteins in lens development. *Dev Dyn, 229*(3), 440-448. doi: 10.1002/dvdy.10467

Ring, B. Z., Cordes, S. P., Overbeek, P. A., & Barsh, G. S. (2000). Regulation of mouse lens fiber cell development and differentiation by the Maf gene. *Development, 127*(2), 307-317.

Robinson, M. L., & Overbeek, P. A. (1996). Differential expression of alpha A- and alpha B-crystallin during murine ocular development. *Invest Ophthalmol Vis Sci, 37*(11), 2276-2284.

Rowan, S., Siggers, T., Lachke, S. A., Yue, Y., Bulyk, M. L., & Maas, R. L. (2010). Precise temporal control of the eye regulatory gene Pax6 via enhancer-binding site affinity. *Genes Dev, 24*(10), 980-985. doi: 10.1101/gad.1890410

Sakai, M., Serria, M. S., Ikeda, H., Yoshida, K., Imaki, J., & Nishi, S. (2001). Regulation of c-maf gene expression by Pax6 in cultured cells. *Nucleic Acids Res, 29*(5), 1228-1237.

Sandilands, A., Wang, X., Hutcheson, A. M., James, J., Prescott, A. R., Wegener, A., . . . Quinlan, R. A. (2004). Bfsp2 mutation found in mouse 129 strains causes the loss of CP49 and induces vimentin-dependent changes in the lens fibre cell cytoskeleton. *Exp Eye Res, 78*(1), 109-123.

Santana, A., & Waiswo, M. (2011). The genetic and molecular basis of congenital cataract. *Arq Bras Oftalmol, 74*(2), 136-142.

Shaham, O., Gueta, K., Mor, E., Oren-Giladi, P., Grinberg, D., Xie, Q., . . . Ashery-Padan, R. (2013). Pax6 regulates gene expression in the vertebrate lens through miR-204. *PLoS Genet, 9*(3), e1003357. doi: 10.1371/journal.pgen.1003357

Shaham, O., Smith, A. N., Robinson, M. L., Taketo, M. M., Lang, R. A., & Ashery-Padan, R. (2009). Pax6 is essential for lens fiber cell differentiation. *Development, 136*(15), 2567-2578. doi: 10.1242/dev.032888

Sharma, K. K., & Santhoshkumar, P. (2009). Lens aging: effects of crystallins. *Biochim Biophys Acta, 1790*(10), 1095-1108. doi: 10.1016/j.bbagen.2009.05.008

Shavit, J. A., Motohashi, H., Onodera, K., Akasaka, J., Yamamoto, M., & Engel, J. D. (1998). Impaired megakaryopoiesis and behavioral defects in mafG-null mutant mice. *Genes Dev, 12*(14), 2164-2174.

Shichi, H. (2004). Cataract formation and prevention. *Expert Opin Investig Drugs, 13*(6), 691-701. doi: 10.1517/13543784.13.6.691

Shiels, A., Bennett, T. M., & Hejtmancik, J. F. (2010). Cat-Map: putting cataract on the map. *Mol Vis, 16*, 2007-2015.

Shiels, A., & Hejtmancik, J. F. (2013). Genetics of human cataract. *Clin Genet, 84*(2), 120-127. doi: 10.1111/cge.12182

Shimokawa, N., Okada, J., & Miura, M. (2000). Cloning of MafG homologue from the rat brain by differential display and its expression after hypercapnic stimulation. *Mol Cell Biochem, 203*(1-2), 135-141.

Sinha, R., Bali, S. J., Kumar, C., Shekhar, H., Sharma, N., Titiyal, J. S., & Vajpayee, R. B. (2013). Results of cataract surgery and plasma ablation posterior capsulotomy in anterior persistent hyperplastic primary vitreous. *Middle East Afr J Ophthalmol, 20*(3), 217-220. doi: 10.4103/0974-9233.114794

Slingsby, C., Wistow, G. J., & Clark, A. R. (2013). Evolution of crystallins for a role in the vertebrate eye lens. *Protein Sci, 22*(4), 367-380. doi: 10.1002/pro.2229

Toki, T., Itoh, J., Kitazawa, J., Arai, K., Hatakeyama, K., Akasaka, J., . . . Ito, E. (1997). Human small Maf proteins form heterodimers with CNC family transcription factors and recognize the NF-E2 motif. *Oncogene, 14*(16), 1901-1910. doi: 10.1038/sj.onc.1201024

Trumler, A. A. (2011). Evaluation of pediatric cataracts and systemic disorders. *Curr Opin Ophthalmol, 22*(5), 365-379. doi: 10.1097/ICU.0b013e32834994dc

Ueda, Y., Duncan, M. K., & David, L. L. (2002). Lens proteomics: the accumulation of crystallin modifications in the mouse lens with age. *Invest Ophthalmol Vis Sci, 43*(1), 205-215.

Vanita, V., Singh, D., Robinson, P. N., Sperling, K., & Singh, J. R. (2006). A novel mutation in the DNA-binding domain of MAF at 16q23.1 associated with autosomal dominant "cerulean cataract" in an Indian family. *Am J Med Genet A, 140*(6), 558-566. doi: 10.1002/ajmg.a.31126

Varadaraj, K., Kumari, S. S., & Mathias, R. T. (2010). Transgenic expression of AQP1 in the fiber cells of AQP0 knockout mouse: effects on lens transparency. *Exp Eye Res, 91*(3), 393-404. doi: 10.1016/j.exer.2010.06.013

Varadaraj, K., Kumari, S. S., Patil, R., Wax, M. B., & Mathias, R. T. (2008). Functional characterization of a human aquaporin 0 mutation that leads to a congenital dominant lens cataract. *Exp Eye Res, 87*(1), 9-21. doi: 10.1016/j.exer.2008.04.001

Wei, J., Richbourgh, B., Jia, T., & Liu, C. (2014). ADAMTS-12: A Multifaced Metalloproteinase in Arthritis and Inflammation. *Mediators Inflamm, 2014*, 649718. doi: 10.1155/2014/649718

Wigle, J. T., Chowdhury, K., Gruss, P., & Oliver, G. (1999). Prox1 function is crucial for mouse lens-fibre elongation. *Nat Genet, 21*(3), 318-322. doi: 10.1038/6844

Wolf, L., Harrison, W., Huang, J., Xie, Q., Xiao, N., Sun, J., . . . Cvekl, A. (2013). Histone posttranslational modifications and cell fate determination: lens induction requires the lysine acetyltransferases CBP and p300. *Nucleic Acids Res, 41*(22), 10199-10214. doi: 10.1093/nar/gkt824

Wride, M. A. (2011). Lens fibre cell differentiation and organelle loss: many paths lead to clarity. *Philos Trans R Soc Lond B Biol Sci, 366*(1568), 1219-1233. doi: 10.1098/rstb.2010.0324

Wurm, A., Sock, E., Fuchshofer, R., Wegner, M., & Tamm, E. R. (2008). Anterior segment dysgenesis in the eyes of mice deficient for the high-mobility-group transcription factor Sox11. *Exp Eye Res, 86*(6), 895-907. doi: 10.1016/j.exer.2008.03.004

Xie, Q., & Cvekl, A. (2011). The orchestration of mammalian tissue morphogenesis through a series of coherent feed-forward loops. *J Biol Chem, 286*(50), 43259-43271. doi: 10.1074/jbc.M111.264580

Xie, Q., Yang, Y., Huang, J., Ninkovic, J., Walcher, T., Wolf, L., . . . Cvekl, A. (2013). Pax6 interactions with chromatin and identification of its novel direct target genes in lens and forebrain. *PLoS One, 8*(1), e54507. doi: 10.1371/journal.pone.0054507

Yamada, R., Mizutani-Koseki, Y., Hasegawa, T., Osumi, N., Koseki, H., & Takahashi, N. (2003). Cell-autonomous involvement of Mab21l1 is essential for lens placode development. *Development, 130*(9), 1759-1770.

Yamazaki, H., Katsuoka, F., Motohashi, H., Engel, J. D., & Yamamoto, M. (2012). Embryonic lethality and fetal liver apoptosis in mice lacking all three small Maf proteins. *Mol Cell Biol, 32*(4), 808-816. doi: 10.1128/mcb.06543-11

Yang, W., Rozan, L. M., McDonald, E. R., 3rd, Navaraj, A., Liu, J. J., Matthew, E. M., . . . El-Deiry, W. S. (2007). CARPs are ubiquitin ligases that promote MDM2-independent p53 and phospho-p53ser20 degradation. *J Biol Chem, 282*(5), 3273-3281. doi: 10.1074/jbc.M610793200

Yang, Y., Stopka, T., Golestaneh, N., Wang, Y., Wu, K., Li, A., . . . Cvekl, A. (2006). Regulation of alphaA-crystallin via Pax6, c-Maf, CREB and a broad domain of lens-specific chromatin. *EMBO J, 25*(10), 2107-2118. doi: 10.1038/sj.emboj.7601114

Yi, J., Yun, J., Li, Z. K., Xu, C. T., & Pan, B. R. (2011). Epidemiology and molecular genetics of congenital cataracts. *Int J Ophthalmol, 4*(4), 422-432. doi: 10.3980/j.issn.2222-3959.2011.04.20

Yoshida, C., Yoshida, F., Sears, D. E., Hart, S. M., Ikebe, D., Muto, A., . . . Melo, J. V. (2007). Bcr-Abl signaling through the PI-3/S6 kinase pathway inhibits nuclear translocation of the transcription factor Bach2, which represses the antiapoptotic factor heme oxygenase-1. *Blood, 109*(3), 1211-1219. doi: 10.1182/blood-2005-12-040972

Yoshida, K., Kim, J. I., Imaki, J., Hiromi, I., Nishi, S., Matsuda, H., . . . Sakai, M. (2001). Proliferation in the posterior region of the lens of c-maf-/- mice. *Curr Eye Res, 23*(2), 116-119.

Zandy, A. J., Lakhani, S., Zheng, T., Flavell, R. A., & Bassnett, S. (2005). Role of the executioner caspases during lens development. *J Biol Chem, 280*(34), 30263-30272. doi: 10.1074/jbc.M504007200

Zhang, X., Friedman, A., Heaney, S., Purcell, P., & Maas, R. L. (2002). Meis homeoproteins directly regulate Pax6 during vertebrate lens morphogenesis. *Genes Dev, 16*(16), 2097-2107. doi: 10.1101/gad.1007602

Zheng, Y., Liu, Y., Ge, J., Wang, X., Liu, L., Bu, Z., & Liu, P. (2010). Resveratrol protects human lens epithelial cells against H2O2-induced oxidative stress by increasing catalase, SOD-1, and HO-1 expression. *Mol Vis, 16*, 1467-1474.

Appendix A

DIFFERENTIALLY REGULATED GENES (DRG) IN *MAFG-/-:MAFK+/-* MUTANT LENS BASED ON MICROARRAY ANALYSIS

Table A.1 Complete list of differentially regulated genes in MafG-/-:MafK+/- mouse lens in comparison to *MafG+/-:MafK+/-* mutant lens from whole genome gene expression profiling by microarrays at 2 months of age.

Differentially up-regulated genes	
Gene ID	**Fold change (F.C)**
DCTN4	6.46
Hmgcs1	4.12
Hmgxb3	3.25
DDIT3	3.24
FDPS	2.64
CYP51	2.63
Arsi	2.55
Gm8163	2.53
SQLE	2.47
SC4MOL	2.42
HMOX1	2.38
KLHL9	2.37
BC032265	2.35
CHRNG	2.28
SQLE	2.24
GM106	2.15
INSIG1	2.03
XBP1	2.02
PSMB5	1.98
CYP26A1	1.98
Rpsa-ps11	1.94
1700123O20RIK	1.93
TMEM14C	1.91
LYZL4	1.90
INSIG1	1.87

Gm3716	1.79
STARD4	1.76
ARSI	1.75
HSD17B7	1.74
CRELD2	1.71
CDK2AP2	1.70
DDIT3	1.69
DLEU2	1.69
RIOK1	1.69
HOPX	1.68
PLK3	1.68
MANBAL	1.67
RPS3	1.67
9430081H08RIK	1.65
NDST1	1.65
NUP160	1.65
CHAC1	1.65
KCTD12	1.64
DNAJB9	1.63
Cldn26	1.63
DHCR24	1.63
CRELD2	1.62
AACS	1.62
SUPT16H	1.61
SERPINF1	1.60
ARFGAP2	1.58
KDELR2	1.57
RPRM	1.56
PNPLA3	1.56
ACAT2	1.56
TMSB10	1.56
Mir17hg	1.56
Vstm4	1.55
INSIG1	1.54
Spaca6	1.53
GAA	1.52

CALR	1.52
TMEM55B	1.52
KLHL22	1.51
SYNPO	1.50
TMEM55A	1.50
Differentially down-regulated genes	
TTC27	-10.91
C630022N07RIK	-10.65
MAFG	-9.11
NCSTN	-8.08
LOC100047628	-5.60
IGK-C	-5.52
TMEM32	-3.89
ALDH3A1	-3.64
WFDC1	-3.63
BGN	-3.48
GJB6	-3.47
ALOX5AP	-3.31
5730507A09RIK	-3.16
ALOX5AP	-3.07
PBLD	-3.05
OPTC	-3.05
PTPN14	-2.92
TAP2	-2.78
LOC381739	-2.75
LOC208642	-2.72
4930402H24RIK	-2.70
SNHG11	-2.68
LOC383579	-2.67
DGAT2	-2.65
LIMS2	-2.58
SULT2B1	-2.57
LIMS2	-2.56
OTTMUSG00000005065	-2.54
LIMS2	-2.52
MAT2A	-2.51

USP39	-2.50
LOC385461	-2.49
PYGO1	-2.49
SEZ6L	-2.49
MAP4K4	-2.47
ERMAP	-2.46
RORC	-2.44
KIF2C	-2.43
OTTMUSG00000001070	-2.40
TREX1	-2.39
2500002E12RIK	-2.37
BC055324	-2.36
NTRK2	-2.36
APOE	-2.35
VAMP8	-2.34
CATSPER4	-2.34
IFT74	-2.33
SNHG11	-2.33
2010204K13RIK	-2.32
CLRN1	-2.31
SHANK2	-2.31
ACOX3	-2.31
PLEKHA4	-2.31
TARS	-2.28
MYO5C	-2.28
TFPI	-2.27
4632417K18RIK	-2.25
C3	-2.25
LOC380998	-2.25
CNDP2	-2.24
FBXW2	-2.24
4933425L03RIK	-2.23
2900017F05RIK	-2.22
WDR93	-2.21
IL1A	-2.21
NUDT7	-2.21

UCHL5IP	-2.21
MYL9	-2.21
PDE6G	-2.20
CCR9	-2.20
1300011L04RIK	-2.20
LRRC66	-2.20
TTC8	-2.19
ALDH1A3	-2.18
1700024C24RIK	-2.18
KLF4	-2.18
POLN	-2.18
BCL2L2	-2.17
MT1	-2.17
ASPHD2	-2.17
CORT	-2.15
HS6ST3	-2.15
LOC380781	-2.14
OLFR676	-2.13
EMP3	-2.13
TLE2	-2.12
1500005I02RIK	-2.12
PPFIBP2	-2.12
CALR4	-2.12
EG434729	-2.12
SH3BGRL	-2.11
2310010J17RIK	-2.11
CAMKK2	-2.11
SLC4A8	-2.10
RHOU	-2.10
1200016D23RIK	-2.09
RGL1	-2.09
AKAP6	-2.07
KIFAP3	-2.07
TRIM44	-2.07
WDR92	-2.07
PTGIR	-2.06

ASAH2	-2.06
CLCA3	-2.06
SFXN4	-2.06
FBLIM1	-2.05
MAD2L1BP	-2.05
ZCCHC3	-2.05
CRABP2	-2.05
C630004H02RIK	-2.04
THEM4	-2.04
BMP4	-2.04
FXN	-2.04
ATF7IP	-2.03
GYLTL1B	-2.03
TMEM166	-2.03
KDELC1	-2.03
SLC6A13	-2.03
IHPK2	-2.03
4932438A13RIK	-2.02
OLFR916	-2.02
C4B	-2.02
NUDT14	-2.01
MTRR	-2.01
D230034L24RIK	-2.01
S1PR4	-2.00
ATG2A	-2.00
ZCCHC3	-1.99
4933401F05RIK	-1.99
A630062H14	-1.99
LOC668433	-1.99
PPFIBP2	-1.99
6430706D22RIK	-1.99
DDX23	-1.99
RRP1B	-1.99
ICA1	-1.98
LOC100044159	-1.98
5730485H21RIK	-1.98

SHF	-1.98
WFDC2	-1.98
LOC634731	-1.98
2610024G14RIK	-1.98
RETNLA	-1.98
LOC384315	-1.98
IFT140	-1.98
HOXC9	-1.98
ZFP273	-1.98
CEACAM2	-1.97
6430527G18RIK	-1.97
2610024G14RIK	-1.97
PDYN	-1.97
P2RY10	-1.97
C1QTNF9	-1.97
PPM1F	-1.97
TXNDC15	-1.97
GP2	-1.96
SPINK12	-1.96
DBF4	-1.96
PVALB	-1.96
IFNE1	-1.96
PARD3B	-1.96
CNGB1	-1.95
2210012G02RIK	-1.95
LOC231069	-1.95
AMT	-1.95
0610040B10RIK	-1.95
OMP	-1.95
MYO5B	-1.95
YPEL2	-1.94
PKD1	-1.94
ZFP474	-1.94
AA467197	-1.94
EHMT1	-1.94
C230060E24	-1.94

PAICS	-1.94
DENR	-1.93
FMOD	-1.93
A230005G17RIK	-1.93
AA408296	-1.93
RNF186	-1.93
RKHD3	-1.93
LOC268652	-1.93
B3GNT5	-1.92
LOC100043972	-1.92
FN3K	-1.92
BC024537	-1.92
TREX1	-1.92
NAB1	-1.92
D330037H01RIK	-1.92
BC024659	-1.92
PCMTD2	-1.91
SLC25A34	-1.91
DEFB12	-1.91
2210021J22RIK	-1.91
SCL0002270.1_1	-1.91
SMPD2	-1.91
DACT2	-1.91
2600011C06RIK	-1.91
ABCA4	-1.91
MARS2	-1.91
RAB1	-1.90
BC017643	-1.90
KRT7	-1.90
ZFP428	-1.90
MTBP	-1.90
STK40	-1.90
EG328264	-1.90
C1QTNF2	-1.90
PIGL	-1.90
IGFBP4	-1.89

4922505G16RIK	-1.89
SULT2B1	-1.89
ZFP262	-1.89
RNF138	-1.89
NANOS2	-1.89
GALE	-1.89
DAP	-1.89
OLFR1394	-1.89
CCRL1	-1.89
JMJD1A	-1.89
ATP6V1G2	-1.89
UMODL1	-1.89
ARHGAP29	-1.88
EG433229	-1.88
MRP63	-1.88
FBXL4	-1.88
EG245376	-1.88
DST	-1.88
CUL1	-1.88
PRELP	-1.88
PGM5	-1.88
IVNS1ABP	-1.88
EG665509	-1.88
MFAP4	-1.88
2610312E17RIK	-1.88
B230342M21RIK	-1.87
PRR15	-1.87
LOC100048372	-1.87
0610030E20RIK	-1.87
1810033B17RIK	-1.87
ITGB1BP1	-1.87
CNKSR1	-1.86
GLRX2	-1.86
FSCN1	-1.86
PSMD12	-1.86
PTGES3	-1.86

1200016E24RIK	-1.86
TAL2	-1.86
KLC2	-1.86
GYLTL1B	-1.86
PLEKHA7	-1.86
STX3	-1.86
SNAP91	-1.86
USP38	-1.86
IL1B	-1.86
CD27	-1.85
YBX2	-1.85
LOC385992	-1.85
WWTR1	-1.85
CDH2	-1.85
BTBD2	-1.85
MYCS	-1.85
DDX25	-1.84
PEO1	-1.84
2610024G14RIK	-1.84
RAP2A	-1.84
TCFE3	-1.84
SOAT1	-1.84
ABCC5	-1.84
LOC239369	-1.84
AGPAT5	-1.84
LOC215098	-1.84
CEACAM10	-1.84
RAMP1	-1.84
SMC6	-1.83
LOC385632	-1.83
EG329123	-1.83
1700041C02RIK	-1.83
CBR2	-1.83
SSPN	-1.83
SLC10A7	-1.83
THNSL2	-1.83

SEH1L	-1.83
LOC100044696	-1.82
ROBO2	-1.82
KRT2	-1.82
ORF9	-1.82
DOCK5	-1.82
D830030K20RIK	-1.82
CHMP7	-1.82
SNAI3	-1.82
NUDT13	-1.82
LOC381892	-1.82
CHMP2B	-1.82
EGFBP2	-1.82
SUSD3	-1.82
RAB26	-1.81
FJX1	-1.81
CCDC9	-1.81
EG666731	-1.81
VDR	-1.81
TLE6	-1.81
A130010J15RIK	-1.81
LOC217372	-1.81
UHRF1BP1	-1.81
LOC100047052	-1.81
PGM5	-1.81
DEADC1	-1.81
FCHSD1	-1.80
TYW1	-1.80
OCIAD2	-1.80
IIGP2	-1.80
SLC17A8	-1.80
TMEM2	-1.80
GLRA4	-1.80
9330157O18RIK	-1.80
CLDN7	-1.80
COL6A2	-1.80

4933421B21RIK	-1.80
NECAP1	-1.80
EIF5B	-1.80
SCML4	-1.80
E130016E03RIK	-1.80
LOC383074	-1.79
4930430E16RIK	-1.79
BMPER	-1.79
GUS-S	-1.79
1110036O03RIK	-1.79
SRPR	-1.79
D430029G22RIK	-1.79
POSH-PENDING	-1.79
PPEF2	-1.79
BXDC1	-1.79
LOC386068	-1.79
MRGPRE	-1.79
SIAT7B	-1.79
4930565A21RIK	-1.79
EGFLAM	-1.79
TNNI3K	-1.79
LOC271697	-1.79
OLFR1390	-1.79
LOC241262	-1.79
KIT	-1.79
TXNIP	-1.78
VMO1	-1.78
LOC386169	-1.78
GLIS2	-1.78
AIFM1	-1.78
ATP8A1	-1.78
ZFP526	-1.78
SSBP1	-1.78
E330022B15RIK	-1.78
HECTD3	-1.78
ZFP467	-1.78

POFUT2	-1.78
STX11	-1.78
FGFR1OP2	-1.78
OTTMUSG00000015529	-1.77
WFDC12	-1.77
ARFRP1	-1.77
LOC100045241	-1.77
6030458B15RIK	-1.77
LTB4R1	-1.77
DTNA	-1.77
LPIN1	-1.77
ALKBH5	-1.77
AVPR2	-1.77
2810402E24RIK	-1.77
C730027P07RIK	-1.77
STAMBPL1	-1.77
OLFR350	-1.77
PCDHAC2	-1.77
4932416G22RIK	-1.77
MTF2	-1.77
FAF1	-1.77
NAPSA	-1.77
INSM1	-1.76
2410005G18RIK	-1.76
TEK	-1.76
LPP	-1.76
ATG4C	-1.76
TRFR2	-1.76
ACOT5	-1.76
MED1	-1.76
NRAS	-1.76
ATP8B2	-1.76
SERPING1	-1.76
9430077A04RIK	-1.76
1500026H17RIK	-1.76
MYBBP1A	-1.76

CP	-1.76
NXPH4	-1.76
RAB39	-1.76
V1RC25	-1.76
HHAT	-1.76
MORF4L1	-1.76
SPNS1	-1.76
NUP88	-1.76
TMEM120B	-1.75
E130012F07RIK	-1.75
LOC100046963	-1.75
GPR124	-1.75
1190020J12RIK	-1.75
CCNT2	-1.75
2010100O12RIK	-1.75
RUSC1	-1.75
LOC385248	-1.75
TXNIP	-1.75
NFU1	-1.75
FANCC	-1.74
E330019D12RIK	-1.74
SLC10A6	-1.74
STEAP1	-1.74
CRBN	-1.74
LOC100041613	-1.74
SFRS14	-1.74
RSU1	-1.74
4921517L17RIK	-1.74
MFSD10	-1.74
NUDT7	-1.74
DDX19B	-1.74
LOC381533	-1.74
HPS3	-1.74
SCL0002827.1_16	-1.73
D630041K24RIK	-1.73
PIK3IP1	-1.73

D930028F11RIK	-1.73
DPEP3	-1.73
S3-12	-1.73
ANKZF1	-1.73
GMCL1	-1.73
ABCC2	-1.73
BC088983	-1.73
ELOVL2	-1.73
E230024B12RIK	-1.73
C9	-1.73
DCXR	-1.73
2410017P07RIK	-1.72
ENSA	-1.72
UBE1X	-1.72
FAIM2	-1.72
PDZRN3	-1.72
CRYGF	-1.72
LOC100046500	-1.72
A730017C20RIK	-1.72
CEP120	-1.72
D930007M19RIK	-1.72
MBOAT2	-1.72
DNAJA3	-1.72
UBR5	-1.72
CDC42EP3	-1.72
LOC382009	-1.72
GNG11	-1.72
TCN2	-1.72
SH3BGR	-1.72
SPRYD4	-1.71
B130019G13RIK	-1.71
A830062E06RIK	-1.71
MAPK14	-1.71
RGS3	-1.71
LOC224054	-1.71
MTRF1	-1.71

SMAD1	-1.71
TNFRSF19	-1.71
DAGLA	-1.71
SCL0003176.1_43	-1.71
SLU7	-1.71
D930008O12RIK	-1.71
LOC245545	-1.71
POPDC3	-1.71
FBXW2	-1.71
SEMA3A	-1.71
CDCA8	-1.71
LBX2	-1.71
CALN1	-1.71
SHROOM4	-1.71
FREQ	-1.71
OLFR1250	-1.71
STRN	-1.71
RIN2	-1.71
MGST1	-1.71
PATZ1	-1.70
IMPDH1	-1.70
EG226957	-1.70
CEBPG	-1.70
SMR1	-1.70
WHSC1	-1.70
P2RX1	-1.70
KLHDC8B	-1.70
CTTNBP2NL	-1.70
C130048P03RIK	-1.70
TMEM47	-1.70
1300018I17RIK	-1.70
HPDL	-1.70
AA407270	-1.70
GSTO1	-1.70
STXBP5	-1.70
SLC6A3	-1.70

KATNAL1	-1.70
ZFP236	-1.70
DENND4B	-1.70
PAX8	-1.70
LARP6	-1.69
LOC100046792	-1.69
1700024G13RIK	-1.69
MRPL1	-1.69
DBI	-1.69
CTTN	-1.69
GNPDA1	-1.69
PCBD1	-1.69
HSD17B11	-1.69
TTPAL	-1.69
5730585A16RIK	-1.69
CCDC69	-1.69
A730069A04RIK	-1.69
1200015N20RIK	-1.69
MYLK	-1.69
ZFP760	-1.69
C730031B13RIK	-1.69
2810408M09RIK	-1.69
D730003I15RIK	-1.69
LY108	-1.69
PDE6B	-1.69
LOC234360	-1.69
CDC25A	-1.69
ANGPTL3	-1.69
GNAT1	-1.69
1810043G02RIK	-1.69
RB1CC1	-1.69
RBBP6	-1.69
COL8A2	-1.69
PPP1R14C	-1.69
MXD4	-1.68
MIXL1	-1.68

LOC669420	-1.68
1700028I04RIK	-1.68
ANKRD28	-1.68
LOC245676	-1.68
PAWR	-1.68
E130112E08RIK	-1.68
5630401D24RIK	-1.68
2310014L17RIK	-1.68
SLC1A3	-1.68
NLN	-1.68
CCNG1	-1.68
4732479B03RIK	-1.68
GAL3ST4	-1.68
TTC5	-1.68
PRX	-1.68
C030045D06RIK	-1.68
IGFBP5	-1.68
H2-DMB2	-1.68
TMEM79	-1.68
DEFB25	-1.68
AGXT2L2	-1.67
SKAP1	-1.67
PLEC1	-1.67
MTAP7D1	-1.67
RAB4A	-1.67
H1F0	-1.67
TIGD2	-1.67
PBX4	-1.67
NEK4	-1.67
LOC100048056	-1.67
NQO2	-1.67
ROD1	-1.67
PPP2R2B	-1.67
PLK2	-1.67
NAPRT1	-1.67
TRIM36	-1.67

AURKB	-1.67
LOC100047419	-1.67
CEP68	-1.67
NUP133	-1.67
NCOA1	-1.67
OCIAD2	-1.67
FBXL6	-1.66
SLC38A8	-1.66
RTN2	-1.66
1700027A23RIK	-1.66
9430014F16RIK	-1.66
A830019P03RIK	-1.66
LOC385130	-1.66
RFFL	-1.66
UFSP2	-1.66
MDK	-1.66
NCRNA00117	-1.66
FZD5	-1.66
41164	-1.66
1600014C23RIK	-1.66
LY96	-1.66
ENTPD5	-1.66
4930579E17RIK	-1.66
TFPT	-1.66
ADD1	-1.66
2310008I22RIK	-1.66
PSMG2	-1.66
4933429F08RIK	-1.66
6030416D17RIK	-1.66
PDGFRL	-1.66
PDYN	-1.66
GSTM4	-1.66
EG665378	-1.66
TERA-PENDING	-1.66
ISLR	-1.66
MFSD3	-1.66

ANKRD40	-1.66
SMAD1	-1.66
CYHR1	-1.66
EG665186	-1.66
A730042J05RIK	-1.66
4833426H15RIK	-1.65
CADPS2	-1.65
B3GALTL	-1.65
EG240549	-1.65
MFSD3	-1.65
FAM109A	-1.65
LOC230592	-1.65
TMEM120B	-1.65
OLFR786	-1.65
LOC381852	-1.65
ANKS6	-1.65
3110057O12RIK	-1.65
2610528B01RIK	-1.65
AI987712	-1.65
CDKL1	-1.65
NOL11	-1.65
FAM108B	-1.65
MSX3	-1.65
EG330503	-1.65
REG1	-1.65
GM817	-1.65
DHX9	-1.65
4930535I16RIK	-1.65
LOC634059	-1.65
PHF14	-1.65
SCL000650.1_5	-1.65
BOLL	-1.65
SERPINA1A	-1.65
NNAT	-1.65
VGF	-1.65
LRRC50	-1.65

SCL0002624.1_576	-1.65
SERPING1	-1.64
PIGA	-1.64
DOCK8	-1.64
POLR3K	-1.64
0610037D15RIK	-1.64
NAPRT1	-1.64
PEX5	-1.64
RNF6	-1.64
OLFR1495	-1.64
USP15	-1.64
OLFR1012	-1.64
LOC100046883	-1.64
4930428E23RIK	-1.64
GRM1	-1.64
OLFR142	-1.64
GM672	-1.64
TREML4	-1.64
GPR146	-1.64
TMEM218	-1.64
4933431K14RIK	-1.64
LOC380858	-1.64
1600002K03RIK	-1.64
MOSPD1	-1.64
FAM19A4	-1.64
CLDN17	-1.64
ADAMTS12	-1.64
BIRC6	-1.64
1700021P04RIK	-1.64
LOC381492	-1.64
LOC100045250	-1.64
CDKN2C	-1.64
A030007L17RIK	-1.64
CTH	-1.64
LOC381019	-1.64
2210418G03RIK	-1.64

LOC214403	-1.63
NR4A2	-1.63
AFMID	-1.63
STEAP3	-1.63
LAS1L	-1.63
NDRG3	-1.63
NSMCE2	-1.63
1810062O18RIK	-1.63
KCNJ10	-1.63
LOC675572	-1.63
4930538K18RIK	-1.63
LOC385642	-1.63
FBXW4	-1.63
UFD1L	-1.63
MMP24	-1.63
TGM2	-1.63
SYNE1	-1.63
NFS1	-1.63
RUFY3	-1.63
RFTN2	-1.63
RHO	-1.63
A930009M04RIK	-1.63
LOC100047264	-1.63
DOC2B	-1.63
GRAMD3	-1.63
COL6A3	-1.63
WDR70	-1.63
RBM12	-1.63
TRFR2	-1.63
ZSCAN20	-1.63
GRIPAP1	-1.63
IL17A	-1.63
A330044P14RIK	-1.63
FBXO46	-1.63
OLFR159	-1.63
TCTE2	-1.63

TK1	-1.63
2410006F04RIK	-1.63
6330403K07RIK	-1.62
LOC100039792	-1.62
DGUOK	-1.62
NARF	-1.62
ZFP644	-1.62
MRGPRF	-1.62
GATS	-1.62
MCM10	-1.62
FOXD2	-1.62
FBXO42	-1.62
TRIB2	-1.62
EDNRB	-1.62
ZBTB1	-1.62
TNNI3K	-1.62
RAB11FIP3	-1.62
IBSP	-1.62
NUP54	-1.62
KLK1B26	-1.62
PKMYT1	-1.62
PQLC2	-1.62
METRN	-1.62
BC022224	-1.62
GPR50	-1.62
D230037D09RIK	-1.62
ZFP93	-1.62
PLAU	-1.62
AGPS	-1.62
LOC381897	-1.62
ANO4	-1.62
WDR53	-1.62
ALS2CR4	-1.62
TEX9	-1.62
YTHDF3	-1.62
IGFBP5	-1.62

CAMK2N2	-1.62
4931429P17RIK	-1.62
6330414G02RIK	-1.62
9330154M19RIK	-1.62
TBC1D8	-1.61
CD93	-1.61
OLFR194	-1.61
1700007N01RIK	-1.61
PLEC1	-1.61
LOC245069	-1.61
PHF21A	-1.61
RARG	-1.61
A130041O12RIK	-1.61
DNAJC30	-1.61
EG381806	-1.61
CABYR	-1.61
ATL3	-1.61
CYP2C70	-1.61
ZFP36L1	-1.61
C130052O15RIK	-1.61
BRD2	-1.61
5330401F18RIK	-1.61
NKX2-3	-1.61
TTC3	-1.61
SCL0003251.1_21	-1.61
HIST1H2BB	-1.61
A730075L14RIK	-1.61
RPL21	-1.61
TAAR8A	-1.61
KRT86	-1.61
BC066107	-1.61
MDK	-1.61
PRMT6	-1.61
D630023F18RIK	-1.61
LOC382029	-1.61
41154	-1.61

IFNGR2	-1.60
CLCA3	-1.60
OTTMUSG00000010750	-1.60
NCBP2	-1.60
CREBL2	-1.60
BGLAP1	-1.60
EG633570	-1.60
3200002M19RIK	-1.60
PREI4	-1.60
MESDC2	-1.60
A930015D01RIK	-1.60
A430085C19	-1.60
4833421E05RIK	-1.60
NT5DC1	-1.60
BC050811	-1.60
EVI1	-1.60
2210012G02RIK	-1.60
GRAMD4	-1.60
STAG2	-1.60
DHRS4	-1.60
SVS6	-1.60
A930005L06RIK	-1.60
IL4I1	-1.60
PRL2C4	-1.60
SULT1E1	-1.60
KCNK9	-1.60
PER2	-1.60
SCL000022.1_12_REVCOMP	-1.60
UCK1	-1.60
CLRN1	-1.60
HSPB1	-1.60
TXNDC11	-1.60
CRIM2	-1.60
AKAP3	-1.60
2510016D11RIK	-1.60
TMEM169	-1.60

IGHA_J00475$V00785_IG_HEAVY_CONSTANT_ALPHA_1 35	-1.60
EDEM2	-1.60
SEMA4A	-1.60
LAMA3	-1.59
OLFR638	-1.59
HS3ST2	-1.59
BC002216	-1.59
DNAJC27	-1.59
3830406C13RIK	-1.59
BDH1	-1.59
LRRC34	-1.59
9430067P06RIK	-1.59
TIMM9	-1.59
HS3ST3B1	-1.59
PYGB	-1.59
CPLX2	-1.59
XPNPEP1	-1.59
RHOX12	-1.59
ASB3	-1.59
LOC100047368	-1.59
D430017M14RIK	-1.59
FBXO4	-1.59
ASPH	-1.59
CTSH	-1.59
TCF12	-1.59
SLC25A20	-1.59
2810423O19RIK	-1.59
PPM1L	-1.59
PLEKHA4	-1.59
LOC386537	-1.59
SLCO3A1	-1.59
MUC13	-1.59
CD44	-1.59
CCDC53	-1.59
LOC207685	-1.59
RNF38	-1.59

OLFR985	-1.59
THNSL2	-1.59
DNASE2B	-1.59
HSD11B1	-1.59
FAM101A	-1.59
SEC11C	-1.59
2010009J12RIK	-1.59
SCLY	-1.59
KLHL2	-1.59
GDF10	-1.59
C4A	-1.59
LOC241593	-1.59
EPB4.1L4B	-1.59
MCF2L	-1.59
PYCR1	-1.59
FDXR	-1.59
EPS15-RS	-1.59
KIF22	-1.59
4933426M11RIK	-1.59
CCDC23	-1.59
CFL2	-1.58
OTTMUSG00000020946	-1.58
PEX16	-1.58
ANKS6	-1.58
RNF31	-1.58
EPB4.1L4B	-1.58
PAFAH1B1	-1.58
KCNG2	-1.58
BCDO2	-1.58
KRTAP8-2	-1.58
E230014G11RIK	-1.58
LOC100040061	-1.58
POLR2A	-1.58
PDCD4	-1.58
TUG1	-1.58
PHKA1	-1.58

HOXD13	-1.58
LOC100046608	-1.58
AQP4	-1.58
BRCA2	-1.58
PPAP2C	-1.58
HBEGF	-1.58
LOC235997	-1.58
RNASEH2B	-1.58
2510049I19RIK	-1.58
2310007H09RIK	-1.58
CHD2	-1.58
TESK1	-1.58
MTUS1	-1.58
PDXP	-1.58
SORCS3	-1.58
2310004N24RIK	-1.58
VANGL2	-1.58
CPA2	-1.58
NAGPA	-1.58
EG245297	-1.58
DEK	-1.58
BC003993	-1.58
ZFP472	-1.58
NLRX1	-1.58
LOC384410	-1.58
2310021H06RIK	-1.57
CHD5	-1.57
SLC24A2	-1.57
RFC4	-1.57
4930504E06RIK	-1.57
TULP3	-1.57
SAP30BP	-1.57
CTTNBP2	-1.57
SUCLG2	-1.57
ZRANB3	-1.57
4833425P12RIK	-1.57

ZFP508	-1.57
E130112L06RIK	-1.57
6430598A04RIK	-1.57
1810060C03RIK	-1.57
2610305D13RIK	-1.57
PAQR6	-1.57
DVL1	-1.57
CCDC94	-1.57
STX11	-1.57
A730096F01RIK	-1.57
RBM24	-1.57
PSMF1	-1.57
CARTPT	-1.57
LOC210535	-1.57
TIMP1	-1.57
ALG8	-1.57
HTR7	-1.57
BCL2L1	-1.57
MORC3	-1.57
A930021K20RIK	-1.57
TEF3	-1.57
LOC380854	-1.57
SERPINA3H	-1.57
PRKCDBP	-1.57
D430044G18RIK	-1.57
CASP4	-1.57
UBE2J1	-1.57
MUP5	-1.57
NSD1	-1.57
LOC382765	-1.57
TMEM218	-1.57
1500041B16RIK	-1.57
ITSN2	-1.57
DTX4	-1.56
ENPP2	-1.56
SLC38A1	-1.56

FBXO16	-1.56
9130005N14RIK	-1.56
GIMAP4	-1.56
LOC100044204	-1.56
5730494M16RIK	-1.56
D13WSU177E	-1.56
OLFR134	-1.56
LOC100047645	-1.56
SPATA7	-1.56
FZD6	-1.56
CACNA1A	-1.56
LOC639001	-1.56
CITED4	-1.56
2410012M07RIK	-1.56
SCTR	-1.56
SLITRK4	-1.56
PFDN1	-1.56
BRP17	-1.56
LOC666979	-1.56
0610009L18RIK	-1.56
LOC383630	-1.56
LOC232974	-1.56
ZFP410	-1.56
LOC194055	-1.56
BC026439	-1.56
EG329763	-1.56
VLDLR	-1.56
LOC381957	-1.56
CLDN18	-1.56
A830086L01RIK	-1.56
MAPRE3	-1.56
AY761184	-1.56
NIPSNAP3A	-1.56
1700029H14RIK	-1.56
TMEM17	-1.56
SCG5	-1.56

D830039M14RIK	-1.56
PDE4DIP	-1.56
COBL	-1.56
ZFP94	-1.56
PSMC4	-1.56
D330006C15RIK	-1.56
DUSP22	-1.56
LOC383262	-1.56
RRAS2	-1.56
CAMK2A	-1.56
2310007H09RIK	-1.56
DDX50	-1.56
FAIM	-1.56
SMPX	-1.56
DDX17	-1.56
2410022L05RIK	-1.55
AHDC1	-1.55
D630011D02RIK	-1.55
RHPN1	-1.55
EPHA1	-1.55
THRAP2	-1.55
AGXT2L2	-1.55
TTC8	-1.55
A730046J19RIK	-1.55
RBBP9	-1.55
AI850995	-1.55
SCL0003723.1_3	-1.55
LOC193533	-1.55
PCDHA7	-1.55
FBLN1	-1.55
D930025M23RIK	-1.55
CXCL14	-1.55
TWSG1	-1.55
LOC633661	-1.55
PM20D1	-1.55
LOC100047839	-1.55

GRAMD1B	-1.55
NNAT	-1.55
SYNGR2	-1.55
E030030K01RIK	-1.55
GZMG	-1.55
GM459	-1.55
LOC385274	-1.55
5730589K01RIK	-1.55
C79407	-1.55
CDCA8	-1.55
BC023835	-1.55
FV1	-1.55
FUSIP1	-1.55
PPP3CA	-1.55
D030044M21RIK	-1.55
CAPRIN2	-1.55
TNIP1	-1.55
2610301G19RIK	-1.55
UMPS	-1.55
KNG2	-1.55
9330175B10RIK	-1.55
FBXL10	-1.55
XRCC6	-1.55
TGFB3	-1.55
MGST1	-1.55
UNC5A	-1.55
LOC545238	-1.54
RARRES2	-1.54
382044	-1.54
OLFR1020	-1.54
PAPOLG	-1.54
NEO1	-1.54
LOC100042270	-1.54
LOC100047749	-1.54
PFKM	-1.54
1500001M20RIK	-1.54

CCRN4L	-1.54
TRAPPC5	-1.54
C87436	-1.54
COX17	-1.54
RGL3	-1.54
2610208M17RIK	-1.54
GRIK2	-1.54
GTPBP10	-1.54
SNX22	-1.54
NTNG1	-1.54
OPN3	-1.54
2010106G01RIK	-1.54
4930471G03RIK	-1.54
V2R8	-1.54
IRF1	-1.54
MBD1	-1.54
DPPA4	-1.54
TOP1	-1.54
LOC100042514	-1.54
1700065O13RIK	-1.54
LOC546090	-1.54
SH2D1B2	-1.54
EIF2C3	-1.54
IL1RAPL1	-1.54
9530064J02	-1.54
OLFR1189	-1.54
VPS26B	-1.54
2310046O06RIK	-1.54
6530401D06RIK	-1.54
EG666668	-1.54
IER3	-1.54
NFATC1	-1.54
HSDL1	-1.54
PROM	-1.54
OSMR	-1.54
JMJD2A	-1.54

PIGC	-1.54
ELK3	-1.54
SH3GLB1	-1.54
OLFR101	-1.54
1700020O03RIK	-1.54
E030034P13RIK	-1.54
1110006G06RIK	-1.54
GM969	-1.54
MYCBP	-1.54
LOC100048684	-1.54
LRRC51	-1.54
ZC3H14	-1.53
F2RL1	-1.53
NOS3	-1.53
ACSL4	-1.53
FBXL10	-1.53
DGKB	-1.53
NUDT8	-1.53
RFC4	-1.53
RGS8	-1.53
PCDH7	-1.53
FGF14	-1.53
CDC37L1	-1.53
LOC213411	-1.53
PTPN4	-1.53
A930025D01RIK	-1.53
D930014E17RIK	-1.53
WDR20B	-1.53
TUBB2B	-1.53
ZBTB45	-1.53
A2LD1	-1.53
PIK3CG	-1.53
PKN1	-1.53
DEFB19	-1.53
LYL1	-1.53
EPB4.1L5	-1.53

FAHD1	-1.53
BAMBI-PS1	-1.53
9530013D10RIK	-1.53
MPDZ	-1.53
LOC380623	-1.53
XPNPEP2	-1.53
MGC117608	-1.53
OLFR1197	-1.53
IRAK1	-1.53
COL1A2	-1.53
9430043O10RIK	-1.53
ZCCHC3	-1.53
CCDC53	-1.53
IFIT2	-1.53
CARD10	-1.53
DCUN1D3	-1.53
AKR7A5	-1.53
NAT15	-1.53
C4A	-1.53
LOC381220	-1.53
LOC386005	-1.53
TBC1D2B	-1.53
NOSIP	-1.53
SCL0002507.1_236	-1.53
IFNA1	-1.53
TCFCP2L1	-1.53
PPP1R3F	-1.53
GRAMD2	-1.53
2610206P12RIK	-1.53
ZFP821	-1.53
GPR85	-1.53
PRR14	-1.53
USP38	-1.53
F730003H07RIK	-1.53
VWA5B2	-1.52
EPN2	-1.52

ENTPD5	-1.52
RNASEH1	-1.52
TRAPPC5	-1.52
EHBP1	-1.52
WDR7	-1.52
MBP	-1.52
PDHX	-1.52
RAD51C	-1.52
RHOC	-1.52
LOC100044439	-1.52
A230003K02RIK	-1.52
NICN1	-1.52
MAT2B	-1.52
E430021E22RIK	-1.52
SPOCK2	-1.52
5730502D15RIK	-1.52
SORBS1	-1.52
LOC385651	-1.52
ZFP748	-1.52
ACTN3	-1.52
OLFR51	-1.52
D6WSU116E	-1.52
4933407L21RIK	-1.52
CAPG	-1.52
NDE1	-1.52
5430435G22RIK	-1.52
TSPAN15	-1.52
SLC35A5	-1.52
MTAP1B	-1.52
ZFP354A	-1.52
OPN1MW	-1.52
NOXO1	-1.52
LOC381981	-1.52
MLLT1	-1.52
MON1A	-1.52
IGFBP5	-1.52

4930533K18RIK	-1.52
PRUNE	-1.52
LOC385923	-1.52
GPR27	-1.52
GANC	-1.52
ORF9	-1.52
CLP1	-1.52
EG217246	-1.52
RARRES2	-1.52
LGALS4	-1.52
E030001I17RIK	-1.52
BC048546	-1.52
EEFSEC	-1.52
4930432M17RIK	-1.52
B430105G09RIK	-1.52
1700087I21RIK	-1.52
FBXO7	-1.52
RELT	-1.52
1810054D07RIK	-1.52
ANKRD13A	-1.52
LTBP4	-1.52
JPH4	-1.52
4930555G01RIK	-1.52
TRPT1	-1.52
G630007B09RIK	-1.52
TARDBP	-1.52
EFCAB4B	-1.52
AR	-1.52
OLFR10	-1.52
ECHDC2	-1.52
4733401O04RIK	-1.52
ACPP	-1.52
TRIM26	-1.52
THOC3	-1.52
2310004N11RIK	-1.52
EG434758	-1.52

GORASP2	-1.52
WIPI2	-1.52
ZFP36L2	-1.52
TRAF6	-1.52
1110003F05RIK	-1.52
METRNL	-1.52
A130022L12RIK	-1.52
EG627743	-1.52
ODZ4	-1.52
CROCC	-1.52
PARD6B	-1.52
CYB5D2	-1.52
GCNT2	-1.52
4632415L05RIK	-1.52
ORF9	-1.52
9430041J12RIK	-1.52
IL17RC	-1.52
DHTKD1	-1.52
SCOTIN	-1.51
D330028D13RIK	-1.51
OLAH	-1.51
RBAK	-1.51
LOC100045266	-1.51
VPS11	-1.51
1500019G21RIK	-1.51
TBRG1	-1.51
6530404N21RIK	-1.51
4933407C03RIK	-1.51
HDAC5	-1.51
MERTK	-1.51
DTX4	-1.51
RAI3	-1.51
PRNPIP1	-1.51
RHOX5	-1.51
2810422J05RIK	-1.51
MAP3K7IP1	-1.51

|	
FAM171A1	-1.51
COL18A1	-1.51
LOC232993	-1.51
EPHA1	-1.51
OPRS1	-1.51
LOC383303	-1.51
MTF1	-1.51
H2-K1	-1.51
PRRX1	-1.51
TRMU	-1.51
1700129I04RIK	-1.51
5430406J06RIK	-1.51
SENP8	-1.51
OLFR692	-1.51
GINS1	-1.51
APOB48R	-1.51
NOC4L	-1.51
GPD2	-1.51
1700001L05RIK	-1.51
TRPT1	-1.51
COX7B	-1.51
TTC33	-1.51
HAP1	-1.51
ELMOD3	-1.51
BAT2D	-1.51
SRP19	-1.51
EXOC7	-1.51
POLR3F	-1.51
TRO	-1.51
UNC5A	-1.51
TRP53BP1	-1.51
SLC4A1	-1.51
CTRB1	-1.51
LASS4	-1.51
ALDH1A7	-1.51
1700025H01RIK	-1.51

EG432879	-1.51
GDPD5	-1.51
GCAP3	-1.51
AU019823	-1.51
MYO5B	-1.51
SYNGR4	-1.51
IFIT3	-1.51
RAB3B	-1.51
RTN4	-1.51
6030470M02RIK	-1.51
TUBB2B	-1.51
TRO	-1.51
NCKIPSD	-1.51
REFBP2	-1.50
D330018I10RIK	-1.50
AKAP2	-1.50
FRAT1	-1.50
1700019G17RIK	-1.50
2900060M06RIK	-1.50
RPGR	-1.50
SEMA3B	-1.50
ARMC9	-1.50
TRP53INP1	-1.50
REV3L	-1.50
MRC2	-1.50
KRT42	-1.50
EGR3	-1.50
E130107G19RIK	-1.50
CAR5B	-1.50
10181072_290	-1.50
WDR17	-1.50
EIF3S1	-1.50
NESPAS	-1.50
HMGB4	-1.50
SLC25A15	-1.50
TTC39A	-1.50

TLCD2	-1.50
2700016E08RIK	-1.50
HDGF	-1.50
TNC	-1.50
CRYZ	-1.50
HLF	-1.50
CCNG1	-1.50
CCRK	-1.50
NUP43	-1.50
EG666756	-1.50
CUL1	-1.50
POLG	-1.50
RPA2	-1.50
IDB4	-1.50
B930076A02	-1.50
DOCK1	-1.50
DOCK4	-1.50
PHKA2	-1.50

Appendix B

IACUC LETTER OF APPROVAL

University of Delaware
Institutional Animal Care and Use Committee
Annual Review
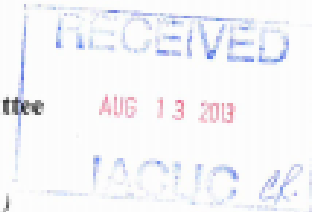
(Please complete below using Arial, size 12 Font.)

Title of Protocol: Investigate the function of genes associated with animal development using mouse and chicken

AUP Number: 1226-2014-2   ← (4 digits only)

Principal Investigator: Salil A. Lachke

Common Name: Mouse, Chicken, Rat

Genus Species: *Mus musculus, Gallus gallus, Rattus rattus*

Pain Category: *(please mark one)*

USDA PAIN CATEGORY: *(Note change of categories from previous form)*	
Category	**Description**
☐ B	Breeding or holding where NO research is conducted
x ☐ C	Procedure involving momentary or no pain or distress
☐ D	Procedure where pain or distress is alleviated by appropriate means (analgesics, tranquilizers, euthanasia etc.)
☐ E	Procedure where pain or distress cannot be alleviated, as this would adversely affect the procedures, results or interpretation

---

Official Use Only

IACUC Approval Signature: _____

Date of Approval: 10/1/2012

135